THE UNIVERSITY
of EDINBURGH

Fission yeast growth polarity decisions depend on integration of multiple internal cues

Sanju Ashraf

Doctor of Philosophy – University of Edinburgh – 2016

Acknowledgements

First, I would like to thank my supervisor Ken Sawin for providing me with an opportunity to work in his lab. I am deeply indebted to Ken for his guidance, patience and encouragement throughout my PhD. Working with Ken has been an absolute pleasure and a great learning experience both scientifically and on a personal level.

I am very grateful to all the past and present members of Sawin lab: Eric Lynch, Weronika Borek, Delyan Mutavchiev, Xun Bao, Harish Thakur, Su Ling Leong, Hayley Johnson, Ye Dee Tay and Marcin Leda. I highly appreciate your friendship and advice both inside and outside the lab. I would also like to thank my second supervisor Andrew Goryachev for all the advice and guidance during my PhD. Further, I would like to thank my PhD committee members Hiro Ohkura and Karl Oparka for their feedback and guidance during my PhD.

I would like to thank Principals Career Development Scholarship and Edinburgh Global Research Scholarship from University of Edinburgh for the financial support during my PhD.

I am very grateful to David Kelly for all the help with microscopy and for making sure the long hours of imaging are never dull.

I would like to thank all my friends in Edinburgh and back home for supporting me throughout my PhD. Your friendship and encouragement has helped me a great deal when the going was tough. A special hug goes out to Tanmay and Simon for their friendship and all the support during my PhD. I would also like to thank Shameer, Lulu, Becky, Bhoomi, Jenny, Hayley, Philipp, Prasmit, Jacob, Jana, Keerthi, Aparna, Pradeep, Phu, Ruth, James, Burak, Lisa and many others for their constant support and motivation.

Finally I would like to thank my loving family for all their unconditional love and support. Uppa, Umma, Simitha, Waseem and Jeeju – without your love and constant support, this thesis would not have been possible. I am very grateful to Heba for always being there for me. Your love and care provided me with great comfort during difficult times.

Declaration

The work presented in this thesis is the original work of the author. This thesis has been composed by the author and has not been submitted in whole or in part for any other degree.

Sanju Ashraf

August 2016

Abstract

The establishment of cell polarity is a vital requirement for cellular processes such as proper cell division, growth and movement. Cell polarization relies on different internal and external cues in order to reorient the cell growth machinery along the axis of polarity. The core mechanisms involved in establishment of polarized growth are highly conserved from yeast to humans. Cells of the fission yeast *Schizosaccharomyces pombe* grow in a highly polarized fashion, with cell growth restricted to the cell tips, making fission yeast an excellent model system to study polarized growth.

Here I describe a system for long-term live-cell imaging of fission yeast polarized growth that is stress free, physiological and accessible to media change and drug addition. I use this improved imaging system along with yeast genetics and drug perturbations to address how cell polarity is established and maintained in fission yeast. I have shown that fission yeast growth polarity depends on competition and cooperation among three distinct internal polarity cues: 1) A microtubule-based cue involving Tea1/Tea4 polarity proteins positively regulates polarized growth, initially at the “old” cell end (i.e., the end that pre-existed in the mother cell) and later at the “new” cell end (i.e. the end that is generated by septation), in order to initiate the transition from monopolar to bipolar growth (also known as New End Take-Off, or “NETO”). 2) An actin cable-based cue “clears” polarity proteins from the new end immediately after cytokinesis thereby reinforcing old-end growth. As a result perturbation of actin cable-based transport by either deleting actin cable nucleator For3 or cable-based transporter Myo52 results in premature bipolar growth. 3) A novel “memory-based” growth polarity cue helps to establish polarized growth in the absence of the microtubule-based cue. This memory-based cue is dependent on the predicted transmembrane proteins Rax1/Rax2. In the absence of both Tea1/Tea4 cue and Rax1/Rax2 cue, cells depend on septation cue and grow exclusively from the cell ends generated by septation. Furthermore, both Tea1/Tea4 and Rax1/Rax2 cue are important to maintain polarized growth under various environmental stresses.

In fission yeast, during interphase, nucleus is positioned at the centre of the cell and this precise positioning of nucleus, which is important for defining the position of cytokinetic ring is thought to be exclusively MT-dependent. Here I show that MT-independent nuclear movement exists in fission yeast and this nuclear

movement is mediated by actin cables and type myosin myo52. Furthermore, I show that actin cable might be important for buffering the pushing forces generated by MTs on the nucleus. In this way both microtubules and actin cables are involved in nuclear movement in fission yeast.

Lay summary

Cells exist in different shapes and sizes in order to perform a wide array of biological functions. This difference in cell size and shape is generated by a fundamental process termed as cell polarization. Loss of polarity is a hallmark of cancer. In this thesis, I use a simple unicellular model organism *Schizosaccharomyces pombe* with powerful genetics and very well defined rod shape to understand how multiple internal cues or landmark proteins regulate growth pattern.

Here I show that establishment of polarized growth in fission yeast depend on multiple, redundant cues that cooperate and compete with each other. Microtubules along with polarity proteins Tea/Tea4 initially establish polarized growth at the old ends and later at the new ends, whereas actin cables clear proteins from the new end thereby promoting growth at the old ends. In the absence of MT-based cue, cells depend on a cue that is inherited from the mother cell – a 'memory'-based cue. Memory-based cue involves transmembrane proteins Rax1/Rax2 and in the absence of both MT-based cue and memory-based cue, cells depend on cue generated from septation. In this way, multiple redundant cues regulate establishment of polarized growth in fission yeast and are also important to maintain polarized growth under environmental stresses.

In fission yeast, nucleus is placed at the centre of the cell, which positions the future division plane of the cell. Hence, after cytokinesis, mother cell will produce two equal daughter cells with same amount of genetic material. Microtubules that span the long axis of the cell are thought to push the nucleus from both sides and position it at the cell centre. In this study, I show that apart from MTs, actin cables are also involved in this process and actin cables might be important to buffer the pushing generated by MTs.

Table of contents

Abbreviations

aa	Amino acid
ARP	Actin Related Protein
ATP	Adenosine Triphosphate
CAP	Cytoskeleton Associated Proteins
CAR	Cytokinetic Actin Ring
CH	Calponin Homology
CRIB	Cdc42/Rac Interactive Binding
DMSO	Dimethyl Sulfoxide
DNA	Deoxyribonucleic Acid
EB	End Binding
EBH	End Binding Homology
EMM	Edinburgh Minimal Medium
ER	Endoplasmic Reticulum
FH	Formin Homology
FP	Fluorescent Protein
FRAP	Fluorescence Recovery After Photobleaching
GAP	GTPase Activating protein
GDI	Guanine nucleotide Dissociation Inhibitors
GDP	Guanosine diphosphate
GEF	Guanine nucleotide Exchange Factors
GFP	Green Fluorescent Protein
GTP	Guanosine triphosphate
HMT	Home-made Taq polymerase
IFT	Intraflagellar Transport
KDa	KiloDalton
LatA	LatrunculinA
LINC	LInkers of Nucleoskeleton and Cytoskeleton
LPA	Lysophosphatidic Acid
MAP	Microtubule Associated Proteins
MBC	Methyl Benzimidazol-2-yl Carbamate
MT	Microtubules
MTOC	Microtubules Organizing Centres
NADH	Nicotinamide Adenine Dinucleotide

NETO	New End Take-Off
O/N	Over night
OD	Optical Density
PAA	Post Anaphase Array
PAK	P21 Activated Kinase
PAR	Partition Defective
PB	Phloxin B
PCI	Phenol/Chloroform/Isoamyl alcohol
PCR	Polymerase Chain Reaction
PEG	Polyethylene glycol
RMSD	Root Mean Squared Deviation
RNA	Ribonucleic Acid
ROS	Reactive Oxygen Species
RP	Replica Plating
RPM	Rotation Per Minute
RT	Room Temperature
SCPR	Search Capture Pull and Release
SIN	Septation Initiation Network
SPB	Spindle Pole Body
TAN	Transmembrane Actin-associated Nuclear lines
TBZ	Thiabendazole
TGN	Trans Golgi Network
TOR	Target Of Rapamycin
TRK	Tropomyosin Receptor Kinase
UTR	Untranslated Region
YE	Yeast Extract
YFP	Yellow Fluorescent Protein
µm	Micron

List of figures

Chapter 1: Introduction

1.1 Cell Polarity: Overview

Cell polarization is a fundamental biological process and is defined as asymmetric organization of cell membranes, intracellular organelles and the cytoskeleton into subdomains along well defined axes with distinct chemical and physical properties in order to facilitate diverse cellular functions (Nelson 2003; Asnacios & Hamant 2012; Bryant & Mostov 2008).

Proper establishment of cell polarity is important for a host of cellular functions, including cell shape, cell division, cell adhesion, cell migration, and cell fate determination (Thompson 2013). For example, polarized epithelial cells have a distinct apical-basal axis of polarity. This organization is important for vectorial transport of nutrients and waste across the epithelium between the internal and external environments (Nelson 2009). In contrast, migratory mesenchymal cells exhibit a front-rear axis of polarity, which is important for persistent, directional cell migration during development and wound healing (Nelson 2009). Loss of apical-basal polarity is thought to be a common feature of cancer progression (Macara & McCaffrey 2013). Similarly, in order to assemble functional neural networks to propagate signals, a morphologically unpolarized neuron need to be polarized into a complex morphology of one long axon and several shorter dendrites (Tahirovic & Bradke 2009). Polarization is also important for asymmetric cell division, especially at the beginning of development of multi-cellular organisms, for differentiation into distinct cell types (Suzuki & Ohno 2006). For example, in the one-celled embryo of *C.elegans*, 'partition defective' (PAR) proteins are segregated asymmetrically after division to give rise to cells of different size, contents and fate (Suzuki & Ohno 2006; St Johnston & Ahringer 2010; Thompson 2013) (Fig.1.1).

Although apical-basal polarity of epithelial cells looks quite different from the polarization of neurons into axon and dendrites, or the asymmetric division of a nematode zygote embryo, the basic molecular mechanisms involved in polarization are highly conserved from single-celled eukaryotic systems such as yeast to cells in tissues of multi-cellular organisms such as worms, flies and mammals (McCaffrey & Macara 2009; Nelson 2003). Establishment of cell polarity is hierarchical and can be broadly classified into the following simple steps. 1) Initially, a spatial cue or

landmark is generated at the cell surface. This is followed by 2) amplification of this signal throughout the cell by different core mechanisms that reorient the inherently polar actin and microtubule network along the axis of polarity. Finally, 3) different proteins and growth factors use these cytoskeletal networks as tracks to move towards the landmark to amplify and maintain polarized cell growth (Nelson 2003; Li & Bowerman 2010; McCaffrey & Macara 2009).

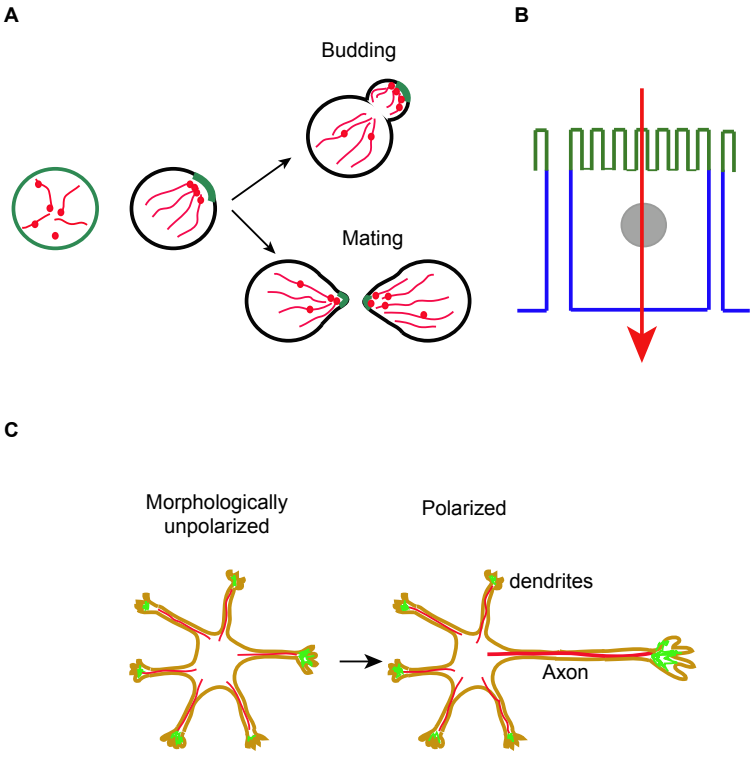

Fig.1.1 Polarization in different eukaroyotic cells. A) Cell polarization process in the life cycle of budding yeast. Initially actin cytoskeleton (red) and Cdc42 (green) are not polarized. In response to cell cycle signals and mating pheromones, actin cytoskeleton and Cdc42 becomes polarized to provide targeted secretion. This is important for budding (cell division) and mating. Adapted from (Slaughter et al. 2009). **B)** Polarized epithelial cells showing two distinct biological compartments - apical membrane (green) and basolateral membrane (blue) important for vectorial transport of ions and solutes (red arrow) between the compartments. Adapted from (Nelson 2003). **C)** Morphologically unpolarized neuronal cell with several equal dendrites polarize to form morphologically polarized neuron bearing an axon. The actin cytoskeleton (green) is more dynamic and microtubules (red) are more stable in axons compared to dendrites. Adpated from (Tahirovic and Bradke 2009).

1.2 Cell polarity in the fission yeast S.pombe

The fission yeast *Schizosaccharomyces pombe* is an excellent model organism for understanding the process of establishment of cell polarity. It is a unicellular, non-motile, rod-shaped organism, 8-14 μm long and 3-4 μm wide (Chang & Martin 2009). Fission yeast cells grow in a highly polarized fashion, which is restricted to cell tips, and they divide by medial fission (Hayles & Nurse 2001).

Polarised growth in fission yeast is highly regulated during the cell cycle (Mitchison & Nurse 1985) (Fig.1.2). After cytokinesis, the new daughter cells initially grow in a monopolar fashion from their old ends, i.e. the ends that were already present in the mother cell during the previous cell cycle. Later, they initiate growth at the new end, i.e. the ends that were generated by septation of the mother cell. This transition in growth from monopolar to bipolar growth is referred to as NETO (new end take off) (Mitchison & Nurse 1985). Using fluorescence microscopy and time-lapse photomicrography on wild-type, size mutants and *cdc* mutants, it was shown that establishment of NETO depends on cells reaching a critical cell length or cells passing the early G2 phase of cell cycle (Mitchison & Nurse 1985). Establishment of NETO is also dependent on growth media in which cells are grown. In nutrient poor minimal medium with ammonium as nitrogen source, NETO is delayed to later in the cell cycle (0.49 of cell cycle) compared to rich medium (0.34 of cell cycle) (Mitchison & Nurse 1985). Finally, upon entering mitosis, cells stop growing at the tips, and the growth machinery relocalizes to the cell equator to form a cytokinetic ring and a septum, and cells undergo medial division to produce two equal daughter cells (Hayles & Nurse 2001). The precise localization of growth to the opposite cell poles, ease of genetic manipulation and power of live-cell imaging make fission yeast an attractive model organism to understand the process of cell polarity (Hayles & Nurse 2001; Chang & Martin 2009).

Similar to higher eukaryotes, establishment of polarized growth in fission yeast depends on the cytoskeleton (mainly actin filaments and microtubules), RhoGTPases, membrane trafficking, spatial landmarks and specific types of lipids (Martin & Arkowitz 2014). The stereotypical shape of fission yeast provides a great advantage to identify proteins important for establishment and maintenance of polarized growth by visualizing morphological mutants (Martin & Arkowitz 2014).

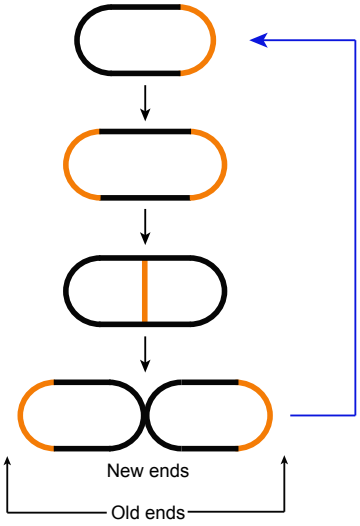

Fig. 1.2. Establishment of NETO in fission yeast. After cell division, *S.pombe* cells only grow (orange) from old-end and once cell enters G2 phase of cell cycle and reaches a particular length, establishes NETO or bipolar growth. Once cell enter mitosis, cell growth ceases at the cell tips and relocalize to cell septum and undergoes cytokinesis to produce two equal daughter cells and continue the cycle.

1.3 Cytoskeleton and regulation of polarity in fission yeast

The fission yeast cytoskeleton consists mainly of microtubules (MTs) and actin filaments (Martin & Arkowitz 2014). Establishment and maintenance of polarized growth in fission yeast depends mainly on MT and actin cytoskeletons (Sawin & Nurse 1998; Feierbach & Chang 2001; Marks et al. 1986; Radcliffe et al. 1998). This is in contrast to budding yeast *Saccharomyces cerevisiae*, a widely used model system to study cell morphogenesis, which mainly depends on actin and septins for spatial cues (Jacobs et al. 1988; Pruyne et al. 1998; Barral et al. 2000; Gladfelter et al. 2001) .

1.3.1 **Microtubules**

MTs are biopolymers made up of repeating tubulin dimers, with each dimer comprising an α- and β-tubulin protein molecule (Desai & Mitchison 1997; Shelley 2016). These cytoskeletal filaments are implicated in a wide range of cellular processes such as intracellular transport, organelle positioning, cell division, cell polarity and morphogenesis, and MTs also provide the structural basis for cilia and flagella (Akhmanova & Steinmetz 2015). Each MT is formed by head to tail association of α/β heterodimers to form 13 linear protofilaments with a three-start helix, which associate laterally to form hollow, cylindrical polymers approximately 25 nm wide (Desai & Mitchison 1997; Nogales 2001). The asymmetry of heterodimer gives MTs an intrinsic directionality or polarity. Thus, the fast-growing end of a MT is referred to as the plus end, and the slow-growing end is referred to as the minus end (Desai & Mitchison 1997; Shelley 2016). Within each protofilament, β-tubulin subunits are pointing towards the plus end of MTs and α-tubulin subunits pointing towards the minus end of the MTs (Desai & Mitchison 1997; Nogales 2001). The general picture of MT polarity is one in which minus ends are anchored at the microtubule organizing centres (MTOCs), usually near the nucleus, and plus ends are reaching the cell periphery (Sawin & Tran 2006; Welte 2004).

MTs are highly dynamic in nature, undergoing stochastic polymerization and depolymerization at the plus ends. This process involves catastrophe (the switch from growing to shrinking) and rescue (the switch from shrinking to growing) and is referred to as dynamic instability (Mitchison & Kirschner 1984; Desai & Mitchison 1997). During the polymerization phase, GTP-tubulin is added to the plus end of the MTs. During or soon after polymerization, GTP-tubulin is hydrolyzed and

subsequently releases the hydrolyzed phosphate (Mitchison & Kirschner 1984; Desai & Mitchison 1997). When the GTP hydrolysis rate is slower than the rate of addition of new subunit, a GTP-tubulin “cap” is formed at the plus end, which protect the MTs from shrinking, while loss of the cap leads to MT shrinkage (Mitchison & Kirschner 1984; Desai & Mitchison 1997). During depolymerization, GDP-tubulin is rapidly lost from the plus ends. Depolymerizing MTs can transit back to the polymerization phase when GTP-tubulin is added to the depolymerizing end (rescue). This rescue event was shown to be directly promoted by GTP-tubulin remnants (GTP-tubulin “islands”) in the MT lattice (Tropini et al. 2012; Gardner et al. 2013). These growing and shrinking events are locally regulated to act as a search-and-capture mechanism for MTs to interact with cellular organelles and membranes (Etienne-Manneville 2013).

The dynamics of MTs and the connections between MTs and cellular structures are mediated by MT-associated proteins (MAPs) and MT-associated motor proteins (Etienne-Manneville 2013; Akhmanova & Steinmetz 2015). MT-based molecular motors include kinesins and dyneins, which transport vesicles, proteins or mRNA from or towards the cell periphery using MTs as tracks. These motor proteins are powered by hydrolysis of ATP to move along MTs. Generally, kinesins move towards the MT plus ends, whereas dynein moves towards the minus ends of MTs (Kardon & Vale 2009; Etienne-Manneville 2013). Although many genes encoding dynein heavy chain have been identified (around 15), only intraflagellar (IFT) dynein and cytoplasmic dynein are known to transport cargoes along MTs. IFT dynein moves cargo exclusively along the flagellar or ciliary axoneme towards the cell body, whereas cytoplasmic dynein performs minus end-directed transport within the cytoplasm as well as several mitotic functions (Karki & Holzbaur 1999; Kardon & Vale 2009). Cytoplasmic dynein is implicated in a wide range of processes, such as neuronal transport, mitosis, transport of wide variety of cargoes including mRNA, viruses and endosomes, nuclear positioning and maintenance of the Golgi apparatus (Mallik & Gross 2004). For example, In both *Aspergillus nidulans* and *Neurospora crassa*, dynein is required for proper nuclear migration, and mutations in the gene encoding dynein results in nuclear clumping and significant inhibition of nuclear migration along the hyphae (Holleran et al. 1998; Karki & Holzbaur 1999). Similarly in the budding yeast *S.cerevisiae*, dynein is important for positioning the nucleus during cell division (Adames & Cooper 2000; Roberts et al. 2013). Cytoplasmic dynein is also important for intracellular transport along MTs. For example in neurons, dynein is involved in transport of endosomes containing tropomyosin receptor kinase (TRK) towards the cell body, where they initiate signalling cascades essential for neuronal survival (Heerssen et al. 2004).

The kinesin superfamily of proteins is implicated in transport of various cargoes from the Golgi to the endoplasmic reticulum (ER) and from the trans-Golgi network (TGN) to the plasma membrane, and also in transport of endosomes and lysosomes (Woźniak & Allan 2006; Eustratios Bananis et al. 2004; Stauber et al. 2006). In neurons, kinesins are important for bidirectional transport of membrane organelles and synaptic vesicle precursors for neuronal polarization and elongation (Hirokawa, Noda, et al. 2009; Hirokawa, Nitta, et al. 2009). For example, during neuronal development, kinesin-I (KIF5)-based transport is involved in the specification of a single axon from multiple neurites (Nakata & Hirokawa 2003). Kinesins are also important for regulating the dynamics of MTs (Walczak et al. 2013). For example, kinesin-13 family members are known to depolymerize the MTs instead of moving along MTs (Moores & Milligan 2006).

A major group of MAPs include +TIP proteins, which consist of structurally and functionally diverse MT regulators that are conserved in all eukaryotes and are concentrated at the plus ends of MTs (Akhmanova & Steinmetz 2008; Akhmanova & Steinmetz 2015). +TIP proteins include plus end- and minus end-directed motors, non-motor MAPs and regulatory and adaptor proteins (Lansbergen & Akhmanova 2006). +TIP proteins can be broadly classified into: 1) end-binding (EB) proteins such as EB1, EB2 and EB3; 2) cytoskeleton-associated protein (CAP) glycine rich proteins such as CLIPs and p150-glued; 3) proteins that contain basic and serine rich (SxIP) sequences such as CLASP1 and APC; 4) HEAT and WD40-repeat proteins such as XMAP125 and lissencephaly-1 (LIS1); and 5) motor proteins such as Tea2 and MCAK (Akhmanova & Steinmetz 2010; Akhmanova & Steinmetz 2008). EBs are considered to be master regulators of +Tip networks because they autonomously track the plus end of MTs independent of any binding partners (Bieling et al. 2007; Bieling et al. 2008; Dixit et al. 2009). They recognize growing plus and minus ends of MTs and recruit a variety of different factors (Goodwin & Vale 2010; Hendershott & Vale 2014; Akhmanova & Hoogenraad 2015). EB proteins have an N-terminal calponin-homology (CH) domain followed by a variable linker region and a coiled-coil domain, which is important for dimerization, an EBH domain (End-binding homology) and a C-terminal flexible region containing EEY/F motif. The CH domain along with the linker region has been shown to be sufficient to recognize and track growing MTs (Slep & Vale 2007; Akhmanova & Steinmetz 2015). The EBH domain and the flexible region containing the EEY/F motif helps EB proteins to interact with different +Tip proteins to recruit them to MT plus ends (Akhmanova & Steinmetz 2010). For example, a single CAP-Gly domain of CLIP-170 along with the adjacent serine-rich region can track growing MT ends (Gupta et al. 2009; Akhmanova & Steinmetz

2010). Proteins with TOG domains such as XMAP125 can bind to MT plus ends to recruit tubulin dimers and increase the rate of tubulin addition to the growing plus ends (Slep & Vale 2007; Brouhard et al. 2008; Akhmanova & Steinmetz 2010).

Apart from regulating MT dynamics, +Tip proteins can also link MT-plus ends with other cellular structures. For example, CLASP-LL5β complex can mediate interaction between MT ends and cell cortex. This accumulation of CLASPs promotes MT stabilization and actin remodelling at the leading edge of migrating cells (Lansbergen et al. 2006). +Tips also participate in crosstalk between MT and actin cytoskeleton. For example, in mammalian cells, CLIP-170 controls the recruitment of formin mDia1, an actin nucleating protein, at the onset of phagocytosis and thereby regulates actin polymerization (Lewkowicz et al. 2008). In addition, in budding yeast, the EB1 homolog Bim1 along with Kar9-Myo2 is involved in transport of MT ends along actin filaments (Liakopoulos et al. 2003).

In fission yeast *S.pombe,* during interphase, MTs are organized into three to five anti-parallel bundles spanning the long axis of the cell such that the plus ends of the MTs are oriented towards the cell tips, whereas the minus ends are oriented towards the nucleus (Piel & Tran 2009; Drummond & Cross 2000). This linear arrangement of MTs along the long axis of the cell is important for establishing polarized growth and positioning organelles in the fission yeast (Drummond & Cross 2000; Tran et al. 2001; Piel & Tran 2009). In fission yeast, MTs undergo striking changes during the cell cycle. During interphase, MTs are nucleated from the spindle pole body (SPB) as well as additional sites on nuclear membrane, on MTs themselves and in the cytoplasm. These microtubule organizing centres (MTOCs) are collectively known as interphase MTOCs (iMTOCs) (Sawin & Tran 2006). During mitosis, astral MTs are nucleated from the cytoplasmic side of the SPBs, and at the end of mitosis, equatorial MTOCs (eMTOCs) nucleate MTs to form post-anaphase arrays (PAA) at the cytokinetic actin ring (Sawin & Tran 2006) (Fig. 1.3).

MT bundles in fission yeast are made up of multiple MTs that are held together by MT bundler Ase1, motor protein Klp2 and Dis1 (XMAP215 homolog). Ase1 is a member of conserved ASC1/PRC1/MAP65 family of MT bundling proteins, and *ase1*Δ cells fail to form overlapping anti-parallel MT bundles, resulting in defects in nuclear positioning and premature mitotic spindle collapse (Loïodice et al. 2005; Akira yamashita et al. 2005; Janson et al. 2007; Roque et al. 2010). Klp2 is a minus end-directed kinesin like protein important for sliding of MTS, which is required for proper organization of interphase MTs (Carazo-Salas et al. 2005). Dis1 and the related protein Alp14 are structurally and functionally redundant proteins known to

stabilize MTs and act as a bridge between plus end of the mitotic spindles and the kinetochore (Nakaseko et al. 2001; Garcia et al. 2001; Garcia et al. 2002).

In fission yeast, MTs play two important roles in cell morphogenesis. Firstly, during polarized growth, MTs are important to transport different polarity proteins to the cell tips to mark the cell tips for polarized growth (discussed in section 1.5.1) (Sawin & Nurse 1998; Mata & Nurse 1997; Martin et al. 2005). Secondly, MTs are important for the central positioning of the nucleus, which determines the future plane of cell division (discussed in chapter 4) (Tran et al. 2001). Previous work by Sawin *et al.* showed that microtubules are not required for maintenance of polarized growth or for establishment of polarity *per se* in fission yeast (Sawin & Snaith 2004). However, when the actin cytoskeleton is perturbed, MTs are important for dictating the sites of re-establishment of polarized growth by accurate delivery of polarity proteins to the cell tips (Sawin & Snaith 2004).

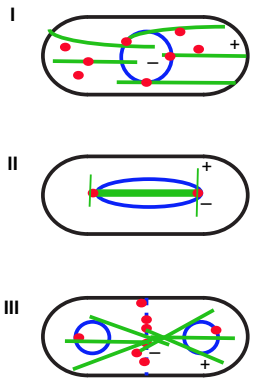

Fig. 1.3. Microtubule organization in fission yeast. (I) Interphase MTs (green) nucleated from MTOCs (red) associated with nuclear envelope (blue), cytoplasm and MTs themselves. (II) Astral MTs nucleated from SPBs on the nuclear envelope. (III) PAA nucleated form the eMTOCs. Adapted from (Sawin and Tran 2006)

1.3.2 Actin cytoskeleton in fission yeast

Actin is a highly conserved protein that is abundant in eukaryotic cells and is involved in a wide range of cellular functions such as polarized growth, cell motility, internalization and transport of vesicles and cytokinesis (Pfaendtner et al. 2010; Pollard & Cooper 2009). Actin mainly exists in two states – monomeric (globular or G) actin and filamentous (polymerized or F) actin and the two states exists in a steady state in the cell controlled by a variety of factors (Pollard et al. 2000; Pfaendtner et al. 2010). Actin monomers spontaneously polymerize into long, stable filaments in a head-to-tail fashion (Pollard 2007a). Similar to MTs, subunits are added and removed only at the ends of actin filaments. The rapidly growing end of the filament is called the barbed end (plus end), whereas the slow growing end is called the pointed end (minus end) (Pollard et al. 2000; Pollard & Cooper 2009).

Eukaryotic cells use more than 100 accessory proteins to maintain the pool of monomeric actin, initiate polymerization, restrict the length of actin filaments, regulate assembly/disassembly of filaments, and crosslink filaments into networks and bundles. Many of these proteins are highly conserved from fungi to animals (Pollard & Cooper 2009). Although several different types of proteins are involved in nucleation of actin filaments, the two main group of proteins involved are actin-related protein (Arp) 2/3 complex and formins (Pollard 2007b). Arp2/3 nucleates branched filaments, mainly responsible for forward pushing of the leading edge of motile cells and for endocytosis. Generally, Arp2/3 complex nucleates new filaments on the pre-existing actin network (Pollard 2007b; Kaksonen et al. 2003). Formins nucleate unbranched filaments, which are mainly involved in organelle transport, filopodia formation, cell adhesion and cytokinetic ring formation (Goode & Eck 2007; Wu et al. 2003; Schirenbeck et al. 2005; Kobielak et al. 2004; Coffman et al. 2013).

Unlike mammalian cells, which has 6 actin isoforms, fission yeast only has a single actin isoform and relies on three types of polymeric actin structure for growth throughout the cell cycle – actin patches, actin cables and the contractile ring (Fig.1.4) (Perrin & Ervasti 2010; Kovar et al. 2011). In this section, I first describe actin patches, followed by actin cables and cytokinetic ring. Actin patches are sites of Arp2/3-dependent polymerization of F-actin. During interphase, actin patches are concentrated at the sites of polarized growth at the cell tips and at the septum during cytokinesis. Early in the cell cycle, when the cell is growing monopolar, actin patches are localized to one end (the old end, as described above), and then in G2 phase, when the cell undergoes NETO, actin patches are localized to both ends (Marks et al. 1986; Pelham & Chang 2001). Actin patches assemble at sites of endocytosis and

are thought to be involved in endocytosis, as in budding yeast (Gachet & Hyams 2005; Kaksonen et al. 2003). In budding yeast, during endocytosis, the actin cytoskeleton is thought to be important for generating force for invagination of plasma membrane against the turgor pressure (Aghamohammadzadeh & Ayscough 2009).

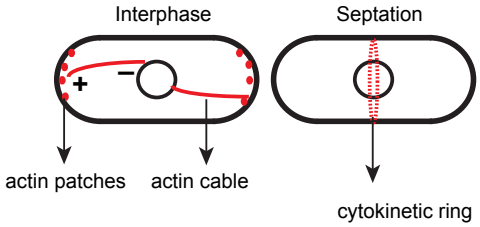

Fig. 1.4. Actin organization in fission yeast. Actin exists as three different structures in fission yeast. During interphase, actin patches are localized to the growing cell tips and are involved in endocytosis. Actin cables span the long axis of the cell and act as tracks for the transport of vesicles. During septation, actin forms cytokinetic ring, which is important for dividing mother cell into two equal daughter cells.

Nucleation of actin patches by Arp2/3 is stimulated by one of the three nucleation promoting factors, Pan1, Wsp1 and Myo1, which are thought to have distinct but overlapping functions (Toya et al. 2001; Lee et al. 2000; Sirotkin et al. 2010). Wsp1 and Myo1 arrive at the patch before internalization and recruit and activate Arp2/3 to nucleate branched actin filament followed by internalization of endocytic actin patches (Sirotkin et al. 2005). Upon internalization, actin patches undergo directed movement along actin cables (Pelham & Chang 2001). The contractile ring is responsible for the process of cytokinesis. Proper assembly of the contractile ring involves actin, myosin-II and host of other cytoskeletal and signalling proteins conserved from yeast to human (Lee et al. 2012). The nucleus determines the initial location of cytokinetic ring by releasing the Anillin-like protein Mid1 upon phosphorylation by Polo kinase Plo1 (Chang & Nurse 1996; Sohrmann et al. 1996; Paoletti & Chang 2000; Bähler, Steever, et al. 1998). Immediately before the start of mitosis, Mid1 recruits Rng2, Myo2, Cdc4, Cdc15 and formin Cdc12 to form cortical nodes (Lee et al. 2012). These nodes later condense into a cytokinetic ring through a process termed as search, capture, pull and release mechanism (SCPR) (Vavylonis et al. 2008), which depends on actin filaments nucleated by Cdc12 and myosin II Myo2 to pull the nodes together into a ring (Vavylonis et al. 2008; Lee et al. 2012). However, in *mid1*Δ cells, even though contractile rings are impaired, cells are still viable, suggesting a cortical node-independent assembly of contractile ring (Huang et al. 2008). This assembly of contractile ring is dependent on the SIN (septation initiation network) pathway (Huang et al. 2008; Lee et al. 2012).

Actin cables are polarized bundles of short parallel filaments spanning the long axis of the cell with barbed ends facing the cell tips (Pelham & Chang 2001; Mishra et al. 2013). In fission yeast, interphase actin cables are nucleated by formin For3, and *for3*Δ cells were reported to have fewer or no actin cables (Feierbach & Chang 2001; Nakano et al. 2002). The polarity proteins Tea1-Tea4, which is transported to the cell tips on the MTs, is important for recruiting For3 to the cell tips to nucleate actin filaments (Feierbach et al. 2004; Martin et al. 2005) (Discussed in section 1.5.2). Actin cables act as tracks for transport of secretory vesicles and molecules involved in cell wall synthesis and remodelling. This transport is mediated by the motor protein myosin-V and is important for polarised growth (Win et al. 2001; Martin et al. 2005; Motegi et al. 2001). For example, type-V myosin Myo52 is thought to be involved in transport of β-1, 3-glucan synthase (Bgs1), a major component of cell wall, to the cell tips and cell equator during polarized growth and septation respectively (Mulvihill et al. 2006). However, cells are still able to establish polarized growth even in the absence of actin cables (*for3*Δ cells), suggesting multiple

redundant pathways in establishment of polarized growth in fission yeast (Feierbach & Chang 2001; Nakano et al. 2002). Previously it was shown that polarized growth in fission yeast depends on both actin cable-based transport and exocytosis and polarized growth is only abolished in the absence of both pathways suggesting that these two pathways play a complementary role in regulation of polarized growth (Snaith et al. 2011; Bendezú & Martin 2011).

Fission yeast formin For3 has a Formin Homology Domain 1 (FH1), which binds to profilin-actin complex, and a Formin Homology Domain 2 (FH2), which has been shown to be necessary and sufficient for actin cable nucleation and elongation (Kovar 2006). For3 activity is inhibited by an intramolecular interaction between the Diaphanous-related formin Inhibitory Domain (DID) and the Diaphanous-related Autoinhibitory Domain (DAD). This autoinhibition is relieved by binding of Rho-GTPase Cdc42-GTP at the N-terminus and Bud6 at the C-terminus of For3 (Martin et al. 2007) (Fig.1.5). Once activated, For3 initiates rapid actin filament assembly, which is then incorporated into the actin bundle. For3 is then released making it partially inactive and occasionally remains bound to the plus end of the actin filament. Polymerization of new actin filament pushes the existing filament away from the cell tip along with the inactive For3. After disassembly of the cable, For3 may return to the cell tip by active transport or diffusion to continue the cycle (Martin & Chang 2006). However, the specific mechanisms by which For3 is activated, partially inactivated and fully inactivated are not yet fully understood.

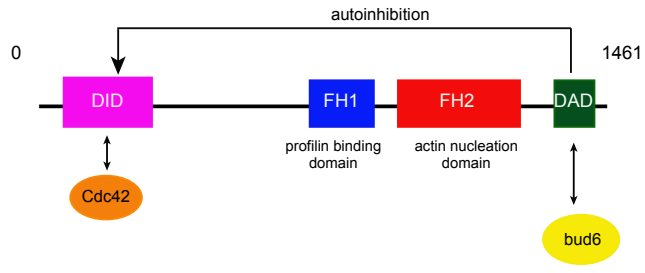

Figure 1.5. Domain architecture of For3. For3 is regulated by an autoinhibition between the C-terminal DID and N-terminal DAD domains. Binding of Bud6 and Cdc42 relieves this autoinhibition, which is important for nucleations of actin cables.

Myosins are motor proteins that bind to F-actin in an ATP-regulated manner and are involved in processes that require force and translocation (Woolner & Bement 2009; Vicente-Manzanares et al. 2009). Around 30 different classes of myosins have been identified in higher eukaryotes and some are conserved from yeast to humans (Woolner & Bement 2009). Myosin motor proteins are implicated in a wide range of cellular processes such as cytokinesis, vesicle transport, Golgi organization and signal transduction (Sweeney & Houdusse 2010).

In fission yeast, five different types of myosins belonging to three different classes have been described. The class-I myosin has a single myosin Myo1, whereas class-II and class-V myosins have two different types each - Myo2 and Myp2 (Class-II) and Myo51 and Myo52 (class-V) (East & Mulvihill 2011). As mentioned before, Myo1 together with Pan1 and Wsp1 is involved in stimulating Arp2/3-dependent polymerization of actin patches (Kovar et al. 2011). Class-II myosins Myo2 and Myp2 play important roles in facilitating the contraction of the cytokinetic ring (East & Mulvihill 2011). Class-V myosins are involved in transport of cargo along actin filaments to discrete cellular locations. Fission yeast has two class-V myosins- Myo51 and Myo52 (Win et al. 2001; Motegi et al. 2001). Myo51 is a component of the cytokinetic ring whereas, Myo52 is involved in transport of vesicles along the actin cables involved in regulation of polarized growth(Mulvihill et al. 2006). In addition, Myo52 regulates the turnover of Tip1 to promote the dynamic instability of MTs at the cell tips (Martín-García & Mulvihill 2009).

1.4 Small GTPases – key regulators of cell polarity

During polarization, cells need to amplify the signals generated by spatial cues or landmarks to reorient the cytoskeleton. These key signalling events are carried out by highly conserved small GTPases (Park & Bi 2007). An important small GTPase involved in polarization is Cdc42. Cdc42 plays a key role in organization of cytoskeleton, control of exo/endocytosis and mating (Martin et al. 2007; Bendezú & Martin 2013; Martin & Arkowitz 2014). Apart from Cdc42, a second small Rho GTPase, Rho1 is also involved in polarization and is essential for cell viability in *S.pombe* (Nakano et al. 1997). Rho1 plays an important role in activation of 1,3-beta-glucan synthase, which is a major component of cell wall and is important for maintaining cell integrity (Nakano et al. 1997). In this section, I will be focusing mainly on the Cdc42 GTPase.

1.4.1 Cdc42 – the centre of cell polarity

Cdc42 is a small GTPase of the Rho family, which plays a central role in establishing cell polarity in all eukaryotic cells (Etienne-Manneville 2004). Cdc42 is highly conserved from unicellular yeasts to multi cellular organisms. In both yeast and multicellular organisms, cells respond to different external cues to organize cell polarity. Depending on the organism or the cell type, they may include pheromones, receptor tyrosine kinases, adhesion molecules and G-protein coupled receptors. This process is controlled by localized recruitment and activation of Cdc42, which then control multiple cellular activities required for polarization (Etienne-Manneville & Hall 2002; Etienne-Manneville 2004).

Much of our current understanding of how diverse polarization signals regulate Cdc42 emerged from studies carried out in budding yeast, where Cdc42 was first discovered (Etienne-Manneville 2004; Park & Bi 2007; Johnson & Pringle 1990). In budding yeast, Cdc42 plays a central role in directional budding. Temperature sensitive mutants of Cdc42 failed to form bud at restrictive temperature and, as a consequence, cells expand isotropically (Adams et al. 1990). Similarly during mating, Cdc42 is important for correct orientation of shmooing along a gradient of secreted pheromones (Pruyne & Bretscher 2000; Etienne-Manneville & Hall 2002).

In multicellular organisms such as *C.elegans*, Cdc42, and the product of 6 PAR (partition defective) genes, and an atypical protein kinase C (PKC-3) regulate establishment of anterior/posterior axis. Inhibition of Cdc42 completely disrupts polarity and delocalizes all PAR proteins (Etienne-Manneville & Hall 2002). Cdc42 has been shown to activate WASP (Wiskott-Aldrich syndrome protein), which in turn recruits and activates the Arp2/3 complex, resulting in the formation of membrane protrusions such as filopodia (Machesky & Insall 1999; Etienne-Manneville 2004; Farhan & Hsu 2015).

Like many GTPases, Cdc42 act as a molecular switch cycling between two conformational states--an active GTP-bound state and an inactive GDP-bound state to control complex cellular processes (Etienne-Manneville & Hall 2002; Etienne-Manneville 2004). Cdc42 is membrane-associated due to cysteine prenylation of its C-terminal CAAX box (A –Aliphatic, X-any amino acid) (Park & Bi 2007; Martin 2015). Cdc42 is positively regulated by guanine nucleotide exchange factors (GEFs) and negatively by GTPase activating proteins (GAPs) and guanine nucleotide dissociation inhibitors (GDIs). GDIs can maintain Cdc42 in an inactive state by

retaining Cdc42 in the cytosol, via shielding the C-terminal domain of Cdc42 (Etienne-Manneville 2004).

In fission yeast, active Cdc42 localizes to growing end of the cells, forming dynamic patches defining the regions of active growth (Tatebe et al. 2008; Das et al. 2012). Since C-terminal and N-terminal tagging of Cdc42 compromise Cdc42 function, active Cdc42 (Cdc42-GTP) is visualized by imaging fluorescently tagged CRIB (Cdc42/Rac interactive binding), which binds specifically to Cdc42-GTP (Tatebe et al. 2008). Recently, a functional fluorescently tagged allele of Cdc42 was constructed in fission yeast (Cdc42-GFP/mCherry sw) by placing the fluorescent protein in the reading frame of Cdc42 and replacing the endogenous genomic copy (Bendezú et al. 2015). Similar to CRIB-GFP, Cdc42-GFPsw was enriched at the cell tips and division sites (Bendezú et al. 2015). In fission yeast, active Cdc42 shows anticorrelated oscillatory dynamics at the two cell tips, indicating the presence of positive and negative feedback controls (Das et al. 2012). In pre-NETO cells, these oscillations were asymmetrical, whereas in bipolar cells, oscillations were symmetrical. Using mathematical modelling, it was shown that the symmetric and asymmetric oscillations were dependent on the abundance or activity of Cdc42 or its regulators. This suggested that asymmetric oscillation (pre-NETO) might be due to decreased Cdc42-GTP or its effectors, whereas symmetric Cdc42 oscillation might be due to increased Cdc42 activation or total levels of Cdc42-GTP or effectors. Indeed *gef1*Δ cells showed lower amount of active Cdc42 and Cdc42 oscillations were asymmetric, whereas overexpression of Gef1 led to increased Cdc42-GTP symmetry (Das et al. 2012). This raises a possibility that these oscillatory dynamics of Cdc42 somehow might be regulating NETO transition (Das et al. 2012; Rincón et al. 2014)

Unlike budding yeast, which has only one GEF (Sc. Cdc24), localization and activation of Cdc42 in fission yeast is dependent on two GEFs - Scd1 and Gef1. Localization and activation of Cdc42 is also dependent on a scaffold protein, Scd2 (Bem1 in budding yeast) (Chang et al. 1994; Coll et al. 2003). During polarized growth, both Scd1 and Gef1 localize to growing cell tips. Scd1 is important for establishing polarity whereas, Gef1 is thought to promote growth at the new end (Kelly & Nurse 2011; Wei et al. 2016; Coll et al. 2003). Although *scd1*Δ*gef1*Δ mutants are lethal, single *gef1*Δ and *scd1*Δ mutants show different morphology, suggesting that these two GEFs have different but overlapping functions (Coll et al. 2003).

During cytokinesis both Gef1 and Scd1 localize to the septum. Recently Wei et al. showed that during cytokinesis, activation of Cdc42 before ring constriction is Gef1-dependent, whereas after ring constriction, Cdc42 activation is Scd1

dependent, suggesting a unique spatiotemporal activation of Cdc42 (Wei et al. 2016). To date, in fission yeast, GTP hydrolysis of Cdc42 is known to be stimulated by two GAPs, Rga4 and Rga6 (Das et al. 2007; Revilla-Guarinos et al. 2016). Rga4 localizes to the cell sides and to the non-growing ends, thereby preventing ectopic activation of Cdc42 in non-apical regions. This exclusion of Rga4 from growing tips has been shown to be dependent on Pom1 kinase (Tatebe et al. 2008; Das et al. 2007). Recently it was shown that Rga6 along with Rga4 might spatially restrict active Cdc42 at the cell tips and maintain cell morphology (Revilla-Guarinos et al. 2016).

Cdc42-GTP specifically binds CRIB domain containing proteins such as WASP, PAK (p21 activated kinases) kinases and activates these effectors to organize cell polarization (Fig.1.6) (Park & Bi 2007; Martin & Arkowitz 2014). In fission yeast, Cdc42 binds to and activates actin cable nucleator formin For3 and is also involved in localization of exocyst complex and tethering of exocytic vesicles to the plasma membrane (Martin et al. 2007; Bendezú & Martin 2011; Rincón et al. 2014). Additionally, Cdc42 binds to Shk1 and Shk2 PAK kinases. Although how Shk1 regulates polarized growth is not fully understood, Shk1 is essential for actin organization and polarized growth (Marcus et al. 1995; Ottilie et al. 1995; Rincón et al. 2014).

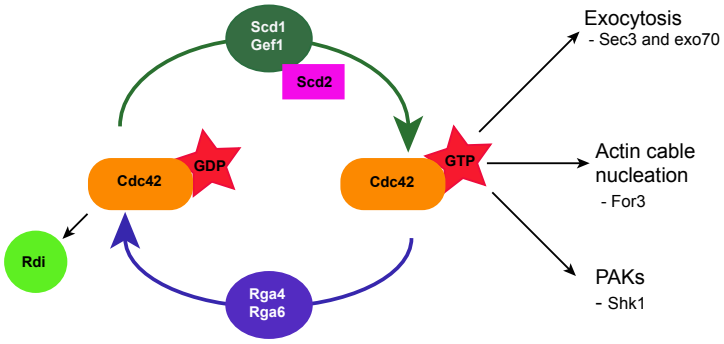

Fig. 1.6. Cdc42 plays a central role in cell polarity by regulating different processes. Schematic representation of Cdc42-GTP/GDP cycle and interactions with downstream effectors. Fission yeast has two GEFs - Scd1 and Gef1 and a scaffold protein Scd2 that are involved in activating Cdc42 to regulate exocytosis, actin cable nucleation and activation of PAK kinases. Two GAPs Rga4 and Rga6 inactivates Cdc42 along with GDI Rdi, which retains Cdc42 in the cytosol.

1.5 Spatial landmarks involved in polarity establishment

Cell polarization depends on both internal and external cues. Cells respond to different external cues such as chemical cues, mechanical forces and electric fields in order to undergo polarization. One of the extensively studied external cues are chemical gradients or chemoattractants (Graziano & Weiner 2014). The process by which a cell move towards a chemical gradient is referred to as chemotaxis (King & Insall 2009). During chemotaxis, cells respond to different chemical cues such as growth factors, yeast mating pheromones, and chemokines. In order to move towards these chemical cues the cell must read the extracellular gradient and transmit this signal inside the cell to elicit changes in cell morphology and move towards the direction of the gradient (King & Insall 2009). For example, during development of the cellular slime mold *Dictyostelium discoideum,* starving cells secrete waves of cyclic adenosine monophosphate (cAMP) that act as chemoattractant for neighbouring cells to aggregate. These aggregates subsequently differentiate into a number of different cell types, which are important for cells to disperse and find a new food supply (King & Insall 2009). This directional migration involves reorientation of the polarity machinery, to define leading and trailing edges by stabilising and forming actin-rich protrusions or lamellopedia (Petrie et al. 2009).

Cell polarization can also be achieved by internal cues such as prelocalized cortical landmarks, which organize intrinsically polar actin filaments and MTs. For example in budding yeast *Saccharomyces cerevisiae*, cells grow isotropically until they reach a particular size in G1 phase at which point they break symmetry in order to grow a bud and later undergo cell division (Slaughter et al. 2009). Different cortical spatial landmarks determine bud-site selection, which determines the axis of cell polarity and, ultimately, of cell division (Park & Bi 2007). Budding yeast cells divide in two separate spatial patterns. In haploid a and α cells, the mother cell and the daughter cell form buds immediately adjacent to the previous site of cell division, whereas in diploid a/α cells, the mother cell and the daughter cell form buds from the proximal or distal poles relative to the previous cell division site (Chant 1999; Park & Bi 2007). The haploid, axial pattern is dependent on Bud3, Bud4, Axl1 and Axl2 landmark proteins, whereas the diploid, bipolar budding pattern is dependent on Bud8, Bud9, Rax2 and Rax1 landmarks. These landmarks recruit the Ras-like protein Rsr1 that cycles between active and inactive state to promote the local activation and recruitment of the small-GTPase Cdc42, a key regulator of cell polarity. Rsr1, its GEF Bud5 and its GAP Bud2 are required for both axial and bipolar

budding patterns. All the three proteins localize to the incipient bud site and are important for correct budding pattern (Park & Bi 2007; Martin & Arkowitz 2014).

In fission yeast, MTs play an important role in positioning the cortical landmarks involved in regulation of polarized growth (Sawin & Nurse 1998; Behrens & Nurse 2002). Polarity proteins Tea1 and Tea4 are transported on the plus end of the dynamic MTs to reach the cell tips, leading to actin cable assembly in order to promote directed cell growth (Martin et al. 2005; Tatebe et al. 2005; Mata & Nurse 1997). In this way accurate positioning of spatial cues is thought to link the MT and actin cytoskeleton to regulate polarized growth (Chang & Martin 2009).

1.5.1 Tea1 an important regulator of polarity in fission yeast

In fission yeast, a key polarity protein involved in regulation of polarized growth is Tea1. Tea1 (Tip elongation aberrant) is an 1147 amino-acid protein with six N-terminal kelch repeats and a largely alpha-helical coiled-coiled C-terminus (Mata & Nurse 1997). Tea1 was initially identified in a screen for cell shape defect mutants (Snell & Nurse 1994). Under various stress conditions such as heat stress *tea1*Δ mutants fail to grow from the cell tips and instead grow from ectopic sites, producing bent or T-shaped cells (Verde et al. 1995; Mata & Nurse 1997). Moreover, *tea1*Δ mutants fail to establish bipolar growth and strictly grow in a monopolar fashion (Mata & Nurse 1997; Verde et al. 1995). During interphase, Tea1 is localized to the cell tips and is also present on the MTs and during septation Tea1 is present at the cell septum along with tip localization (Mata & Nurse 1997).

Tea1 is transported on the plus end of the MTs along with microtubule-associated proteins Tea2 (Kip2 homolog), Mal3 (EB1 homolog) and TIP1 (CLIP-170 homolog) to reach the cell tips (Brunner & Nurse 2000; Busch et al. 2004; Browning et al. 2003). Tea2 and Tip1 interact with each other and move along the plus end of the MTs. This localization of both Tip1 and Tea2 to the growing MT is dependent on Mal3 (Busch et al. 2004; Busch & Brunner 2004; Browning et al. 2003). Mal3 localizes to the growing ends of MTs and the MT lattice and is involved in initiation and maintenance of MT growth by providing a binding site for +TIP proteins (Busch & Brunner 2004; Sandblad et al. 2006). In this way Tip1, Tea2 and Mal3 are required for proper cytoplasmic MT organization, which in turn helps in accurate delivery of Tea1 to the cell tips. Mutants of *tip1*, *mal3* and *tea2* have shorter MTs and hence

cannot deliver Tea1 to the cell tips resulting in bent or branched cells (Behrens & Nurse 2002; Browning et al. 2003; Busch & Brunner 2004).

Apart from being transported on MTs, Tea1 might have some role in regulating dynamics of MTs. In the absence of Tea1, some cells show defects in MT organization where MTs curl around at the cell tips (Mata & Nurse 1997; Behrens & Nurse 2002; Snaith & Sawin 2003). Moreover, cells in which Tea1 is overexpressed have shorter MTs (Mata & Nurse 1997). This role of Tea1 in MT organization seems to independent of Tea1's role in cell polarity. This is based on the evidence that in *tea1Δ200* cells, which lack the Tea1 C-terminal coiled-coil region, Tea1 fails to accumulate at cell tips, and tip growth is affected. However, *tea1Δ200* continue to bind MTs and did not affect MT dynamics. This suggests that Tea1 retention at cell tips, which is important for its role in cell polarity is not important for Tea1's role in MT organization (Behrens & Nurse 2002).

Once at the cell tips, Tea1 is released from the MT ends and is anchored at the cell tips with the help of a prenylated membrane protein Mod5 (Snaith & Sawin 2003). In *mod5Δ* cells, Tea1 is delivered to the cell tips at the same rate as wild type cells but is not anchored properly at the cell tips (Snaith & Sawin 2003). Interestingly, in *tea1Δ* cells, Mod5, which is normally localized to cell tips, is no longer restricted to cell tips and instead is present all over the plasma membrane. Based on this interdependent localization of Tea1 and Mod5 to the cell tips, it was proposed that Tea1 and Mod5 might be involved in a positive feedback loop to regulate cell polarity (Snaith & Sawin 2003). Tea1 and Mod5 exhibit different dynamics at cell tips and Mod5 act as a catalyst and helps in the incorporation of Tea1 into a polymeric cluster network. Thus interaction between Tea1 and Mod5 maintains a stable polarity landmark that is robust to fluctuations in MT dynamics by ensuring that only Tea1 delivered to the centre of cell tips gets incorporated into the network and reinforces the polarity, whereas Tea1 delivered farther away from the centre will be recycled back to the cytoplasm (Bicho et al. 2010).

1.5.2 Tea4 acts as link between actin and MT cytoskeleton to regulate cell polarity

Similar to Tea1, the SH3-domain protein Tea4 is also transported on the plus end of MTs to reach the cell tips and is required for establishment of bipolar growth (Martin et al. 2005; Tatebe et al. 2005). Tea4 binds directly to Tea1 *in vitro* and the C-terminal half of Tea1 was necessary and sufficient to bind Tea4 (Martin et al.

2005). Tea4 and Tea1 colocalize on MT plus ends and at cell tips. Moreover, Tea4 localization at the cell tip is dependent on same proteins involved in localization of Tea1, such as Mod5, Tip1 and Tea2, as well as Tea1 itself (Martin et al. 2005). Tea4 also interacts with Win1 MAPKKK of the stress-activated MAP kinase cascade. Consistent with this, *tea4*Δ cells and *tea1*Δ cells show more severe polarity defects under stresses that activate the MAP kinase pathway (Tatebe et al. 2005).

Once the Tea1-Tea4 complex reaches the cell tip on the plus end of the MTs, Tea4 is thought to recruit actin cable-nucleating protein For3 to the cell tips (Martin et al. 2005). At the cell tips, For3 interacts with Bud6 and Cdc42 to relieve its auto-inhibition and nucleate actin cables (Martin et al. 2007). These actin cables act as a track for myosin-V -mediated transport of secretory vesicles and molecules involved in cell wall synthesis and remodelling (Motegi et al. 2001; Mulvihill et al. 2006). In this way, Tea1-Tea4 can act as a link between MT and actin cytoskeleton to achieve polarized growth (Fig.1.7). Indeed, in *tea4*Δ cells, MT-based polarity proteins such as Tea1, Tea3 and Mod5 are localized to the non-growing end, whereas actin, For3, and Myo52 are localized to the growing end, suggesting that Tea4 might be acting as a link between MT and actin network (Martin et al. 2005).

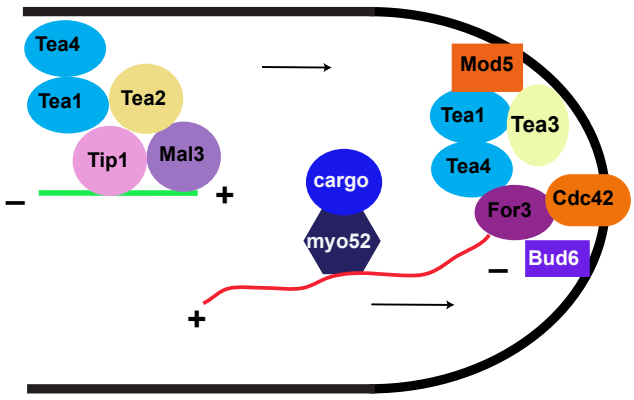

Fig. 1.7. Tea1-Tea4 act as a link between microtubule and actin cytoskeleton to regulate polarized growth. Tea1-Tea4 is transported on the plus end of the MTs to reach the cell tip with the help of MT-associated proteins Tip1, kinesin Tea2 and EB1 homolog Mal3. At the cell tips, Tea1-Tea1 is anchored to the cell tips by prenylated protein Mod5 and Tea3. Tea4 recruits actin cable nucleating protein For3 to the cell tips where it relieves auto-inhibition by binding to Bud6 and Cdc42 and nucleate actin cables. These cables provide a track for MyoV-based transport of secretory vesicles and cell wall synthases. In this way Tea1-Tea4 act as a link between MT and actin network.

It is important to note that this is a rather simplified model, because Tea1/Tea4-independent recruitment of For3 to the cell tips exists. For3 is still localized to one of the old end in both *tea1*Δ and *tea4*Δ cells suggesting Tea1/Tea4 independent For3 recruitment (Feierbach et al. 2004; Martin et al. 2005). Similarly, Tea1/Tea4 independent recruitment of For3 was also shown by using micro-fabricated chambers to bend the cells. In these bent cells, MTs were contacting the cell sides and were able to recruit polarity proteins such as For3, Cdc42 and Bud6 independent of Tea1/Tea4 pathway, but rather was dependent on Mal3 (Tip1 homolog), Moe1 (Mal3 interactor) and Scd1 (Cdc42 GEF). However, these ectopic sites failed to show any cell growth (Minc et al. 2009; Terenna et al. 2008). Moreover, recently it was shown that ectopic targeting of Tea4 to the cell sides promotes the local activation of Cdc42. This activation is dependent on type 1 phosphatase (PP1) Dis2, Gef1 recruitment (Cdc42 GEF) and Rga4 exclusion (CdC42 GAP) at the ectopic sites (Kokkoris et al. 2014). However, even though ectopically localized Tea4 was able to recruit and activate Cdc42 to the cell sides, these ectopic sites failed to show proper growth suggesting that there might be additional factors required to initiate growth.

1.5.3 Tea1/Tea4 binding partners at the cell tips

Tea1/Tea4 transported on the plus end of the MTs interact with a large number of experimentally characterized proteins (Martin 2009). Indeed, Tea1 is present in several complexes in 12S, 25S, 40S and 75S in sucrose gradients (Feierbach et al. 2004). Tea1/Tea4 complex is necessary for the localization of dual-specificity tyrosine phosphorylation-regulated kinase Pom1, which forms gradients from the cell tips (Tatebe et al. 2005; Padte et al. 2006; Bähler & Pringle 1998). *tea1*Δ, *tea4*Δ and *pom1*Δ cells share similar monopolar growth phenotype and grow from ectopic sites after various stresses (Niccoli et al. 2003; Martin 2009). The Tea1-Tea4 complex and Pom1 gradient have also been shown to prevent assembly of the division septum at cell tips (Huang et al. 2007). Recently it was shown that Pom1 directly phosphorylates F-BAR protein Cdc15, a key component of cytokinetic ring and this regulation is important to inhibit septum formation at the cell tips (Ullal et al. 2015).

Apart from Pom1's role in providing positional information for polarized growth and septum formation, Pom1 is also thought to act as a cell size ruler and regulate

mitotic entry through the Cdr2-Cdr1-Wee1 pathway (Moseley et al. 2009; Martin & Berthelot-Grosjean 2009). Pom1 associates with the plasma membrane by Tea4-dependent dephosphorylation of Pom1 through the protein phosphatase 1 Dis2. Pom1 forms a polar gradient through the cell cortex shaped by lateral diffusion and auto-phosphorylation-dependent detachment (Hachet et al. 2011). However, Pom1 gradients showed large cell-to-cell variability and fluctuations suggesting that changes in Pom1 gradient according to cell length may be less consistent (Saunders et al. 2012; Wood & Nurse 2015). Moreover, *pom1*Δ cells show cell size homeostasis suggesting that cells might employ an additional mechanism to sense the cell length (Wood & Nurse 2013). Recently an alternative model has been proposed where cells sense their surface area as opposed to cell length as a part of cell size mechanism (Pan et al. 2014). In this model, Cdr2, a peripheral membrane protein kinase use levels of Cdr2 to sense the size (surface area) of the cell instead of the cell length. When cells reach a critical size, Cdr2 which is localized to the cell sides accumulate to a particular concentration which might trigger start of cell division (Pan et al. 2014).

Apart from Tea1 and Tea4, another polarity protein Tea3 is also transported on the MT plus ends to the cell tip (Arellano et al. 2002). Tea3 shares 21% identity (45% similarity) and share similar domain structure with Tea1 (Arellano et al. 2002) Similar to *tea1*Δ and *tea4*Δ mutants, *tea3*Δ cells also failed to establish bipolar growth suggesting a role for Tea3 in polarized cell growth (Arellano et al. 2002). Tea3 interacts with Tea1 and Mod5 independently of the other protein, and different regions of Tea1 and Tea3 are required for their interaction with a central region of Mod5 (Snaith et al. 2005). Similar to Mod5, Tea3 is also important for cortical localization of Tea1, specifically at the non-growing cell tip and localization of Tea3 is dependent on Tea1 and Mod5 (Snaith et al. 2005).

1.6 Symmetry breaking: Spontaneous self-polarization of Cdc42

Symmetry breaking in biology is defined as transformation of an initially homogenous distribution into a more structured and polarized state (Li & Bowerman 2010). This phenomenon of self polarization is particularly evident at the cellular level, to polarize in the absence of any internal or external cues (Martin 2015). In the past, the study of how cells establish polarity was mainly focused on different external and internal cues. However, different experimental and modelling work began to focus on the intrinsic ability of cells to break symmetry without any cues

(Wedlich-Soldner & Li 2003). For example, chemotactic cells such as neutrophils and *Dictyosetelium* normally orient and grow towards a gradient of chemical cues. However, if cells are exposed to a uniform chemical gradient, surprisingly, cells are still able to polarize and initiate motility, albeit in random directions (King & Insall 2009; Graziano & Weiner 2014). Similarly, in budding yeast as mentioned before, a key player in bud-site selection is small GTPase Rsr1. However, cells are still able to polarize in the absence of Rsr1, albeit randomly. More surprisingly, simply expressing a constitutive active Cdc42 in a non-polarized G1-arrested cells resulted in random polarization (Wedlich-Soldner & Li 2003; Chant & Herskowitz 1991).

Ground breaking work carried out in budding yeast has greatly improved our understanding of how cells spontaneously self polarize. Different mechanisms have been proposed for spontaneous polarization of Cdc42 in budding yeast. In the first mechanism, a stable Cdc42 axis is generated by a positive feedback loop in which a stochastic increase in local concentration of activated Cdc42 at the plasma membrane enhances actin polymerization, which further reinforces the transport of Cdc42 to the growth axis, via actin filaments (Wedlich-Soldner & Li 2003; Marco et al. 2007). The second mechanism is dependent on the Cdc42 scaffold protein Bem1. In this mechanism, Bem1 recruits Cdc24, the only guanine nucleotide exchange factor (GEF) of Cdc42, and promotes local activation of Cdc42. Stochastic increase in local concentration of activated Cdc42 recruits more Bem1 and Cdc24 and promotes a positive feedback loop, which further reinforce the Cdc42 cluster (Howell et al. 2009; Kozubowski et al. 2008; Goryachev & Pokhilko 2008; Irazoqui et al. 2003). In these different mechanisms, positive feedback loops generate polarized growth triggered by stochastic fluctuations. Even though such stochastic fluctuations occur at multiple sites, an important question is why budding yeast cells only have one “front”. The formation of a single front in these cells might be due to competition for polarity factors (Goryachev & Pokhilko 2008; Howell et al. 2009). Indeed, by experimentally manipulating the exchange of polarity proteins Bem1 and Cdc24 between the membrane and interior of the cell, they were able to create and maintain multiple polarity clusters or “fronts” in these cells (Wu et al. 2015). Recently, Bendezu *et al.* showed that in fission yeast, the local accumulation of active Cdc42 by positive feedback loops might be independent of two Cdc42 recycling routes – actin cable-mediated transport of vesicles and exchange between cytoplasm and membrane by GDI-mediated extraction (Bendezú et al. 2015).

Project aims

The main aim of my PhD was to understand how multiple internal cues or landmarks regulate polarized growth in fission yeast. In order to achieve this, in chapter 3, I first set out to optimize a live-cell imaging module in fission yeast, which is physiological and optimal for long-term imaging without inducing any stress. In chapter 5, using this optimized live-cell imaging, yeast genetics and drug perturbations, I aim to understand what are the different internal cues involved in establishment of polarized growth in fission yeast and how these internal cues are regulated. Further, in chapter 6, I investigate how a growth memory-based cue independent of cytoskeleton is involved in establishment of polarized growth and how this cue is regulated.

Finally, in chapter 4, I focus on investigating a new role for actin cables in nuclear movement in fission yeast, which was earlier thought to be exclusively MT-dependent and to understand what other molecular players are involved in this actin-cable based movement.

Chapter 2: Materials and Methods

2.1 Growing fission Yeast stains

Fission yeast strains were grown in rich yeast extract medium (YE5S) or Edinburgh minimal medium (EMM). The composition of YE5S and EMM are as follows:

YE5S : 0.5% (w/v) Difco Yeast Extract, 3.0% (w/v) glucose, 250mg/L each of adenine, histidine, leucine, lysine, hydrochloride and uracil.
EMM : 14.7 mM potassium hydrogen phthalate, 15.5 mM Na2HPO4, 2% glucose, 1X salts (50X salt solution : 52.5 g/L MgCl2.6H2O, 0.735 mg/L CaCl2.2H20, 50g/L KCl, 2g/L Na2SO4), 1X vitamins (1000X vitamin stock: 1g/L pantothenic acid, 10g/L nicotinic acid, 10mg/L biotin), 1X minerals (10000X mineral stock: 5g/L boric acid, 4g/L MnSO4, 4g/L ZnSO4.7H2O, 2g/L FeCl2.6H2O, 0.4 g/L CuSO4.5H2O, 10g/L citric acid), and 2.2 g/L NH4Cl or 3.75 g/L L-glutamic acid monosodium salt. Amino acid supplements are added as required (200mg/L).

2% Difco agar was added for growth on solid plates. For selection, G418 (Geneticin), norseothricin (CloNat), and hygromycin were added at 100µg/ml. For checking dead and diploid cells, replica-plating (RP) to YE5S + 5mg/L Phloxin B was used. Dead/diploid cells take up Phloxin B more readily than living/haploid cells and give a dark pink staining.

2.2 Genetic crosses

Mating of fission yeast was carried out on SPA plates [2% Difco Bactor agar, 30 g/L glucose, 5g/L KH2PO4, amino acid supplements and 1X vitamins (as for EMM)]. h+ and h- strains to be mated were streaked onto SPA plates and mixed using a small volume of distilled water (10 µl). The plates were incubated at 25ºC or 28ºC for 3X or 2X overnight respectively to form asci. Asci were streaked onto YE5S plates and incubated at 32˚C for 1 hr. This helps to break the ascus wall making it easier to do tetrad dissection. A Singer dissector was used to separate tetrads from a single cross and the plates placed at a suitable temperature to allow the spores to germinate (32˚C for non-temperature sensitive strains and 25˚C for temperature-sensitive strains). Once colonies appear, the donor plate was replica plated onto subsequent selection plates to select for desired genotype.

Random spore analysis was carried out to isolate spores. A small patch of crossed strain was dissolved in 300 µl of distilled water to which 9 µl of helicase (*Helix Pomatia* juice, Life technologies) were added. The mixture was incubated at 32ºC for 4-5 hours to digest the ascus and vegetative cell walls. The samples were sonicated to separate spores and the number of spores was counted using a haemocytometer. Spores were plated in YE5S plates to get a final density of 200 spores per plate.

2.3 PCR based strain construction

C-terminal tagging and deletion of fission yeast genes were carried out using the PCR based method described by Bahler *et al.* (Bähler, Wu, et al. 1998). The 5' ends of the forward and reverse primers have approximately 80 nucleotide sequence homology to the genomic sequence of interest and the 3' ends of the primers have 20-24 bases of sequence homology to tagging cassettes. Plasmids containing antibiotic resistance (G418, hygromycin, nourseothricin) or mEcitrine, mCherry, 3xmEcitrine, 3xmCherry or *ura4+* were used as templates for the PCR. PCR amplification of the plasmid was carried out using a MJ research Thermal Cycler. The PCR reactions were carried out using Phusion High-Fidelity DNA polymerase (Thermo Scientific). The following reaction and cycling conditions were used.

PCR using Phusion polymerase

Component	***Concentration***
HF buffer	1X
Forward primer	0.2µM
Reverse primer	0.2µM
Template DNA	20ng/50µl
dNTPs (dATP,dTTP,dGTP,dCTP)	500 µM each
Phusion polymerase	0.02 U/µl

Cycling conditions:

1. 98ºC 30 sec
2. 98ºC 15 sec
3. 60ºC 30 sec
4. 72ºC 4 min
5. Repeat steps 2-4 for 30-35 cycles

6. 72ºC 10 min
7. 20ºC hold

2.4 Transformation of PCR product into yeast cells

Approximately 20-30 µg of DNA was used for each transformation. Before transformation, PCR amplified DNA was cleaned using phenol/chloroform/isoamyl alcohol (PCI) extraction. An equal volume of PCI was added to amplified DNA, vortexed and spun at 13000 RPM for 5 minutes in a microfuge. The supernatant was collected and transferred to a fresh tube. PCI extraction was then repeated and supernatant collected again. Chloroform was added to the DNA, and samples were then vortexed and spun for 5 minutes. The supernatant was recovered to which NaOAc (pH 5.2) was added to a final concentration of 0.3M, followed by 2 volumes of ethanol. Samples were mixed and incubated at RT for 10 minutes, followed by cold spin for 10 min in a microfuge at 4ºC. Supernatant was removed and DNA pellets were then washed with 70% ethanol, dried, and resuspended in 50µl of TE buffer. DNA recovery was verified by running a small sample of PCI cleaned product on a 1% agarose gel and comparing to known amount of DNA.

PCI cleaned DNA was used for transformation into parent fission yeast strain. Cells were grown overnight in YE5S media at 30ºC to an O.D of around 0.8. 20 mL of cells were spun at 4000 RPM for 5 minutes, washed with an equal volume of dH2O, spun again. The cells were then washed with I mL of 0.1M LiOAc (pH 7.5) and spun at 13000 RPM for 1 min. Cells were then resuspended again with 0.1M LiOAC/TE to a final volume of 100 µl. Approximately 20-30 µg of PCI- cleaned DNA was added to this and incubated at room temperature (RT) for 10 minutes. 260 µl of freshly prepared 40% PEG in LiOAc/TE was then added with gentle mixing and incubated at 32ºC for 45 minutes. 43 µl of DMSO was added followed by a heat shock at 45ºC for 5 minutes. Cells were then washed with 1 mL of dH2O, plated onto 2 YE5S plates and incubated at 32ºC. One day later, plates were replica plated to appropriate antibiotic containing plates and incubated at 32ºC for 2 days. Colonies were picked and streaked onto sectors of YE5S plates and incubated at 32ºC so that individual cells could form colonies under non-selective conditions. These plates were then replica plated onto drug plates to identify stable integrants. Only those plates in which all the colonies were able to grow on drug plates were selected. Stable colonies were then checked for c-terminal tagging or gene deletion using colony PCR and fluorescence microscopy.

2.5 Colony PCR

Colony PCR was carried out to confirm that cassetes are integrated at the right place in the genome during gene deletions, C-terminal tagging of proteins and also to prepare genomic DNA for sequencing. To confirm gene deletions and C-terminal protein tagging, oligos are designed in such a way that the forward primer has homology to the resistance gene in the casette and the reverse primer has homology to the 3' untranslated region (UTR) of the gene of interest (deletion or C-terminal tagging). DNA was always prepared from fresh patch of cells (1 day old) and a pin-head amount of cells were collected using sterile tips and resuspended in 25µl of 0.25% SDS/TE. Cells were then boiled for 5 min and centrifuged to remove the cell debris and supernatant containing DNA was collected. DNA was amplified using a combination of Pwo and homemade Taq (HMT) polymerases. The following PCR rection and cycling conditions were followed.

PCR using HMT/Pwo polymerase:

Component	*Concentration*
Buffer IV	1X
Forward primer	0.2µM
Reverse primer	0.2µM
Template DNA	1ng/µl
dNTPs (dATP,dTTP,dGTP,dCTP)	500 µM each
MgCl2	3.5mM
HMT polymerase	0.2U/µl
Pwo polymerase	0.003U/µl

Cycling conditions:

1. 95ºC 2 min
2. 95ºC 15 sec
3. 50-70 ºC 30 sec
4. 72ºC 6 min
5. Repeat steps 2-4 for 30 cycles
6. 72ºC 5 min
7. 20ºC hold

2.6 DNA sequencing

DNA sequencing was carried out to confirm certain fission yeast mutations. In order to do this, the region carrying the mutation was amplified using the cPCR protocol described above (see section 2.5). The PCR product was then gel-purified and used as a template for sequencing reaction. For sequencing of plasmids, plasmid DNA was directly used for amplification. The sequencing reaction contained 100-250ng of DNA, 0.5μM primer, 2μl BigDye terminator mix v3.1 (Applied Biosystems), 2μl 5X sequencing buffer (Applied Biosystems) in a final volume of 10μl. The following cycling condition was used:

1. 96°C for 30 sec
2. 50°C for 15 sec
3. 60°C for 4 min
4. Steps 1-3 for 25 cycles
5. 4°C hold

Sequencing sample was sent to University of Edinburgh sequencing facility, using ABI 3730 capillary sequencing instruments (Applied Biosystems). Analysis was carried out using Seqman sequence analysis software (DNASTAR Inc).

2.7 Sample preparation for imaging

Cells were imaged in both EMM and YE5S media. A liquid culture was made from a fresh patch of cells and grown at 25ºC O/N. Cells were then grown to get an OD_{595} between 0.3-0.8. Sample preparation was carried out on 35mm MatTek dishes (MatTek Corp, USA) or 4-chamber glass bottom micro-slides (Ibidi; 80427). 4-chamber glass bottom micro-slides were only used for imaging cells in YE5S media because imaging cells in EMM in 4-chamber slide seems to affect polarized cell growth. Both MatTek dish and 4-chamber glass bottom micro-slides were coated with 20μl or 7μl of 1mg/mL of soybean lectin (SigmaAldrich) respectively, air dried for 10 minutes and rinsed with deionized water. Approximately 400-600 μl or 100-200μl of cells were added to the MatTek dish and 4-chamber dish depending on the O.D and allowed to settle down for 25 minutes at 25ºC. In the case of some mutants with morphology defects, cells were allowed to settle down for a longer time (~30 minutes) to get more cells sticking to the lectin. Excess cells were washed with pre-

warmed YE5S (25˚C) or “conditioned” pre-warmed EMM. “Conditioned” EMM media was prepared by growing a large volume of culture (of the same cells as being imaged) to mid-log phase density, centrifuging the culture, and recovering the supernatant. After washing out the excess cells, 400 µl or 100 of conditioned EMM/YE5S was added to the MatTek dish or 4-chamber and transferred immediately to the temperature controlled microscope chamber for imaging.

2.8 Microscopy

Depending on the experiments, three different microscopes were used in this study. All the experiments showed in chapter 5 and chapter 6 were carried out on a customized spinning-disc confocal microscope and all the experiments from chapter 4 were carried out on a Deltavision Elite system unless otherwise stated. All the figure legends were denoted with the corresponding microscope used for image acquisition.

Spinning-disc confocal microscope

Spinning-disc confocal microscopes are routinely used for high-speed, live-cell imaging of fluorescently labeled cells. Unlike point scanning confocal microscope, which scans the sample pixel by pixel, spinning-disc confocal microscope uses an array of pinholes to simultaneously excite the sample and hence can achieve faster acquisition with lower phototoxicity and photobleaching. Moreover, unlike conventional wide-field fluorescence microscope, spinning-disc confocal microscope uses a pinhole to remove out of focus light, thereby improving the spatial resolution.

In this study, I used a customized spinning-disc confocal microscope setup made up of a Nikon TE2000 inverted microscope equipped with a 100x/1.45 NA Plan Apo oil objective (Nikon) and an MS-2000 automated stage with CRISP autofocus (ASI), which enabled multipoint imaging with autofocusing. The spinning-disc unit used is a Yokogawa CSU-10 unit (Visitech), which is placed between the microscope and the EMCCD camera. The Yokogawa spinning disc is made up of a collector disc with an array of microlenses and a pinhole disc with pinholes corresponding to each microlens placed axially at the focal plane of each microlens. Spinning disc confocal microscope uses a wider beam of light to illuminate the sample, which passes through the array of microlenses placed on the collector disc and focuses the light to

pass through the pinhole and illuminates the sample. The resulting emission wavelength is reflected by dichroic mirror placed between the two discs and is collected by an EMCCD camera (Fig 2.1). For imaging of CRIB-3xmCitrine, a 514/594 dichroic mirror was typically used to collect signal and for imaging of GFP-tagged proteins, a 488/594 dichroic mirror was used (Chroma Technology Corp., Vermot, USA). The fluorescence signal was collected using an iXon+ Du888 EMCCD camera with a pixel size of 1024X1024 and with a maximum readout rate of 30 MHz and chilled to -90˚C (Andor Technology, UK). EMCCD camera (90% efficiency) was used because of its higher quantum efficiency compared to a photomultiplier tube (PMT) detector (30-40%)The microscope was also equipped with an Optospin IV filter wheel (Cairn Research, UK), which can be controlled using the metamorph software to use appropriate filter set. Multi-line laser bank (Cairn Research, UK) with 488nm, 514nm, 561nm and 594nm laser lines were used for illumination and were controlled using Metamorph software. Additionally an OptoLED Lite (Cairn Research, UK) was used for brightfield imaging. Imaging temperature was maintained at 25˚C using a temperature-controlled chamber (OKOlab, Italy). The microscope was controlled using Metamorph software, which can control laser lines, filter wheels and also all other imaging parameters (Molecular Devices, USA).

All the fluorescence live-cell imaging carried out in chapter 4 (except where stated) was carried out on DeltaVision Elite system with a solid-state illumination, UltimateFocus™, and environmental stage (Applied Precision). Imaging was performed using a 100X/1.40 UPLS Apo oil objective and acquired using a Cascade EMCCD camera (photometrics). All the imaging was carried out at 25ºC using a temperature-controlled chamber.

Autofluorescence and photo-bleaching experiments were performed using a Leica SP5 laser scanning confocal microscope. Imaging was performed with an inverted Leica microscope with a 100X/1.4 PL Apo oil objective. The fluorescence emission was collected using hybrid detectors with different bandwidths as required.

Microscope	**Strain**	**Laser power/exposure**	**Media**	**Z**
Spinning disc confocal	CRIB-3xmCitrine	514 -2% 100ms	C-SGALU	11Zs, 0.6µm 2X2 bin
	CRIB-3xmcitrine	514 -2% 50ms	YE5S	11Zs, 0.µm 2X2 bin
	LifeAct-mCherry	594 -30%100ms	YE5S/C-SGALU	11Zs, 0.6µm 2X2 bin

	Rax2-3xmCitrine	514-2% 500ms	C-SGALU	4Zs, 0.6µm 4X4 bin
	Bgs4-Cherry	594-30% 100ms	C-SGALU	11Zs, 0.6µm 2X2 bin
	Tea1-GFP	488-30% 100ms	C-SGALU	11Zs, 0.6µm 2X2 bin
	Tea1-mEcitrine/3xmCitrine	514- 2% 100ms	C-SGALU	11Zs, 0.6µm 2X2 bin
	Tea1mCherry/3xmCherry	594 – 30% 100ms	C-SGALU	11Zs, 0.6µm 2X2 bin
Deltavision	CRIB-3xmCitrine	514- 2% 100ms	C-SGALU	9Zs, 0.µm 2X2 bin
Leica SP5	LifeAct-mCherry	561- 5%	C-SGALU	11Zs, 0.59µm

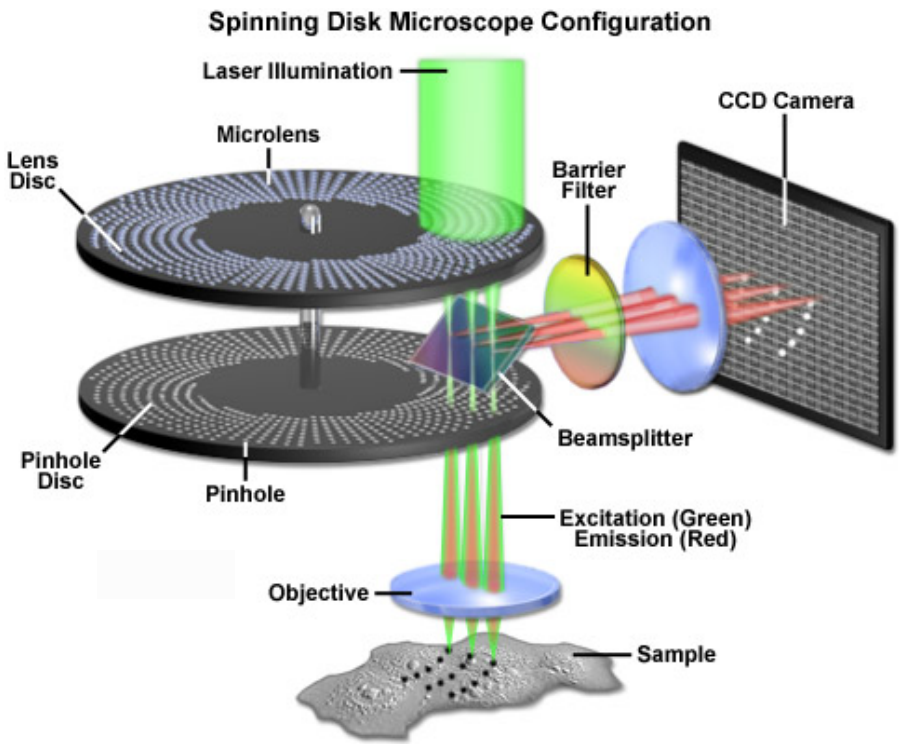

Figure 2.1 Light path of Spinning disc confocal microscope. Spinning disc confocal microscope uses a wide beam of laser light to illuminate the sample. The laser light passes through the Yokagawa spinning disc unit placed between the microscope and the EMCCD camera. The illuminating laser light passes through an array of microlenses, which focuses the light to pass through a pinhole to remove out of focus light and the illuminate the sample. The emitted light passes back and is selected using a dichroic mirror placed between the two lenses and the desired wavelngth is collected by the EMCCD camera. Figure adapted from Andor

2.9 FRAP experiments

FRAP experiments were carried out on the spinning-disc confocal system as described above (see section 2.8). The FRAP module on the spinning-disc confocal microscope used an ILAS2 targeted laser illumination for real-time control of laser illumination (Cairn Research, UK). A 473nm laser line was used for performing FRAP. Laser line and imaging parameters were controlled using the Metamorph software. Typically, cell tips were bleached with a 473nm laser for 350ms. During pre-bleach, two images with 5 sec time interval were captured. Post-bleach images were captured every 10 minutes for 1 hour. Recovery curves were calculated manually using ImageJ.

2.10 Drug perturbations

Depolymerization of microtubules was carried using Methyl benzimidazol-2yl carbamate (Carbandezim, MBC). Media containing 25µg/ml MBC and 1% DMSO (all final concentration) was added to cells to depolymerize microtubules. Control cells were imaged in media containing 1% DMSO.

Depolymerization of actin was carried out by adding media containing 50µm LatrunculinA (LatA) and 1% DMSO (all final concentration). Control cells were imaged in 1% media containing DMSO. During LatA washout experiments, LatA was removed by removing the LatA containing media and adding fresh media using 1 ml Pasteur pipettes. Washing out was carried out 18 times to get maximum LatA wash out.

2.11 Image analysis

Analysis of raw images aquired was carried out using Metamorph (Molecular Devices) and ImageJ (NIH). All the movies are processed by taking either sum, or maximum projection of all the Z planes. Kymographs were plotted using multiplekymograph plugin of imageJ. Different parameters such as cell length, intensity etc. were calculated using analyze function of imageJ.

2.12 List of strains and oligos used in this study

Strain no	Genotype	Source
Ks 136	h- tea1Δ::ura4+ ade6-M210 ura4-D18	Sawin lab
KS 390	pom1Δ::ura4+ ura4-D18 h-	Sawin lab
KS 423	pom1Δ::ura4+ tea1Δ::ura4+ ura4-D18 h+ (2B2)	Sawin lab
KS 515	ade6-M216 ura4-D18 leu1-32 h+	Sawin lab
KS 516	ade6-M210 ura4-D18 leu1-32 h-	Sawin lab
KS 953	h+ for3Δ::kanMX ura4-D18 leu1-32 ade6-M216	Sawin lab
KS 2136	h- for3YFP::kanMX6 leu1-32 ura4-D18 ade6	Sawin lab
KS 2324	h+ myo51Δ::ura4+ ade6-M216 leu1-32 ura4-D18	Sawin lab
KS 2325	h- myo52Δ::ura4+ ade6-M216 leu1-32 ura4-D18	Sawin lab
KS 2654	h- tea3Δ::natMX6 ade6-M216 leu1-32 ura4-D18	Sawin lab
Ks 3137	h-tea1-mCherry:natMX6 ade6-210 leu1-32 ura4-D18	Sawin lab
KS 4152	h- tea4Δ ::hphMX6 ura4-D18 leu1-32 ade6-M210	Sawin lab
KS 4410	h+ myp2Δ::kanMx ade6-216 leu1-32 ura4-D18	Sawin lab
KS 5110	h+ mto1-427 ade6-216 leu1-32 ura4-D18	Sawin lab
KS 6666	Z:ADH15:mCherry-Atb2:natMX6 tea1-GFP:kanMX6 ade6 ura4-D18 leu1-32 h+	Sawin lab
KS 6696	leu1-32[pAct1-lifeact-mCherry-leu1+] ade6-M216 ura4-D18 h+	Sawin lab
KS 6697	leu1-32[pAct1-lifeact-mCherry-leu1+] ade6-M216 ura4-D18 h-	Sawin lab
KS 6715	natMX6:Z:ADH15:mCherry-Atb2 ade6 leu1-32 ura4-D18 h-	Sawin lab
Ks 6716	natMX6:Z:ADH15:mCherry-Atb2 ade6 leu1-32 ura4-D18 h+	Sawin lab
KS 7144	h- ade6<<mCh-psy1 ura4-D18	This study
KS 7145	h+ ade6<<mCh-psy1 uch2-mCherry:ura4+ hphMX6:nmt81:GFP-atb2 ura4-D18 leu1-32	This study
KS 7146	h- Z:ADH15:mCherry-Atb2:natMX6 tea1-GFP:kanMX6 ade6<<mCh-psy1 ura4-D18	This study
KS 7263	h- tea1-mEcitrine-KanMX	This study
KS 7264	h- Tea1-mEcitrine-NatMX6	This study
KS 7265	h-Tea1-mEcitrine.hphMX6	This study
KS 7305	h- CRIB-3xmECitrine:LEU2 KanMX6 ade6-M210 ura4-D18	Sawin lab

	leu1-32	
KS 7306	h- CRIB-3xmECitrine:LEU2 KanMX6 ade6-M210 ura4-D18 leu1-32	Sawin lab
KS 7340	h- CRIB-3xmECitrine:LEU2 for3Δ KanMX6 ade6-M210 ura4-D18 leu1-32	This study
KS 7362	h+CRIB-3xmECitrine:LEU2 ade6-M210 ura4-D18 leu1-32	This study
KS 7363	h- myo51Δ::ura4+ CRIB-3xmECitrine:LEU2 ade6-M210 ura4-D18 leu1-32	This study
KS 7364	h? CRIB-3xmECitrine:LEU2 for3Δ :KanMX6 leu1-32[pAct1-lifeact-mCherry-leu1+] ade6-M216 ura4-D18	This study
KS 7365	h+leu1-32[pAct1-lifeact-mCherry-leu1+]CRIB 3xmCitrine:LEU2 ade6-M210 ura4-D18	This study
KS 7366	h+ CRIB-3xmCitrine:LEU2 myo52Δ::ura4+ ade6-M216 leu1-32 ura4-D18	This study
KS 7368	h+ tea1Δ(434-586)mEcitrine:hphMX6 ura4-D18 leu1-32 ade6-M210	This study
KS 7369	h+ tea1(10A)mEcitrine:hphMX6::ura4+ ura4-D18 leu1-32 ade6-M210	This study
KS 7459	h+ for3-I930A-3GFP-ura4+ ade6-M216 leu1-32 ura4-D18	Sawin lab
KS 7464	h+ bud6Δ::KanMX6 ade6-M216 ura4-D18 leu1-32	This study
KS 7465	h+ for3-3GFP-ura4+ CRIB-3xmCitrine:LEU2 ade6-M216 leu1-32 ura4-D18	This study
KS 7466	h- for3-I930A-3GFP-ura4+ CRIB-3xmCitrine:LEU2 ade6-M210 ura4-D18 leu1-32	This study
KS 7497	h? myp2Δ::KanmMX CRIB-3Xmcitrine:Leu2 ade6-216 leu1-32 ura4-D18	This study
KS 7509	h+ bud6Δ::KanMX6 ade6-M216 ura4-D18 leu1-32	This study
KS 7512	h+ bud6Δ::KanMX6 CRIB-3xmCitrine:LEU2 ade6-M216 ura4-D18 leu1-32	This study
KS 7513	h- bud6Δ::KanMX6 CRIB-3xmCitrine:LEU2 ade6-M216 ura4-D18 leu1-32	This study
KS 7514	h+ CRIB-3xmECitrine:LEU2 myo52Δ::ura4+ myo51Δ::KanMX6 ade6-M216 leu1-32 ura4-D18	This study
KS 7515	h+ CRIB-3xmECitrine:LEU2 myo52Δ::ura4+	This study

	myo51Δ::KanMX6 ade6-M216 leu1-32 ura4-D18	
KS 7593	h+ Scd1-mECitrine::KanMX Sty1Δ:NatMX ade6-M216 ura4-D18 leu1-32	Sawin lab
KS 7620	h- ima1Δ::KanMX6 CRIB-3xmEcitrine:hphMX6 Ura4-D18 leu1-32 ade6-216	This study
KS 7621	h- kms1Δ::KanMX6 CRIB-3xmEcitrine:hphMX6 Ura4-D18 leu1-32 ade6-216	This study
KS 7657	h+ gef1Δ::ura4+ CRIB-3xmECitrine:LEU2 ade6-M210 ura4-D18 leu1-32	Sawin lab
KS 7750	h+ tea1-3xmEcitrine:hphMX6 ura4-D18 leu1-32 ade6-M216	This study
KS 7751	tea1-3xmCherry:KanMX6 ura4-D18 leu1-32 h-	This study
KS 7752	h? mto1-427 CRIB-3xmEcitrine:LEU2 Ura4-D18 leu1-32 ade6?	This study
KS 7753	h? mto1-427 CRIB-3xmEcitrine:LEU2 Ura4-D18 leu1-32 ade6?	This study
KS 7770	h- tea4-3xmEcitrine:hphMX6 ura4-D18 leu1-32 ade6-M216	This study
KS 7811	h- rax2Δ::KanMX6 CRIB-3xmEcitrine:leu2 ade6-M210 Ura4-D18 leu1-32	This study
KS 7812	h- rax1Δ::KanMX6 CRIB-3xmEcitrine:leu2 ade6-M210 Ura4-D18 leu1-32	This study
KS 7867	h- rax2-3xmEcitrine:hphMX6 leu1-32 Ura4-D18 ade6-M216	This study
KS 7907	h+ rax2Δ::KanMX6 adh13-CRIB-3xmECitrine:LEU2 leu1-32 ura4-D18 ade6-M210	This study
KS 7908	h+ rax1Δ::KanMX6adh13-CRIB-3xmECitrine:LEU2 leu1-32 ura4-D18 ade6-M210	This study
KS 7909	h+ for3YFP::kanMX6 leu1-32 ura4-D18 ade6	This study
KS 7919	h? adh13-CRIB-3xmECitrine:LEU2 rga4Δ:: ura4+ leu1-32 ura4-D18 ade6-M210	Sawin lab
KS 7950	h- rax2Δ::KanMX6 adh13-CRIB-3xmECitrine:LEU2 leu1-32 ura4-D18 ade6-M210	This study
KS 7951	h+ rax2Δ::KanMX6 tea1Δ::ura4+ adh13-CRIB-3xmECitrine:LEU2 leu1-32 ura4-D18 ade6-M210	This study
KS 7952	h- rax2Δ::KanMX6 rax1Δ::KanMX6 adh13-CRIB-3xmECitrine:LEU2 leu1-32 ura4-D18 ade6-M210	This study

KS 8055	h? rax2Δ::KanMX6 for3YFP::kanMX6 leu1-32 ura4-D18 ade?	This study
KS 8056	h- rax2Δ::KanMX6 tea4Δ ::hphMX6 adh13-CRIB-3xmECitrine:LEU2 leu1-32 ura4-D18 ade6-M210	This study
KS 8057	h? rax2Δ::KanMX6 rga4Δ:: ura4+ adh13-CRIB-3xmECitrine:LEU2 leu1-32 ura4-D18 ade6-M210	This study
KS 8058	h- tea3Δ::natMX6 adh13-CRIB-3xmECitrine:LEU2 leu1-32 ura4-D18 ade6-M210	This study
KS 8068	h+ rax2-mEcitrine:KanMX6 ade6-M216 ura4-D18 leu1-32	This study
KS 8069	h+ rax1-3xmEcitrine:hphMX6 ade6-M216 ura4-D18 leu1-32	This study
KS 8070	h- pom1Δ::ura4+ adh13-CRIB-3xmECitrine:LEU2 leu1-32 ura4-D18 ade?	This study
KS 8081	h+ tea1Δ::Ura4+ adh13-CRIB-3xmECitrine:LEU2 leu1-32 ura4-D18 ade6-M210	This study
KS 8082	h+ rax2Δ::KanMX6 rax1Δ::KanMX6 adh13-CRIB-3xmECitrine:LEU2 leu1-32 ura4-D18 ade6-M210	This study
KS 8110	h+ rax2Δ::KanMX6 tea3Δ::natMX6 adh13-CRIB-3xmECitrine:LEU2 leu1-32 ura4-D18 ade6-M210	This study
KS 8111	h? pom1Δ::ura4+ rax2Δ::KanMX6 adh13-CRIB-3xmECitrine:LEU2 leu1-32 ura4-D18 ade6-M210	This study
KS 8112	rax2Δ::KanMX6 for3Δ::KanMX6 adh13-CRIB-3xmECitrine:LEU2 leu1-32 ura4-D18 ade6-M210	This study
KS 8113	h? rax1Δ::KanMX6 rax2-3xmEcitrine:hphMX6 leu1-32 ura4-D18 ade6-M210	This study
KS 8116	h- sty1.T97A CRIB-3xmECitrine:LEU2 ade6-M210 ura4-D18 leu1-32	Sawin lab
KS 8130	h+ tea1Δ::ura4+ adh13-CRIB-3xmECitrine:LEU2 leu1-32 ura4-D18 ade6-M210	Sawin lab
KS 8196	h+ Pbgs4+::Cher-12A-bgs4+:leu1+ bgs4Δ::ura4+ leu1-32 ura4-D18 his3-D1	Sawin lab
KS 8197	h? tea1Δ::ura4+ rax1Δ::KanMX6adh13-CRIB-3xmECitrine:LEU2 leu1-32 ura4-D18 ade6-M210	This study
KS 8198	h? tea1Δ::Ura4+ rax2-3xmEcitrine:hphMX6 leu1-32 Ura4-D18 ade6?	This study
KS 8240	h? tea4Δ ::hphMX6 adh13-CRIB-3xmECitrine:LEU2 leu1-	This study

	32 ura4-D18 ade6-M21?	
KS 8241	h? rax2Δ::KanMX6 adh13-CRIB-3xmECitrine:LEU2 leu1-32[pAct1-lifeact-mCherry-leu1+] ade6-M21? ura4-D18	This study
KS 8242	h? rax2Δ::KanMX6 tea1Δ::ura4+ leu1-32[pAct1-lifeact-mCherry-leu1+] ade6-M21? ura4-D18	This study
KS 8290	h? rax2Δ::KanMX6 tea3Δ::natMX6 tea4Δ ::hphMX6 adh13-CRIB-3xmECitrine:LEU2 leu1-32 ura4-D18 ade6-M210	This study
KS 8291	rax2Δ::KanMX6 tea1Δ::ura4+ sty1.T97A adh13-CRIB-3xmECitrine:LEU2 leu1-32 ura4-D18 ade6-M210	This study
KS 8292	h+ rax2-3xmEcitrine:hphMX6 Pbgs4+::Cher-12A-bgs4+:leu1+ bgs4Δ::ura4+ leu1-32 ura4-D18 ade6?	This study
KS 8302	h+ scd1Δ::kan ade6-M216 leu1-32 ura4-D18 + pREP42-Scd1	Sawin lab
KS 8325	h+ Sty1Δ::NatMX CRIB-3xmECitrine:LEU2 ade6-M21? ura4-D18 leu1-32	This study
KS 8326	pom1Δ::ura4+ tea1Δ::ura4+ adh13-CRIB-3xmECitrine:LEU2 leu1-32 ura4-D18 ade6?	This study
KS 8327	rax2Δ::KanMX6 tea3Δ::natMX6 tea1-3xmCherry:KanMX6 adh13-CRIB-3xmECitrine:LEU2 leu1-32 ura4-D18 ade6-M210 h?	This study
KS 8335	h+ Pbgs4+::Cher-12A-bgs4+:leu1+ bgs4Δ::ura4+ leu1-32 ura4-D18 ade?	This study
KS 8336	h- Pbgs4+::Cher-12A-bgs4+:leu1+ bgs4Δ::ura4+ leu1-32 ura4-D18 ade?	This study
KS 8337	h? rax2Δ::KanMX6 tea4Δ ::hphMX6 Sty1Δ::NatMX adh13-CRIB-3xmECitrine:LEU2 leu1-32 ura4-D18 ade6-M21?	This study
KS 8498	h? rax2-3xmEcitrine:hphMX6 scd1Δ::kan ade6-M216 leu1-32 ura4-D18	This study
KS 8499	h- gef1Δ::ura4+ rax2-3xmEcitrine:hphMX6 leu1-32 Ura4-D18 ade6-M21?	This study
KS 8500	tea1-mCherry:natMX6 CRIB-3xmECitrine:LEU2 ade6-M210 ura4-D18 leu1-32 h?	This study
KS 8501	tea1-3xmCherry:KanMX6 CRIB-3xmECitrine:LEU2 ade6? ura4-D18 leu1-32 h?	This study

Number	Sequence	Source

OKS 244	agacggatttcatgaagttattggttaaaagcggcctctcaaatcctccagctaaagaa ccagtccatgacaacgaaaatcggatccccgggttaattaa	Sawin lab
OKS 246	CCAATTTGTTAAAATCCCTTTG	Sawin lab
OKS 251	GAAGGGGTGGTTGAAGTTTTTGAAAAATTTGGTTTGGTCG GTTTATGCGCAGATCCTTTATTCCTTTTAAATAAAAAAGAC ATGATTTAACAAAGCGACTATA	Sawin lab
OKS 2550	TTCCTTACCATTTATTCCTTAATCAGCTTCGTTAGTATCTTT TTTACAACCAAATTACCAGTTTGGTATGTTAATTCATACGC CAGGGTTTTCCCAGTCACGAC	This study
OKS 2551	TCTTTCAGACAAATCGTCAATGTATGTAATGTACAGATATA CTGTTCTAAAAATCCATCCTAGAAAGAACAATGGAGCAAA GCGGATAACAATTTCACACAGGA	This study
OKS 2552	TTCCTTACCATTTATTCCTTAATCAGCTTCGTTAGTATCTTT TTTACAACCAAATTACCAGTTTGGTATGTTAATTCATACGG ATCCCCGGGTTAATTAA	This study
OKS 2553	TCTTTCAGACAAATCGTCAATGTATGTAATGTACAGATATA CTGTTCTAAAAATCCATCCTAGAAAGAACAATGGAGCAAG AATTCGAGCTCGTTTAAAC	This study
OKS 2593	TTTATTGTTTTAAGTTTAAGTTGAACTTTCAATCCTTTTTTT GCGATTAGGATCATTGCTTTACTCATCTATTGGGACCACG GATCCCCGGGTTAATTAA	This study
OKS 2594	CAATTAAAGTTAAAAAAAGTAAAAAAAAAATACACAAACTG GCATACAATCATTGCCAAATCGAATAAAACTTATGCACAGA ATTCGAGCTCGTTTAAAC	This study
OKS 2603	ACTGTTGCAAAGAGCAGCGGTGT	This study
OKS 2604	TAGGCTCGGAATGTTGGGTTTC	This study
OKS 2605	TCTTTCTAGGATTTTTATTTTG	This study
OKS 2606	TCTAGATTTTTTATAGAACTGAGA	This study
OKS 2607	AAGATGAAAACGAAAACGAAACTG	This study
OKS 2608	CGGATGCTGATGACCTTACTGAT	This study
OKS 2609	GCCGTCTGGTTCGATTTATCAGCT	This study
OKS 2610	CATTGCTGATTGTCTTGATAATCAA	This study
OKS 2624	TTATTCCTTCTTTTGATATAGTTTTCCTTTTATACCACAGAA GATATTTTATTTTCAAAAGAAAGTAATTAAAAATTGCTCGG ATCCCCGGGTTAATTAA	This study
OKS 2625	TACATAGCACATCGAAACTCAAGTTACCCGATTTATAACTT TATTCCTTCTTTTGATATAGTTTTCCTTTTATACCACAGCGG ATCCCCGGGTTAATTAA	This study
OKS 2626	TACATAGCACATCGAAACTCAAGTTACCCGATTTATAACTT	This study

	TATTCCTTCTTTTGATATAGTTTTCCTTTTATACCACAGCGG ATCCCCGGGTTAATTAA	
OKS 2627	TGAAGTTACTATATGATGCTTTGAATTAACAGAGAATGATA AGAATATAGTATTAATGAGTACTAATATAAATTAAAAATGAA TTCGAGCTCGTTTAAAC	This study
OKS 2628	ACATCTATTTTTGTGTGTAAACAAAACGCTGTGTTTAGTTT AAATTAGGCGTTCGGGGAGTCTTGTAATTTCTACCGGTCC GGATCCCCGGGTTAATTAA	This study
OKS 2629	ACATCTATTTTTGTGTGTAAACAAAACGCTGTGTTTAGTTT AAATTAGGCGTTCGGGGAGTCTTGTAATTTCTACCGGTCC GGATCCCCGGGTTAATTAA	This study
OKS 2640	GCCTTTATATTAAAAATGATCTA	This study
OKS 2641	AATATACTTTCTTTTCAGTCT	This study
OKS 2642	TCTTCAGAAAATAAAATGTTAAAC	This study
OKS 2643	CTTTTTGAGGACTACAATGAA	This study
OKS 2661	TCACTGTAGGCAACGTAGCCGACAATGATGTACAGAACTC GAGCGACGAAGAAAATCAAGTACCAAATGGTATTAAAGTT CGGATCCCCGGGTTAATTAA	This study
OKS 2662	CCCAGCTCCAAATTTTGAAAGTAAAACCCCTAATTAGGGA ATAAATAAGTAGGCAGAGCACCTTGAAAAATAACTAGATA GAATTCGAGCTCGTTTAAAC	This study
OKS 2663	AGAGTGCTAAGTCACTACTTGCAGAACTAACTAACGGGTC TAATGCTTCAAATCTAGTTGAAAATGACCGCCAAAAACAAC GGATCCCCGGGTTAATTAA	This study
OKS 2664	TCTTTCAGACAAATCGTCAATGTATGTAATGTACAGATATA CTGTTCTAAAAATCCATCCTAGAAAGAACAATGGAGCAAG AATTCGAGCTCGTTTAAAC	This study
OKS 2665	AAATTCAAAACTGAATCCCATTCCCACTAGAATTGTGGTTC GTTTCCTGTATAATTATAATTGCCAGTTCCCTTTCCAAACG GATCCCCGGGTTAATTAA	This study
OKS 2666	TTATGAAATGCACGCAGCTTTATGATAAATTCTAACAAAAA AATTCAAAACTGAATCCCATTCCCACTAGAATTGTGGTTCG GATCCCCGGGTTAATTAA	This study
OKS 2667	AGCACTGATTTTTTTTTTAGAAAAAAAAAATCTTTCGCTAG CATCTTCATTTTCGTCATTATTTATTAGTCGCCTAATTAGAA TTCGAGCTCGTTTAAAC	This study
OKS 2668	TATGTACAAAAAGTTGAAAAAGGGTAAAGCAATTTAAATCA GCACTGATTTTTTTTTTAGAAAAAAAAAATCTTTCGCTAGAA TTCGAGCTCGTTTAAAC	This study

OKS 2669	ACTTGTTGTTTCCCTTTTTTTTTTTAAATTTGCACACACAGG ATTCTATGAGAACTTTGCATTAAATGGTATAATGGGAACGG ATCCCCGGGTTAATTAA	This study
OKS 2670	GGATAAATTAATGAATGATTGGTTTGCAAAAGAATATATTC CATATTACTTTGCATCCACTTCTTTAAATAGTAACCAGAGA ATTCGAGCTCGTTTAAAC	This study
OKS 2677	ATTCCATATTACTTTGCATCCA	This study
OKS 2678	ATTCCAAAATTGGATAAATTAA	This study
OKS 2708	GTGAAGGAGACGCCACCTAT	This study
OKS 2709	AATCCGACACAATATTGAGG	This study
OKS 2714	CAAAACACATCAAACCATAT	This study
OKS 2715	TTTTAAAGTTGACCTTTATT	This study
OKS 2782	TTTACAAGCATCTGAAAAACGCCT	This study
OKS 2783	GAACAAGCTTTTTATCCTCGGAAT	This study
OKS 2786	CCTCGGACTTGGATGATATTTTTGCTAACGTATTGAAGGG TTTATCAGATGAGATGGCCTCCCTCTTAAATACGAATCGC CGGATCCCCGGGTTAATTAA	This study
OKS 2787	ATTTTATAGCGCTCAATAATCCGAATCATACCCGCACATTG AATTTTAGACCTTTATACAACTATGGTATGCTGTTAGTTGA ATTCGAGCTCGTTTAAAC	This study
OKS 2826	CAATATTCGTGCTTTCGATAATTGTTTTAATAGTGGGTGCA AACACAGCAATATTTAGCTGTGTTCCTTCTATTCGTCTACG GATCCCCGGGTTAATTAA	This study
OKS 2827	AAGAGGATCCACAACTTCAAAAAAACAAAAGAATGATAAAA AAAATGCAAAAAGGAGTGGAATGGAACGAAATCGACAGG GAATTCGAGCTCGTTTAAAC	This study
OKS 2828	AGATTATTCATTGGTTCTTTTCGGAGCATGTCGAAACGTTG CACGACTATTCGAATTTTTTAAAAGAATTAAAGACCCAGCG GATCCCCGGGTTAATTAA	This study
OKS 2829	CCTTCCACTGATCATATCAGTATTTAAACTTCAAAATTTGTA TGTTTTAAGATAGCCTCCTTAGTACTGTGCATAATCATGAA TTCGAGCTCGTTTAAAC	This study
OKS 2830	ATCCGCTGTATTTTTTTTGATACACATTAAAATCGGATTAAT TTAGGAACTCTAGTACTTGTCTTGAGGTGGTTGTCTGACG GATCCCCGGGTTAATTAA	This study
OKS 2831	CACTTTGTGTCATCTGACATTTGAAACTAAAGCGGAACCA ATCCGCTGTATTTTTTTTGATACACATTAAAATCGGATTAC GGATCCCCGGGTTAATTAA	This study
OKS 2832	AAGAGGATCCACAACTTCAAAAAAACAAAAGAATGATAAAA	This study

	AAAATGCAAAAAGGAGTGGAATGGAACGAAATCGACAGG GAATTCGAGCTCGTTTAAAC	
OKS 2833	TATTGAATAATTTGATTTTTAAAAGAAATGACTAAACAAAAA GAGGATCCACAACTTCAAAAAAACAAAAGAATGATAAAGA ATTCGAGCTCGTTTAAAC	This study
OKS 2834	TTACTCAAGTCCTGGTTTACTAGGCTCCGTTTGACGGCTT AATGCATCGGCGGCTTTTTGTCTCACGTTTTTAGTATATTC GGATCCCCGGGTTAATTAA	This study
OKS 2835	CAGCATAAAAAGTCACATTTTAAAATCCTTTTTCTTTTCATT ACTCAAGTCCTGGTTTACTAGGCTCCGTTTGACGGCTTCG GATCCCCGGGTTAATTAA	This study
OKS 2836	CCTTCCACTGATCATATCAGTATTTAAACTTCAAAATTTGTA TGTTTTAAGATAGCCTCCTTAGTACTGTGCATAATCATGAA TTCGAGCTCGTTTAAAC	This study
OKS 2837	ATGCATCAGTAAAAGTCGACTTATTAAAAGCATTTTTCTTC CTTCCACTGATCATATCAGTATTTAAACTTCAAAATTTGGA ATTCGAGCTCGTTTAAAC	This study
OKS 2844	TTATAACGTTAAAGGTAATGT	This study
OKS 2845	GATAGTGTCGCCATTTCGGGC	This study
OKS 2846	TAAGGAATCCATGTACACCAC	This study
OKS 2847	TCCGTTATTAGGAAATGAATG	This study
OKS 2848	AAAGATCAACGAGCAATTAAA	This study
OKS 2849	GTTTAGGTCAGCAAGCCTTTC	This study
OKS 2850	ATCAGTAAAGAGCAAGTTAAAA	This study

Chapter 3: Designing an imaging platform for live-cell imaging of fission yeast under stress-free conditions

3.1 Introduction

Live-cell imaging is an important tool in cell biology to study subcellular localization, intracellular transport, protein-protein interactions, and cellular processes such as division and polarized growth (Lippincott-schwartz et al. 2001). When studying processes such as polarized growth, it is crucial that cell viability is always maintained as physiological as possible. This will ensure that the biological processes that are under study are not altered in any way (Frigault et al. 2009). Most cells and tissues are normally not exposed to extremes of light exposure during their life cycle, so it is crucial that the amount of light exposed to these cells is minimal and does not cause any phototoxic effect (Frigault et al. 2009).

I am interested in understanding how cell polarity is regulated in fission yeast. To address this, I primarily use live-cell fluorescence imaging, drug perturbations and yeast genetics. Traditionally, live-cell imaging of fission yeast cells were carried out by mounting cells on agarose pads and sealed with a coverslip. These pads helps to keep the cells in place and also provide a good environment for growth (Tran et al. 2004; Sveiczer et al. 1996; Sawin 1998). However, since these agarose pads are sealed, addition of media or drug during imaging is not possible. Moreover, cells are imaged in an anaerobic environment, which might induce various stresses on the cells and affect their growth. In this chapter, I will focus on how I optimized an imaging system for fission yeast that allows immediate physiological growth without any adaptation period, causes minimal phototoxic stress, and is accessible to drug addition during imaging.

3.2 Results

3.2.1 An "open-dish" system is more physiological for long-term live-cell imaging of fission yeast cells

Previously in the lab, live-cell imaging of fission yeast was carried out on agarose pads that contain growth medium and are sealed with a coverslip (Fig. 3.1A). Previous unpublished work in the lab suggested that cells imaged in this "closed-pad" system were under various stresses, resulting in decreased growth. Under normal conditions, actin patches are present at the growing tips of interphase cells (Pelham & Chang 2001). When cells were imaged in the closed pad system, actin patches marked by Lifeact-mCherry became depolarized within a few minutes, suggesting that cells were under stress (data not shown).

Instead of the closed-pad system, I used an "open-dish" system in which cells are placed on a 35mm MatTek plastic petri dish with a coverslip bottom, coated with lectin (Fig.3.1B). Lectin can bind to the mannose on the cell wall of fission yeast cells and hence were used as a 'adhesive' onto which cells can attach (Huang & Snider 1995). When cells were imaged on the open-dish system, actin patches marked by LifeAct-mCherry were localized to the growing cell tips and showed normal growth without any stress. Hence i decided to use the open-dish system for all further imaging. Moreover, with the open-dish system, it was possible to add drugs or change the media during imaging, which is not possible with closed-pad system.

Even though imaging in the open-dish system did not affect the localization of actin patches, which are important for polarized cell growth, compared to the closed-pad system, I faced three main challenges while using the open-dish imaging system:

1. When cells were imaged in Edinburgh minimal medium (EMM2), some cells showed an initial growth-lag before growing normally. This resulted in a population of cells showing non-homogenous cell growth with different cells initiating polarized growth at different times into imaging.
2. Since most of the proteins of interest were tagged with green fluorescent protein (GFP), I used 488 nm laser to excite the cells. Excitation of cells with 488nm laser also gave higher cellular autofluorescence making it difficult for analysis and quantification of protein levels, localization, and dynamics.

3. Since I was interested in doing long-term live cell imaging to study polarized growth in fission yeast, prolonged light exposure to the cells posed a threat of causing light-induced stress to the cells.

A

“Closed” imaging system

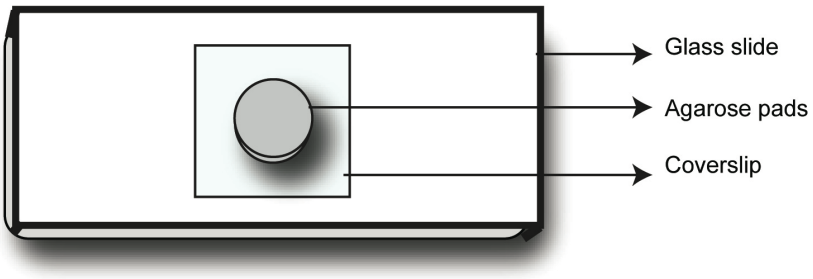

B

“Open” imaging system

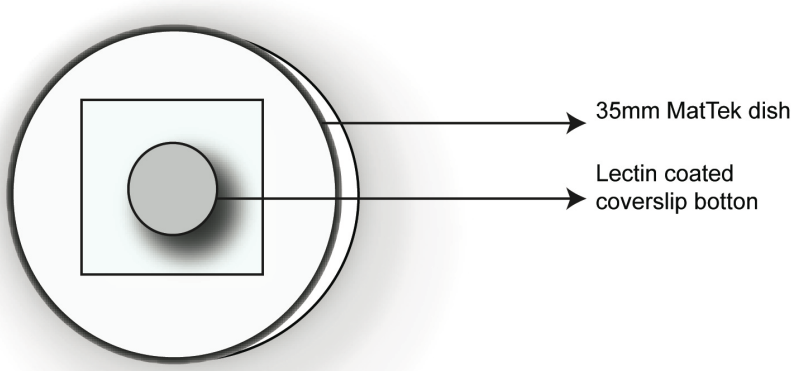

Figure 3.1 “Closed” system vs. “open” imaging system. A) “Closed” imaging system is made up of a glass slide with agarose pads containing growth media onto which cells are mounted and sealed with a coverslip. B) “Open” system is a 35mm MatTek dish with a coverslip bottom and coated with lectin to bind cells. “Open” system is more physiological and is accessible to media change and drug addition during imaging.

3.2.2 Imaging cells in "conditioned" media give improved cell growth.

One of the main issues during imaging in the open-dish system was an initial lag in cell growth. When cells were imaged in normal EMM2, I found that before growing normally, some cells showed an initial lag in growth. I predicted that this growth-lag could be due to cells not being accustomed or adapted to the medium. Therefore, in order to avoid the initial growth-lag, I decided to hold cell preparations for a few hours prior to imaging ("waiting" the cells). I tested different "waiting" times and found that waiting cells for 3 hours prior to imaging decreased the growth-lag. However, it was not the case that all cells waited for 3 hours prior to imaging completely avoided the growth-lag, and this resulted in non-homogenous growth among cells (Fig.3.2A). In addition, waiting 3 hours before imaging was time-consuming, especially for experiments requiring long periods of imaging. Therefore, I decided to "condition" the medium to test if this could prevent lag in cell growth. Cells were prepared and imaged in the same medium in which they were previously grown (known as conditioned medium; see Materials and Methods) (Rupes et al. 1999; Sveiczer et al. 1996).

Cells prepared and imaged in conditioned medium showed improved and homogenous cell growth (i.e. all the cells started growing at the beginning of imaging) compared to cells that were prepared in normal minimal medium and waited 1 hour prior to imaging (Fig.3.2B). Importantly, the homogenous growth observed with cells in conditioned media occurred even when imaged immediately after sample preparation, making it no longer necessary to "wait" cells prior to imaging. Thus I was able to achieve homogenous growth without any growth-lag in cells imaged in EMM by conditioning them. One possible explanation for improved growth in conditioned medium is that because fission yeast cells secrete nutrients into the growth medium, there is increased availability of growth nutrients in conditioned medium as cells were previously growing in this medium. As a result, cells are able to grow without any lag in conditioned medium compared to normal minimal medium. Additionally, conditioned medium might have a different pH to fresh medium and this difference in pH might make conditioned medium more conducive for cell growth.

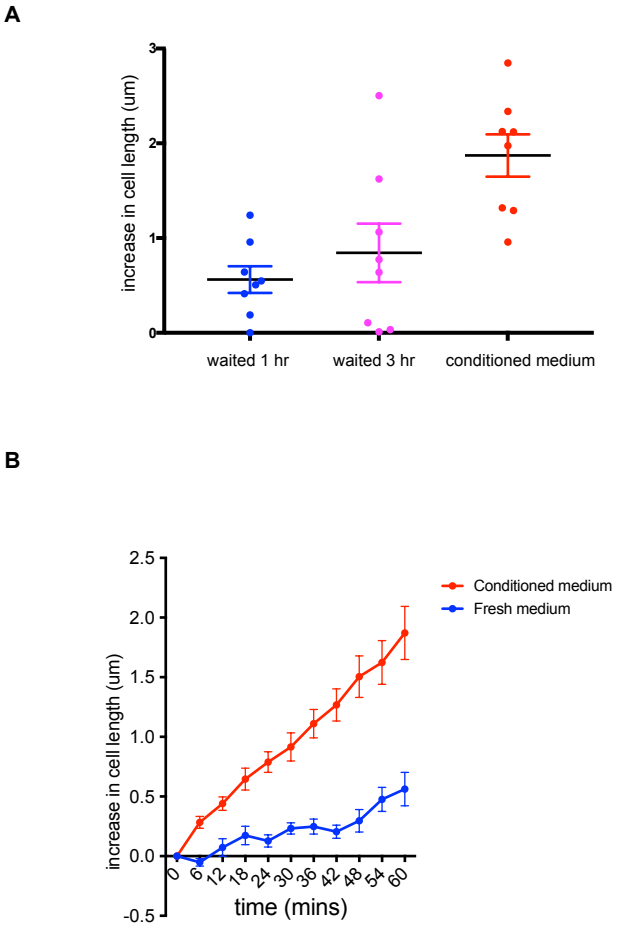

Figure 3.2. Cells imaged in "conditioned" medium show homogenous and improved cell growth comapred to fresh medium. A) Graph showing increase in cell length for cells waited for 1 hour and imaged, waited for 3 hours and imaged and imaged immediately in "conditioned" medium. Cells imaged in "conditioned" medium shows higher increase in cell growth compared to cells waited 1 hour and 3 hours. Moreover, all the cells show cell growth in "conditioned" medium (homogenous) vs. only some cells in 'waited 1 hour and waited 3 hours (non-homogenous) (n=8 cells). **B)** Graph showing increase in cell length in cells imaged in "conditioned" and fresh (waited 1 hour) medium. Cells imaged in "conditioned" medium conitue to grow over time, whereas cells imaged in fresh medium show very slow growth over time (n=8 cells).

3.2.3 Cells excited with 514 nm laser exhibit decreased cellular autofluorescence compared to cells excited with 488 nm laser.

One of the main challenges faced in imaging faint fluorescent signals under physiological conditions is to distinguish a fluorescent signal of interest from other fluorescent species within the biological material. Natural fluorescence emission, arising from endogenous fluorophores, is an intrinsic property of many cells and is termed “autofluorescence” (Knight & Billinton, 2001; Monici, 2005). Autofluorescence greatly hinders the proper visualization and quantification of fluorescent signals arising from exogenous markers. The majority of autofluorescence in animal cells is from mitochondria and lysosomes (Monici 2005).The most common source of cellular autofluorescence include flavins and nicotinamide adenine dinucleotide (NADH) (Knight & Billinton 2001; Monici 2005). Most of these molecules are excited at wavelengths close to 488 nm (Knight & Billinton 2001). Initially, I used GFP as the fluorescent protein to tag proteins of interest. GFP is typically excited at wavelength of 488 nm. As a result, along with the protein of interest, I was also exciting molecules causing autofluorescence. Molecules like flavin also have similar emission spectra to GFP (Monici 2005). This made it difficult to visualize and quantify the signal. Previously, when cells were imaged in the closed-pad system, autofluorescence was not a major issue because in the closed-pad system since we use a lot of cells and close the system, these cells might take up all the oxygen and therefore this might prevent the generation of reactive oxygen species (ROS). ROS are known to enhance autofluorescence in cells (Wu et al. 2010) and this resulted in reduced autofluorescence in the closed-pad system compared to the open-dish system.

I wanted to investigate the levels and spectrum of autofluorescence in cells excited with 488nm laser (GFP channel). The motivation behind this experiment was to check if I could decrease the autofluorescence by adjusting the emission bandwidth used to detect GFP. For example, if the GFP emission spectrum were very broad, and the flavin emission spectrum were more narrow, it might be possible, through appropriate use of emission filters, to remove much of the flavin fluorescent signal without removing too much of the GFP signal. Simultaneously, I was also interested in directly comparing the autofluorescence levels in cells excited with 488nm and 514nm (used to excite yellow fluorescent protein) lasers, to determine if I could use yellow fluorescent protein (YFP) to tag proteins of interest, as an alternative route to decreasing autofluorescence. Cells were excited with 488nm and 514nm lasers on scanning confocal microscope and corresponding emissions were

collected in bandwidths of 15nm to assay the autofluorescence emission spectrum. I found that total autofluorescence levels in cells excited with 514nm laser were lower compared to cells excited with 488nm laser (Fig.3.3A). Moreover, the emission spectrum of autofluorescence in 488nm channel was broad and fall in the emission spectra of GFP (Fig.3.3B) and hence the bandwidth of emission cannot be shortened to decrease cellular autofluorescence. On the other hand, emission spectrum of autofluorescence in 514nm channel was narrower compared to 488nm channel and therefore the bandwidth of emission can be adjusted to decrease the cellular autofluorescence.

As a proof of principle, I compared the fluorescent intensity of polarity protein Tea1 tagged with GFP and mEcitrine, an enhanced, monomeric, modified form of YFP excited by 514nm laser. Tea1 is a polarity protein transported on the plus end of the MTs to reach the cell tips (Mata & Nurse 1997; Sawin & Snaith 2004). Using the open-dish system, a direct comparison of autofluorescence levels between Tea1-GFP and Tea1-mEcitrine excited with similar laser power showed that level of cellular autofluorescence relative to Tea1-FP signal is lower in Tea1-mEcitrine cells as compared to Tea1-GFP cells (Fig.3.3B). Moreover, In Tea1-GFP cells, Tea1 “packets” were difficult to visualize, due to cellular autofluorescence whereas these packets were easy to visualize in Tea1-mEcitrine cells (Fig.3.3B). This indicate that YFP is a better choice of fluorescent protein to study the dynamics of weakly expressed proteins such as Tea1, due to decreased cellular autofluorescence.

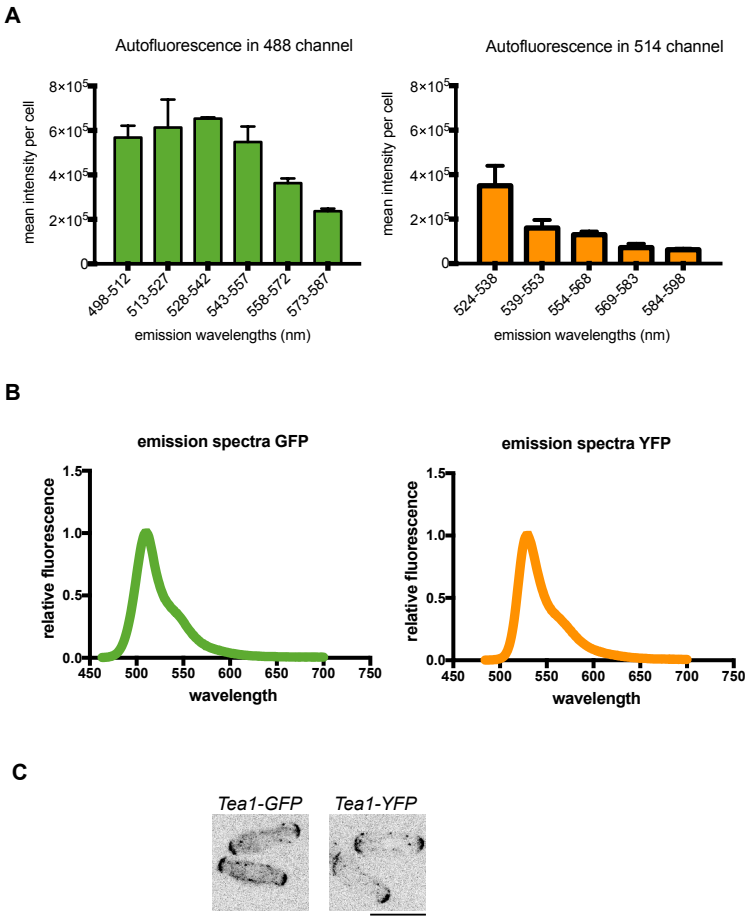

Figure 3.3. Cellular autofluorescence is higher in cells excited with 488nm laser comapred to cells excited with 514nm laser. **A)** Total autofluorescence levels in cells excited with 488nm is higher and broader compared to autofluorescence in cells excited with 514nm laser. **B)** Emission spectrum of GFP and YFP. Autofluorescence due to 488nm excitation falls in the emission spectra of GFP making it difficult to adjust the emission bandwith to decrease autofluorescence. **C)** Tea1-GFP cells show higher cellular autofluorescence compared to Tea1-YFP cells excited with similar amount of laser power. Scale, 10µm.

3.2.4 Prolonged exposure to 488nm laser causes phototoxic damage and affects cellular growth in S.pombe cells

In order to study dynamic processes such as polarized growth, cells may need to be imaged over an entire cell cycle or longer. This prolonged light exposure to cells could result in phototoxicity and photobleaching. The main reason for phototoxicity in fluorescence live-cell imaging is the production of reactive oxygen species (ROS) due to excited fluorophores (Hoebe et al. 2007). ROS react with different types of easily oxidizable components, such as proteins, nucleic acids, lipids and fluorophores, resulting in loss of fluorescent signal (photobleaching) and cell cycle arrest or cell death (phototoxicity) (Hoebe et al. 2007). Decreasing the excitation light can minimize phototoxicity and photobleaching. However, this also directly affects the fluorescent signal, thereby decreasing the signal to noise ratio making it difficult to visualize the desired signal/protein.

I wanted to investigate if prolonged exposure of cells with 488nm or 514nm laser resulted in phototoxic damage, which in turn affects cell growth. In order to investigate this, I used cells expressing LifeAct-mCherry, which labels the actin patches along with actin cables and cytokinetic ring (Huang et al. 2012; Riedl et al. 2008). Localization of actin patches act as a good readout to check cellular stress because under conditions of stress, actin patches are depolarized from the cell tips (Chowdhury & Gustin 1992). In order to determine the effect of 488 and 514 nm laser illumination on cells, *LifeAct-mCherry* cells were excited with either: (a) 30% 488nm plus 5% 561nm laser; or (b) 30% 514nm plus 5% 561nm laser; or (c) 10% 561nm only (maximum power of laser – 100%). Cells were excited with 561nm laser to excite LifeAct-mCherry to study the localization of actin patches. Note that the imaging system (scanning confocal) I used had almost similar laser power for 488nm and 514nm laser (488nm – 5.53 mW and 514nm – 5.86 mW). I measured the increase in cell length over time (2 hrs) for cells excited with 488nm, 514nm and 561 nm lasers. I found that in conditions (b) and (c), cells continue to grow throughout the 2 hours of imaging whereas, in condition (a), cells stopped growing after 1 hour of imaging, suggesting that cells might be undergoing phototoxic stress (Fig.3.4A).

To confirm if cessation of growth in cells excited with 488nm laser light is due to phototoxic stress, I examined the organization of actin patches in these cells and compared it to cells excited with 514 nm laser light. Cell excited with 514 nm light showed normal polarized actin patch localization at the growing ends of the cell. However, in cell excited with 488 nm light, actin patches were depolarized by 2 hours (Fig.3.4B-C). Representative kymographs of cells excited with 488 nm show that

depolarization of actin patches correlate with the time at which cell stops growing (Fig.3.4B). This shows that prolonged exposure of 488 nm laser results in phototoxic damage to the cells causing arrest of cell growth. Therefore YFP appears to be a better choice of fluorescent protein to tag proteins of interest for long-term live cell imaging.

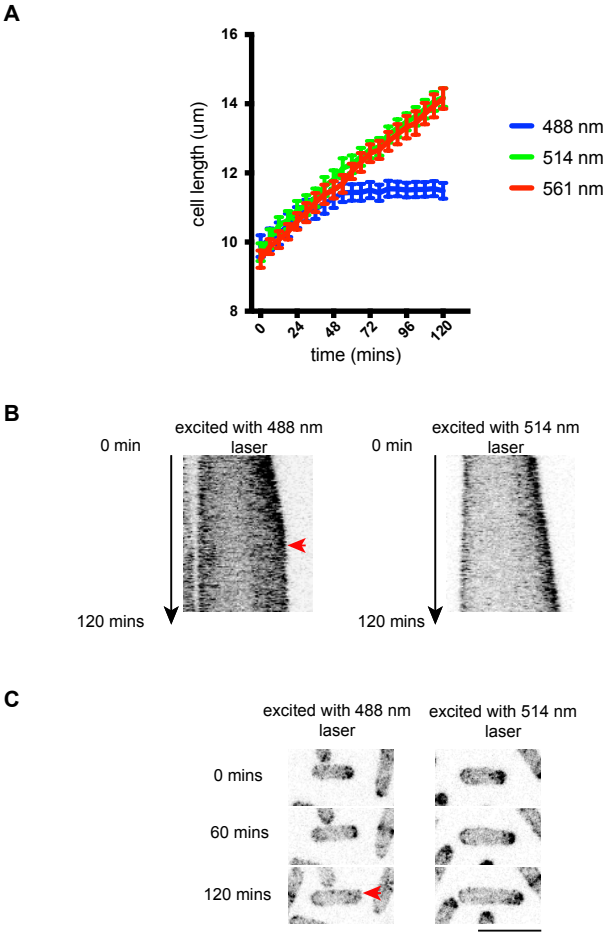

Figure 3.4. Prolonged 488 nm laser exposure to cells cause phototoxicity, whereas 514nm laser does not cause phototoxicity. A) Graph showing increase in cell length in cells excited with 488nm, 514nm and 561nm lasers. Cells excited with 514nm and 561nm continue to grow, whereas cells excited with 488nm stop growing after 1 hour. B) Kymographs obtained from live-cell imaging of *LifeAct-mCherry* cells excited with 488nm and 514nm laser. Cells excited with 488nm stop growing after 1 hour and actin patches labelled by LifeAct depolarize (red arrow), whereas cells excited with 514nm laser shows polarized actin patches at the cell tips and cells continued to grow normally. C) Still images obtained from live-cell imaging of *LifeAct-mCherry* cells excited with 488nm and 514nm lasers. Actin patches remain polarized in cells excited with 514nm laser, whereas actin patches become depolarized in cells excited with 488nm laser (red arrow). Scale, 10µm.

3.3 Discussion

In this chapter, I have optimized a long-term live-cell imaging system (open-dish system) in fission yeast, which is physiological, stress-free and accessible during imaging for drug and media additions. Traditionally agarose pads were used for live-cell imaging in fission yeast. However, apart from being “closed” and hence not accessible for drug additions or media change during imaging, we also found that this imaging in this closed-pad system induces subtle stresses to the cells and hence is not suitable for long-term live-cell imaging. In the open dish system, I was able to image cells for a long period of time compared to closed system without causing any stress and hence is more conducive for studying polarized growth.

In order to study fundamental process such as polarized growth, it is important to ensure that cells grow normally without any growth lag. Here, I have shown that when cells were imaged in synthetic minimal medium, some cells showed an initial growth lag and therefore, cells were not growing continuously under the microscope, making the study on polarized growth difficult to interpret. I have shown that by conditioning the growth medium this growth lag could be avoided and cells grow in a normal polarized manner. Since conditioned medium is prepared from media in which cells were previously growing, it is possible that there is improved nutrient availability in conditioned medium compared to fresh medium. Alternatively, cells that were previously growing in the medium might change the pH of the fresh medium to a more suitable pH and hence cells grow readily in conditioned medium compared to fresh medium. Similar to minimal medium, fission yeast cells can also be grown and imaged in rich complex medium (YE5S). Imaging fission yeast cells in rich medium did not show any growth-lag and hence doesn’t need conditioning (data not shown). However, rich medium shows batch-to-batch variability and also has a higher autofluorescence making it imaging in rich medium tricky.

Fluorescent proteins such as GFP, YFP, and mCherry have been extensively used to tag proteins of interest to visualize proteins under the microscope. Studying of polarized growth in fission yeast sometimes require long-term live-cell imaging of fission yeast cells under the microscope to track growth patterns from one cell cycle to another. As a result, cells are exposed to laser light for long period of time. This is especially tricky in the case of weak signals since higher laser power is needed to visualize them. I have found that prolonged exposure of cells to 488nm laser light resulted in phototoxic damage to cells compared to 514nm laser light. GFP is one of the most extensively used fluorescent protein in fission yeast to visualize proteins of interest and is typically excited at a wavelength of 488 nm. It is easy to overlook

effect of prolonged laser exposure to cells causing phototoxic damage because we found that phototoxicity appears before photobleaching of the sample. Therefore, proper care should be taken in choosing the right fluorescent protein and also choosing the amount of laser light exposed to the cells. Apart from inducing phototoxic stress to the cells, cells excited with 488nm laser also showed higher cellular autofluorescence compared to cells excited with 514nm. Common sources of autofluorescence such as flavins and NADH are typically excited at 488nm and therefore using 488nm laser to excite GFP also excites other molecules resulting in autofluorescence. Moreover, the spectrum of autofluorescence in cells excited with 488nm is broad and therefore, difficult to adjust the emission bandwidth to avoid autofluorescence signal. As a result we found that YFP excited by 514nm laser might be a better choice of fluorescent protein for tagging of proteins in order to do long-term live-cell imaging.

Chapter 4: Actin cables together with microtubules position the fission yeast nucleus.

4.1 Introduction

The positioning of the nucleus inside the cell is dynamically controlled in space and time depending on cell type, stage of the cell cycle, migratory status and differentiation status (Gundersen & Worman 2013; Dupin & Etienne-Manneville 2011). Nuclear movement is mediated by the cytoskeleton, which transmits pushing or pulling forces that act on the nuclear envelope (Dupin & Etienne-Manneville 2011). The physical interaction between the nucleus and the cytoskeleton is important for a broad range of cellular functions, such as cell polarization, cell migration, and positioning of division plane (Isermann & Lammerding 2013). Because of this, it is not surprising that defects in nuclear positioning can lead to cellular dysfunction. Studies from human subjects with inherited diseases and mouse models have shown that changes in proteins involved in nuclear positioning are associated with several different pathologies such as muscular dystrophy, dilated cardio myopathy, lissencephaly and premature ageing (Dupin & Etienne-Manneville 2011; Isermann & Lammerding 2013; Gundersen & Worman 2013).

The molecular machinery involved in nuclear positioning consists mainly of components of the cytoskeleton and protein complexes of the nuclear envelope. The cytoskeletal components generate forces to move the nucleus, whereas the protein complexes spanning the nuclear envelope mediate interaction between cytoskeleton and the nuclear envelope. MTs, actin filaments and associated motor proteins are the main cytoskeletal components involved in nuclear positioning (Gundersen & Worman 2013).

MTs have long been implicated in nuclear movement and are responsible for nuclear movement in majority of the cases (Reinsch & Gönczy 1998). MTs can achieve nuclear movement in two different ways. In the first case, nucleus is tightly associated with a microtubule-organizing centre (MTOC) like centrosome or spindle pole body (SPB) and in this case position of the nucleus follows the position of the MTOC. In the second case, nucleus moves laterally along the microtubules (Reinsch & Karsenti 1997; Reinsch & Gönczy 1998; Gundersen & Worman 2013). These two basic types of nuclear movement are illustrated by the migrations of male and female pronuclei in the newly fertilized egg of many species. Nuclear movement of the male pronucleus corresponds to the first type of nuclear movement, whereas the female pronuclear movement represents the second type of nuclear movement (Reinsch &

Gönczy 1998). For instance, in the *Xenopus* eggs, the male pronucleus nucleates MTs from its centrosome to form the sperm aster. These asters push the pronucleus towards the centre of the cell whereas, the female pronucleus driven by cytoplasmic dynein laterally moves along these astral MTs emanating from the pronuclear centrosome complex (Reinsch & Gönczy 1998; Reinsch & Karsenti 1997). The male pronuclear type of movement is also observed in early *C.elegans* embryo, *Drosophila* oocytes and cultured mammalian cells (Gundersen & Worman 2013; Reinsch & Gönczy 1998) . Similarly, the female pronuclear type of movement is observed during interkinetic nuclear migration of radial glial progenitor cells. This movement depends on both kinesin-3 and dynein for nuclear movement towards the basal and apical surfaces respectively (Dupin & Etienne-Manneville 2011).

In the budding yeast *Saccharomyces cerevisiae*, during mitosis the nucleus first moves towards the mother-bud neck and then into the neck. Nuclear movement towards the neck is mainly mediated by the capture of MT ends at one cortical region at the insipient bud site or bud tip followed by microtubule depolymerization (Similar to male pronuclear migration), whereas movement into the neck is mediated by MT sliding along the bud cortex, which also requires dynein and dynactin (similar to female pronuclear migration). This nuclear migration to the bud neck is important for proper segregation of genetic material to daughter cells (Reinsch & Gönczy 1998; Adames & Cooper 2000).

Although the majority of nuclear movements studied to date are mediated by MTs, the actin cytoskeleton has also been implicated in nuclear movement and positioning, in at least two different ways. Firstly, the actin network can restrain the nucleus. For example, in *C.elegans*, the outer nuclear membrane protein Anc-1, which associated with actin, is essential for anchoring nuclei in the syncytial hypodermal and intestinal cells (Starr & Han 2002; Gundersen & Worman 2013). Similarly in *Drosophila*, the differentiating oocyte is connected to a syncytium of 15 nurse cells via cytoplasmic bridges. In these cells, nuclear position is maintained with the help of an extremely stable network of actin bundles extending from the plasma membrane to the nucleus (Dupin & Etienne-Manneville 2011). In addition to its role in nuclear anchoring, the actin cytoskeleton is also involved in actively moving the nucleus.

A direct role for actin in nuclear movement has been shown in experiments using wounded monolayers of serum-starved NIH3T3 fibroblasts treated with lysophosphatidic acid (LPA), which stimulates cell polarization, but not protrusion or migration. In these cells, the force generated by the rearward-moving actin cables induced by the small GTPase Cdc42 brings about rearward nuclear movement. This

movement of actin cables is likely to be powered by myosin-II, as inhibition of myosin-II by blebbistatin prevents actin flow and nuclear movement (Gomes et al. 2005; Gundersen & Worman 2013)

Recent work carried out by Luxton et *al.* shows that LINC (linker of nucleocytoskeleton and cytoskeleton) complex, which spans the inner and outer nuclear membranes are involved in connecting actin cables to the nucleus. LINC complex components nesprin 2G and SUN2 form linear assemblies termed transmembrane actin-associated nuclear (TAN) lines, which provide a direct linkage between the nucleus and retrograde moving dorsal actin cables. TAN lines are anchored by A-type lamins, and this helps to transmit the forces generated by the actin cytoskeleton to the nuclear envelope to move the nucleus (Luxton et al. 2011; Luxton et al. 2010; Gundersen & Worman 2013). Additionally Samp1, a component of TAN lines, has also been shown to provide additional anchorage by binding to SUN2 (Borrego-Pinto et al. 2012). Recently D'Alessandro et *al.* showed that the BAR domain-containing protein amphiphysin/Bin1 plays a central role in connecting the nuclear envelope with the actin and MT cytoskeletons by binding to nesprin and actin, as well as to the microtubule-binding protein CLIP-170. Impairment of amphiphysin/BIN1 in *C. elegans*, mammalian cells, or muscles from patients with centronuclear myopathy affects the shape and position of the nucleus in these cells. In this way, amphiphysin, which was previously well studied for its role in endocytosis and recycling, acts as a bridge between actin and MT networks to position the nucleus (D'Alessandro et al. 2015).

In the genetically tractable model organism fission yeast, during interphase, the nucleus is positioned at the geometric centre of the cell even when cell is growing in an asymmetric manner from 7 to 14 um in length. This suggests that an active process is involved in positioning the nucleus at the centre of the cell with respect to growth at the cell tips (Mitchison & Nurse 1985; Tran et al. 2001). In fission yeast, MTs have been thought to be important for proper positioning of the nucleus at the centre of the cell. Disruption of the MTs either by mutations of tubulin genes or treatment with MT depolymerizing agent like TBZ results in an off-centred nucleus (Hagan & Yanagida 1997; Tran et al. 2001). The precise positioning of the nucleus has been shown to be important for defining the future plane of cell division (Chang & Nurse 1996). Displacing the nucleus from the cell middle by cell centrifugation in the absence of MTs, or by using optical tweezers, resulted in the relocalization of contractile rings and septa to the new position of the nucleus. This relocalization of the nucleus can occur until early mitosis. However, if the nucleus is displaced after the cytokinetic ring is assembled, the position of the ring does not change (Daga et

al. 2006; Tolic-Nørrelykke et al. 2005; Rincon & Paoletti 2012). Anillin-like protein Mid1 has been shown to play an important role in the assembly of contractile ring in the middle of the cell (Sohrmann et al. 1996). Mutations in *mid1* or *mid1*Δ results in aberrant contractile ring formation with very strong morphological defects (Sohrmann et al. 1996; Rincon & Paoletti 2012). During interphase, Mid1 is mainly present in the nucleus and once cell enter mitosis, Mid1 is shuttled from the nucleus to the cortical nodes, which then recruit other components of the cytokinetic ring (Paoletti & Chang 2000; Rincon & Paoletti 2012; Almonacid et al. 2009). In this way localization of Mid1 in the nucleus during interphase plays an important role in assembly of cytokinetic ring. These experiments demonstrate that the position of the nucleus has a positive impact on the assembly of the cytokinetic machinery and hence misplaced nucleus results in improper assembly of cytokinetic ring leading to inaccurate segregation of genetic material.

Previous work carried out by Tran et *al.* showed that in fission yeast, interphase MTs exist as antiparallel bundles, and these microtubules are thought to be responsible for positioning of nucleus at the cell centre by exerting pushing forces on the nucleus through MT polymerization (Tran et al. 2001). Tran et *al.* showed that the spindle pole body (SPB), which is associated with the nucleus, oscillates along the direction parallel to the long axis of the cell, and these oscillations are greatly diminished upon MT depolymerization. They also showed that in cells containing MTs, the nuclear membrane exhibits frequent and transient deformations, whereas when MTs were depolymerized, these deformations were abolished. This suggests that the deformations in the nuclear membrane are due to pushing action of MTs. Finally, simple mathematical modelling suggested that a balancing of these pushing MT forces can maintain nucleus at the centre of the cell (Tran et al. 2001). The main aim of this chapter is to address whether nuclear movement in fission yeast is exclusively MT-dependent, or if other cytoskeletal components are also involved in the process of nuclear positioning.

4.2 Results

4.2.1 Microtubule-independent movement of the fission yeast nucleus

Although the concept that microtubule-dependent forces position the fission yeast nucleus in the cell centre has been in the field for many years, surprisingly it has never been directly tested whether or not the nucleus can move in cells lacking MTs. Therefore, I first wanted to investigate if MTs are essential for nuclear movement. I depolymerized MTs using the drug methyl benzimidazol-2-yl carbamate (MBC) and carried out live-cell imaging to assay nuclear movement in relation to cell growth over several hours. Previously, thiabendazole (TBZ) was used as a microtubule-depolymerizing drug (Sawin & Nurse 1998). However, in addition to depolymerizing MTs, TBZ also results in transient depolarization of actin patches, leading to a transient arrest in cell elongation, whereas MBC does not affect actin cytoskeleton or cell elongation (Sawin & Nurse 1998; Sawin & Snaith 2004). I therefore decided to use MBC to depolymerize MTs to study nuclear movement. In order to visualize the nucleus and cell growth simultaneously, I used Cdc42/Rac Interactive Binding (CRIB) -3xmcitrine cells. CRIB binds to GTP-bound form of Cdc42 and can be used as a reporter for active Cdc42 (Tatebe et al. 2008, Mutavchiev et.al. 2016). In addition to labelling the cell tips and septum, where active Cdc42 is localized during tip growth and septation, respectively, CRIB-3xmcitrine also shows artifactual localization to the nucleus and is thus a good reporter for nuclear positioning and movement (Fig.4.1A). In my analysis of nuclear movement I considered only monopolar-growing cells, i.e. cells growing in only one direction. This is because in a monopolar growing cell, nucleus need to move in “real space” to position itself at the new centre of the cell. Whereas in a bipolar growing cell since cell grows from both the ends, nucleus could potentially remain at the centre of the cell without moving to maintain a central nuclear position (Fig.4.1B).

Kymographs were plotted using the ‘multiplekymograph’ plugin of imageJ to visualize the nuclear position with respect to the growing end of the cell (Fig.4.1C). Kymograph of control monopolar growing cell imaged in 1% DMSO shows nuclear movement in the direction of the growing end of the cell marked by CRIB-3xmcitrine, such that nuclear position was always approximately in the centre of the cell (Fig. 4.1D). Surprisingly, kymographs of cells treated with 25µg/ml of MBC continued to show nuclear movement in the direction of the growing end of the cell. However, the nuclear centring in MBC-treated cells was not as efficient as wild-type cells (Fig.

4.1D). In order to confirm depolymerization of MTs, *atb2-GFP*, which labels MTs, were imaged in the presence of MBC. MTs were depolymerized within 15 mins of MBC addition (Fig.4.1E). Moreover, MBC-treated cells showed a “cut” phenotype and abnormal mitoses, which is a characteristic of disruption of MTs during mitosis (Uemura & Yanagida 1986; Tran et al. 2001). These results indicate that nuclear movement in fission yeast is not exclusively microtubule-dependent, and that a different or additional mechanism is also involved in this process.

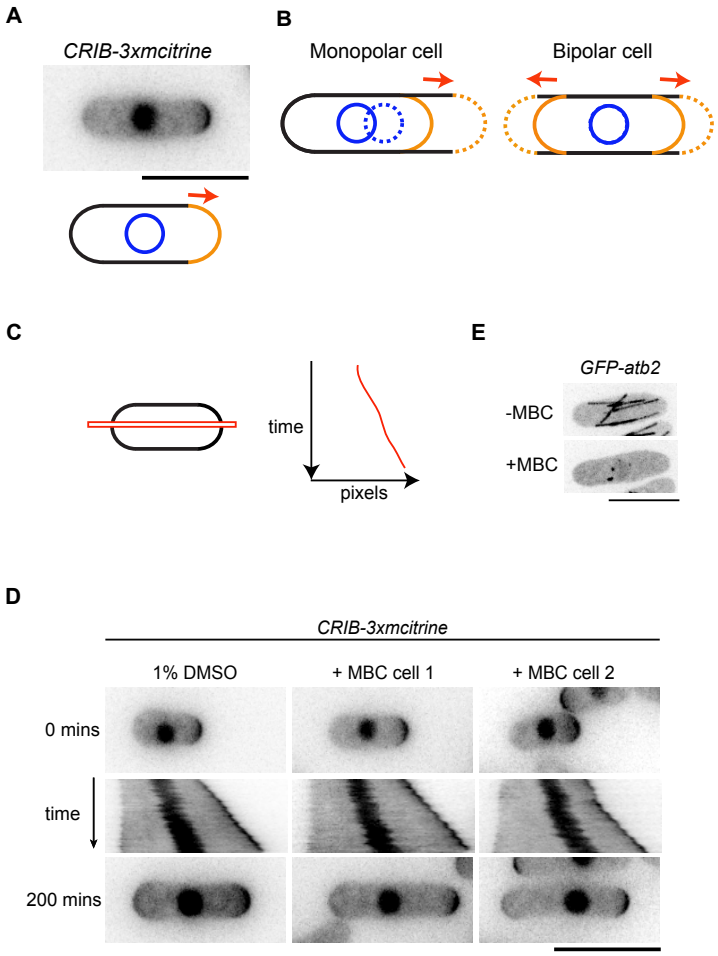

Figure 4.1. Microtubules are not essential for nuclear movement in fission yeast. A) *CRIB-3xmcitrine* labelling monopolar growing end and nucleus as a reporter for nuclear movement. **B)** Schematic diagram showing nuclear movement in monopolar cell compared to bipolar cell. Dotted line represents the new postion of the nucleus and the cell tip. **C)** Schematic representation of plotting a kymograph. X-axis shows time and Y-axis shows pixel. **D)** Kymographs showing nuclear movement in wild-type 1% DMSO treated and MBC-treated *CRIB-3xmcitrine* cells. **E)** MTs labelled by *GTP-atb2* cells showing depolymerization of MTs upon 25 µg/ml MBC addition. Scale, 10µm.

4.2.2 Actin cables are also involved in nuclear movement in fission yeast

Since the nucleus continued to move in MBC treated cells, I wanted to investigate how nuclear movement is achieved in the absence of MTs. Apart from MTs, the actin network has also been implicated in nuclear movement and positioning in different biological systems. Based on this I hypothesized that actin might be playing a role in nuclear movement in cells where MTs are depolymerized. Fission yeast actin exists as a single isoform and is organized into three distinct polymer structures – actin patches, actin cables and contractile ring. Out of these three structures, only actin cables span the long axis of the cell and localize near the nucleus during interphase (Kovar et al. 2011). Therefore, I hypothesized that actin cables might be playing a role in nuclear movement in the absence of MTs. In order to investigate this hypothesis, I used a low concentration of actin depolymerizing drug LatrunculinA (LatA) to check if actin cables are involved in nuclear movement along with MTs. LatA at a low concentration has been reported to selectively depolymerize actin cables without affecting actin patches (Martin & Chang 2006; Lo Presti & Martin 2011). Based on this I used 2μM LatA and 25μg/ml of MBC simultaneously to look at nuclear movement in *CRIB-3xmcitrine* cells. Live-cell imaging showed that even though actin cables and MTs were depolymerized, CRIB was mislocalized from cell tips to ectopic sites (Fig.4.2A). Moreover unpublished results from our lab show that depolymerization of actin results in activation of Sty1-mediated stress signalling pathway (Mutavchiev *et al.,* 2016). As a result polarized growth was affected in these cells making it difficult to study nuclear movement.

In fission yeast, interphase actin cables are nucleated by formin For3 (Feierbach & Chang 2001). Therefore, I decided to construct *for3*Δ *CRIB-3xmcitrine* strain to investigate the role of actin cables in nuclear movement. Deletion of *for3* was confirmed by yeast colony PCR. *for3*Δ cells displayed slow growth and a range of abnormal cell shapes consistent with previously published results (Feierbach & Chang 2001) (Fig. 4.2B). Previously Feierbach *et al.* showed that interphase actin cables were absent in *for3*Δ cells, and these cells also contained depolarized actin patches (Feierbach & Chang 2001). However, Nakano *et al.* reported that actin cables were visible in *for3*Δ cells, albeit reduced in number and shorter in length than in wild-type cells (Nakano et al. 2002). In order to confirm if actin cables are absent in *for3*Δ cells, I constructed a *for3*Δ *lifeact-mCherry* strain. Lifeact is a 17 amino-acid peptide that stains filamentous actin structures in eukaryotic cell (Riedl et al. 2008). Live-cell imaging of *for3*Δ *lifeact-mCherry* cells showed few actin cables and shorter in length similar to Nakano *et al.* observation (Fig.4.2C). However, it is difficult to

distinguish if these cables are fully functional and behave similar to For3 nucleated actin cables or whether the polarity of actin cables is affected.

Kymograph plotted from live-cell imaging of *for3*Δ *CRIB-3xmcitrine* cells treated with MBC showed no nuclear movement (Fig.4.2D). This shows that actin cables are involved in nuclear movement in the absence of MTs, and lack of both MTs and actin cables result in failure of nuclear movement. Next, I wanted to investigate if actin cables are required for nuclear movement when MTs are intact. In order to check this, I performed live-cell imaging of *for3*Δ *CRIB-3xmcitrine* cells in the absence of MBC. Kymographs plotted from movies of these cells revealed nuclear movement in the direction of the growing end of the cell maintaining a central nuclear position (Fig.4.2D). Together these results suggest that both MTs and actin cables are involved in nuclear movement in fission yeast. Having shown that actin cables are also involved in nuclear movement along with MTs, I wanted to investigate if MTs and actin cables by themselves are sufficient to position the nucleus at the cell centre. In order to address this, I calculated the distance from the centre of the nucleus to both the cell ends. The longer distance between the nucleus and the cell tip was denoted as 'a' and the shorter distance was denoted as 'b' and ratio of a/b gave the efficiency of nuclear centring. If the nucleus was centred perfectly, ratio will be 1, whereas if the nucleus was off-centred it will be below 1 with 0.1 being the maximum off-centred (Fig.4.2E). I found that similar to wild-type cells, 90% of the *for3*Δ cells (lacking actin cables) showed efficient nuclear centring with a value of 0.9 (1 being perfectly centred), whereas in MBC-treated cells more than 50% of the cells showed a value below 0.9 (Fig.4.2F). This suggests that MT-based nuclear movement is important for nuclear centring, whereas actin-cable based nuclear movement might be playing a different role during nuclear movement.

Next, I wanted to investigate if actin cable-mediated nuclear movement might be important for accurate positioning of septum. In order to investigate this, I calculated the ratio of distance between septum and the two cell tips. I used CRIB-3xmCitrine cells to label the septum and cell tips and calculated the distance from cell septum to both the cell tips. In wild-type cells, majority of the cells showed accurate positioning of septum (Fig.4.2.G) whereas, in *for3*Δ cells, more than 40% of the cells showed misplaced septum. This suggests that actin cable-based nuclear movement might be important for septum positioning, which in turn is important for accurate division of mother cell into two equal daughter cells.

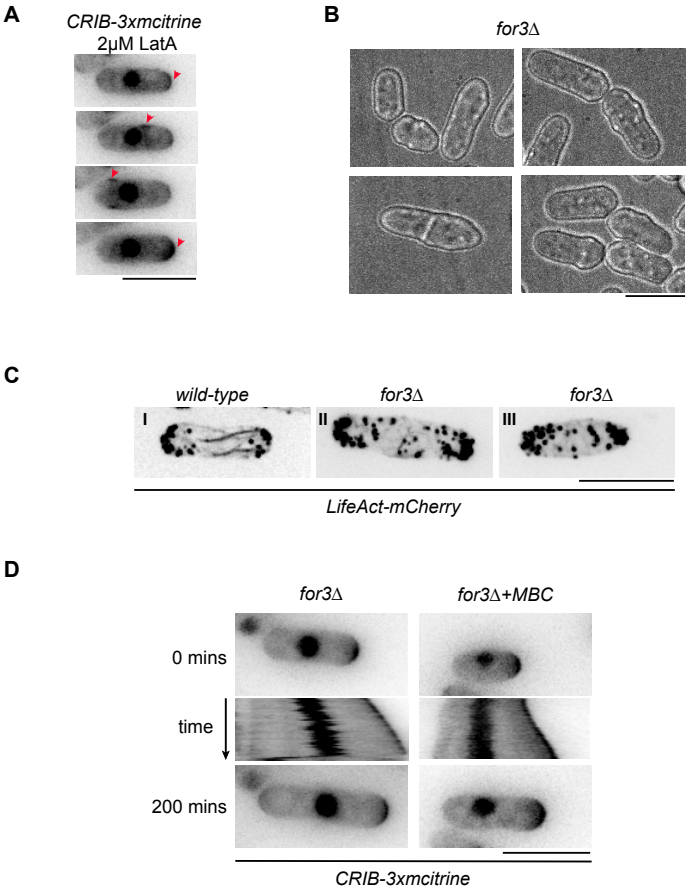

Figure 4.2. Actin cables are involved in nuclear movement in fission yeast. A) Low concentration of LatA is not suitable to check a role for actin cable in nuclear movement. 2μM LatA results in mislocalization of CRIB from the cell tips to ectopic sites (red arrow) and therefore affects polarized growth. **B)** Bright-field image of *for3*Δ cells showing aberrant cell morphology. **C)** *LifeAct-mCherry* cells showing actin organization in (I) wild-type cell and (II-III) *for3*Δ cells. Actin cables that are spanning the long axis of the cell present in the wild-type cell are absent in *for3*Δ cells. **D)** Kymographs showing nuclear movement in *for3*Δ cells and *for3*Δ cells treated with MBC. Nucleus continue to move in *for3*Δ cells towards the growing end of the cell marked by *CRIB-3xmcitrine*, whereas nuclear movement was completly abolished in *for3*Δ cells treated with MBC. This suggests that both MTs and actin cables are involved in nuclear movement in fission yeast. Scale, 10μm.

E

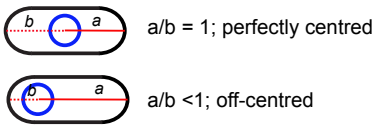

F

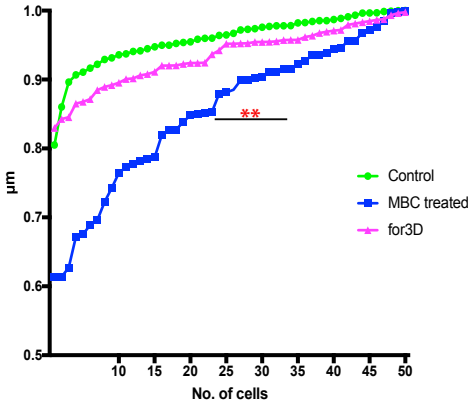

Figure 4.2. E) Schematic representation of nuclear centring. Nuclear centring efficiency is calculated by calculating the distance between nuclear centre and cell tips with longer distance being 'a' and shorter distance being 'b'. a/b gives the efficiency of nuclear centring with 1 being perfectly centred and 0.1 being maximum off-centred. F) Graph showing nuclear centring efficiency in wild-type, MBC-treated and *for3*Δ cells. *for3*Δ cells show efficient nuclear centring similar to wild-type cells, whereas more than 50% of the cells show nuclear centring below 0.9 in MBC-treated cells. Two-tailed unpaired T-test used to check statistical significance. p value = 0.004

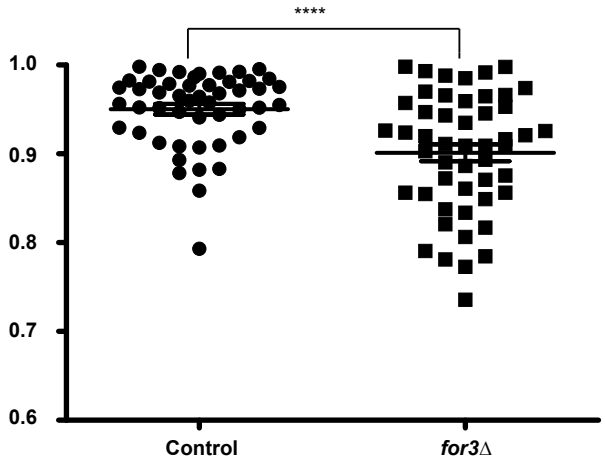

Figure 4.2.G. *for3*Δ cells show misplaced septum compared to wild-type cells. Positioning of septum was calculated by measuring the ratio of distance from septum labelled by CRIB-3xmCitrine to both the cell tips labelled by CRIB-3xmCitrine. A ratio of 1 suggests a prefectly centred septum whereas, ration less than 1 suggests misplaced septum with 0.1 being most misplaced. Two-tailed unpaired T-test used to check statistical significance. p value = 0.0001

4.2.3 Actin cable nucleation property of For3 is important for its role in nuclear movement.

For3 is a multidomain protein that has been shown to nucleate actin cables (Fig. 4.3A). The formin homology 2 (FH2) domain of For3 is important for nucleating actin filaments and binds stably to the growing barbed end of the filament, whereas the adjacent formin homology 1 (FH1) domain binds profilin, which promotes nucleotide exchange on actin and increases the rate of formin-mediated end elongation (Kovar 2006; Goode & Eck 2007). For3 is regulated by autoinhibition through an intramolecular interaction between a Diaphanous Autoregulatory Domain (DAD) and Diaphanous Inhibitory Domain (DID) (Martin et al. 2007). For3 localizes transiently to the cell tips and interact with Bud6 and Cdc42 to relieve the auto inhibition of For3, thereby promoting nucleation of actin cables (Martin & Chang 2006; Martin et al. 2007). Additionally, N-terminal of For3 also interacts directly with the polarity protein Tea4, which is important for bipolar growth in fission yeast (Martin et al. 2005). Because of these different interactions mediated by For3, I wanted to check whether the role played by For3 in nuclear movement is A) a direct role – i.e. role in actin cable nucleation or B) indirect role – i.e. recruiting other proteins important for nuclear movement.

In order to differentiate between these two possibilities, I used a strain with a single point mutation in the conserved actin-binding region of the FH2 domain (I930A) (Martin & Chang 2006). However, 3xGFP-tagged *For3-I930A* still localizes to cell tips and hence can still interact with Bud6, Cdc42 and Tea4 (Martin & Chang 2006). *for3-I903A* cells are therefore ideal for testing whether the requirement for For3 in microtubule-independent nuclear movement reflects a need for For3 more generally or a need for the actin-nucleation capacity of For3 specifically. I constructed a *for3-I930A-3xGFP CRIB-3xmcitrine* strain ~~to~~ assay nuclear movement after MBC treatment. Kymographs plotted from movies of *for3-I930A-3xGFP CRIB-3xmcitrine* cells treated with MBC showed no nuclear movement, similar to *for3*Δ cells treated with MBC (Fig.4.3B), whereas *for3-I930A* cells with intact MTs continued to show nuclear movement (Fig.4.3B). This suggests that failure of nuclear movement in *for3*Δ cells treated with MBC is specifically due to lack of functioning actin cables and not due to a more indirect effect.

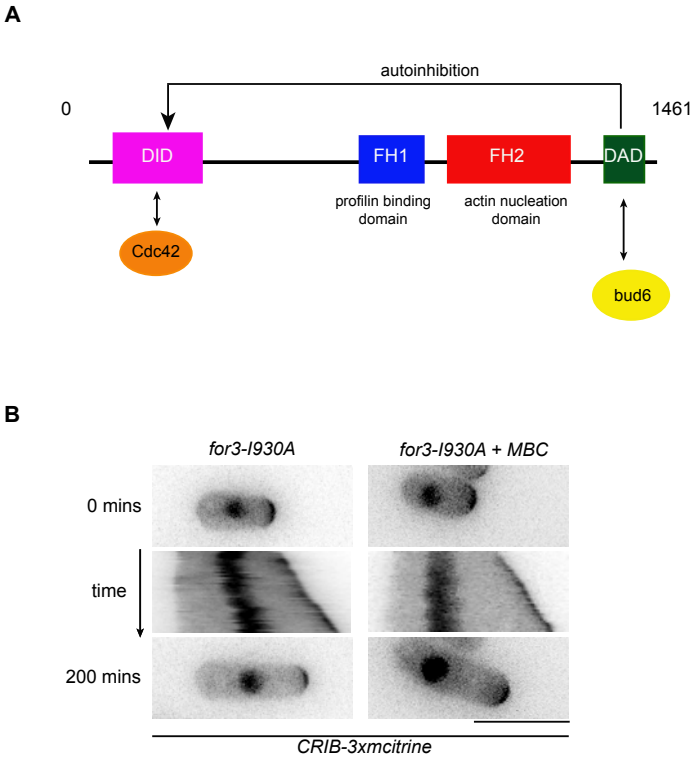

Fig. 4.3 Actin cable nucleation property of For3 is important for its role in nuclear movement. A) Domain architecture of For3. For3 is regulated by an autoinhibition between the C-terminal DID and N-terminal DAD domains. Bud6 and Cdc42 interacts with For3 to relieve this autoinhibition to facilitate nucleation of actin cables. **B)** Nuclear movement was completely abolished in kymographs obtained from live-cell imaging of FH2 domain mutant (I930A) cells treated with MBC suggesting that role of For3 in nuclear movement is due to its actin nucleation property. *for3-I930A* cells with intact MTs continued to show nuclear movement towards the growing cell end. Scale, 10µm.

4.2.4 Actin cables move the nucleus by pulling the nucleus

Having shown that actin cables are important for nuclear movement in the absence of MTs, I wanted to investigate how actin cables contribute to nuclear movement. Actin cable-based nuclear movement can be either by pushing the nucleus, similar to microtubule-based nuclear movement, or by pulling the nucleus (Fig.4.4A). Previously I have shown that in a monopolar growing cell treated with MBC, the nucleus always moves in the direction of the growing end of the cell, i.e., the end from which For3 normally nucleates actin cables. This suggests that actin cables might be moving the nucleus by pulling the nucleus in the direction of growing end of the cell. In order to prove this more conclusively, I used a method to artificially displace the nucleus from the cell centre (Daga & Chang 2005; Daga et al. 2006) . Cells were centrifuged for 3 minutes at 14000 rpm to displace the nucleus from the cell centre. In *CRIB-3xmcitrine* cells with intact MTs, the nucleus returned to the cell centre in approximately 17 minutes, as previously reported (Daga et al. 2006). This re-centring of nucleus was shown to be a microtubule-dependent process because in MBC-treated cells, most of the cells failed to re-centre the nucleus (Daga et al. 2006).

In order to confirm that actin cable-based nuclear movement is achieved by pulling the nucleus, I first depolymerized the MTs and then centrifuged the cells to move the nucleus towards one of the cell ends as described above. The nucleus was displaced arbitrarily either towards growing or non-growing cell ends, which can be distinguished by CRIB-3xmcitrine (Fig.4.4B). Kymographs obtained from live-cell imaging of MBC-treated, centrifuged cells showed that in cells in which the nucleus was displaced towards the growing end of the cell, the nucleus continued to show nuclear movement (Fig.4.4C). However, when the nucleus was displaced towards the non-growing end of the cell, the nucleus failed to show any overall directional movement (Fig.4.4C). In order to quantify nuclear movement in cells where nucleus is displaced to growing and non-growing ends, I calculated the nuclear distance from the growing cell tip at the start (C-start) and at the end (C-end) with respect to cell length at the start (d start) and end (d end). Plotting ‘C-start’ over Δc-Δd showed that in the cells where nucleus is closer to the growing end at the start of the movie (small C-start value), nuclear movement was observed (small Δc/Δd value), whereas cells with larger C-start value showed no net nuclear movement (high Δc/Δd value)

(Fig.4.4 D-E). This selective nuclear movement shows that in cells where nucleus was displaced to the growing end – the end from which actin cables are nucleated, actin cables might be able to physically pull the nucleus and hence can move the nucleus. However, in cells where nucleus was displaced to the non-growing end, actin cables might not be able to physically reach the nucleus and hence failed to move the nucleus. This suggests that actin cables are moving the nucleus by pulling the nucleus unlike MTs, which are moving the nucleus by pushing the nucleus.

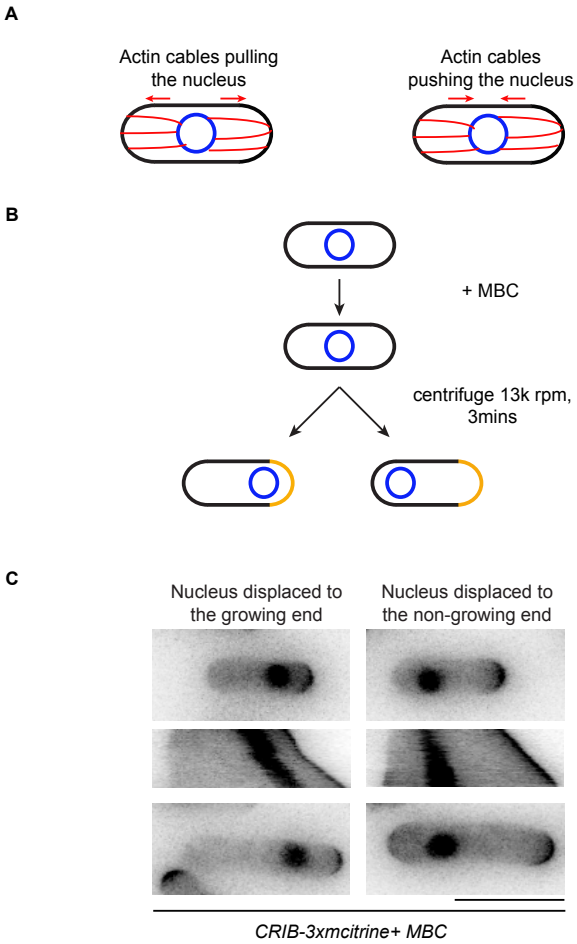

Figure 4.4. Actin cables need to physically reach the nucleus to pull the nucleus to achieve nuclear movement. A) Two possible mechanisms by which actin cables can move the nucleus - either by pushing the nucleus, or by pulling the nucleus. **B)** Simple diagramatic representation of artificially displacing the nucleus to cell ends by centrifugation. Initially, MTs are depolymerized followed by centrifuging the cells for 3 mins at 13k rpm to displace the nucleus arbitrarily to growing or non-growing end distinguished by CRIB labelling (orange). **C)** Kymographs showing nuclear movement in MBC treated, centrifuged *CRIB-3xmcitrine* cells with nucleus displaced to growing or non-growing ends. Nucleus continued to move in cells where nucleus was displaced to the growing end, whereas nucleus failed to move in cells where nucleus was displaced to the non-growing ends**.** This shows that actin cables move the nucleus by pulling the nucleus and actin cables need to physically reach the nucleus to pull the nucleus.Scale, 10 µm.

D

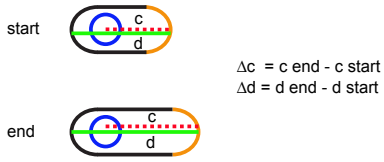

E

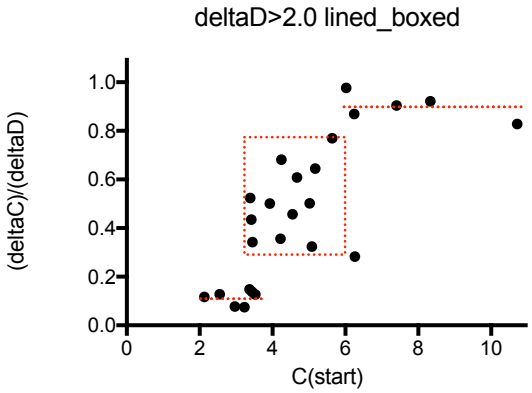

Figure 4.4. D) Diagrmatic representation of how Δc and Δd are calculated. c (start) and c (end) are the distance between the growing cell tip and centre of the nucleus at the start and end of the movie respectively and d (start) and d (end) are the cell length at the start and end of the movie respectively. **E)** Graph showing c(start) plotted against Δc/Δd shows the position of the nucleus at the start of the movie from the growing cell tip vs. the position of nucleus at the end of the movie from the growing cell tip relative to the increase in cell length. Lower c (start) represents cells, which are closer to the growing end and shows a lower Δc/Δd suggesting nuclear movement, whereas higher c (start) represents cells, which are closer to the non-growing end and shows a higher Δc/Δd (closer to 1) suggesting no net nuclear movement.

4.2.5 Actin cables might be important to buffer the pushing force generated by microtubules

Previously Tran *et al.* showed that microtubule-dependent pushing forces result in nuclear oscillations (Tran et al. 2001). Oscillations were observed by tracking the position of SPB, which is associated with the nucleus, and oscillations were greatly diminished in cells treated with TBZ (Tran et al. 2001). Similarly, using kymograph analysis, I observed that wild-type monopolar *CRIB-3xmcitrine* cells show nuclear oscillations, and these oscillations were reduced in MBC-treated cells. Surprisingly, I found that kymographs of *for3*Δ cells, in which actin cables are not properly organized showed more pronounced nuclear oscillations compared to wild-type cells (Fig. 4.5A). In order to quantify the nuclear oscillations in control and *for3*Δ cells, I used an imageJ plugin developed by Dr. David Kelly (Wellcome Trust Centre for Cell Biology) for this purpose. The plugin tracks the nucleus over time and calculates the amplitude of these oscillations. Root mean squared deviation (RMSD) of nuclear oscillations was calculated for each cell and plotted for wild type vs. *for3*Δ cells (Fig. 4.5B). Wild-type cells (n=12) showed a mean RMSD of 0.13um, whereas *for3*Δ (n=8) cells showed a mean RMSD of 0.19um. This shows that amplitude of nuclear oscillations is higher in *for3*Δ cells compared to wild type cells. Since *for3*Δ cells showed aberrant morphology, it was difficult to stick them to lectin, which made it difficult to do long-term imaging without cells moving around. As a result it was difficult to obtain higher cell number for automated analysis of nuclear oscillations.

The most plausible explanation for this increase in amplitude of nuclear oscillation in *for3*Δ cells is that actin cables may normally be involved in buffering the pushing forces exerted by MTs, such that the lack of actin cables—or, to be more specific, the lack of properly organized actin cables--results in increased nuclear oscillations. An increase in nuclear oscillations was also observed in kymographs of *for3-I930A* mutant cells (Fig. 4.5A).

An alternative explanation, which I do not favor, depends on a previous observation by Feierbach *et al.*, who claimed that *for3*Δ cells have defects in MT organization and an increase in number of MT bundles (Feierbach & Chang 2001). This suggested the possibility that increased nuclear oscillations in *for3*Δ cells might be due to an increase in MT-based pushing (rather than the absence of actin-based buffering). However, Feierbach *et al.* did not investigate MT bundles in any detail and did not present any statistical analysis in their work. To validate the claims of Feierbach *et al.*, I constructed *for3*Δ *atb2-mCherry*. I imaged Atb2-mCherry in wild-type and *for3*Δ strains and quantified the number of MT bundles per cell in each

stain. In both the strains, ~50% of the cells showed 3 MT bundles and ~38% of the cells showed 4 MT bundles and remaining cells showed 2 or 5 bundles (Fig. 4.5C). This shows that number of MT bundles in wild type and *for3*Δ cells is similar and increase in nuclear oscillations in *for3*Δ cells is not due to defects in MT organization.

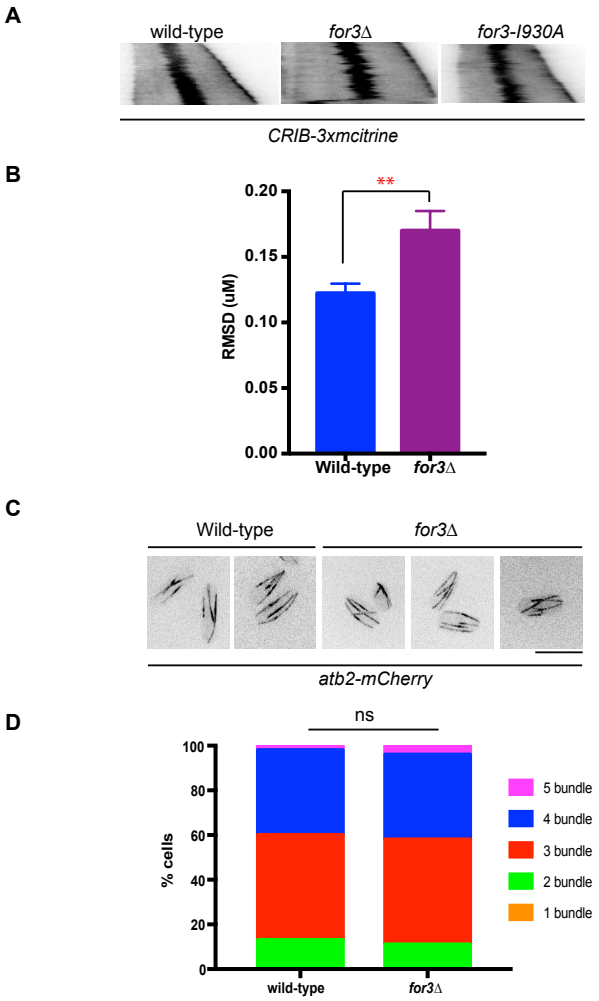

Figure 4.5. Actin cables might be important to buffer the pushing forces generated by MTs. A) Kymographs plotted from live-cell imaging of control, *for3*Δ and *for3-I930A* mutant cells showing increased nuclear oscillations in *for3*Δ and *for3-I930A* cells compared to wild-type cells. **B)** RMSD of amplitude of nuclear oscillation was calculated using an in-house ImageJ plug-in. Amplitude of nuclear oscillations were higher in *for3*Δ cells compared to wild-type cells suggesting that actin cables might be important to buffer the pushing forces generated by MTs on the nucleus. Unpaired t-test to check statistical significance. p value - 0.0037 **C)** MT bundles labelled by *atb2-mCherry* in wild-type and *for3*Δ cells show similar number of MT bundles. **D)** Graph showing number of MT bundles calculated in wild-type and *for3*Δ cells suggests that both wild-type and *for3*Δ cells have similar number of MT bundles and therefore, increased nuclear oscillation in *for3*Δ cells is not due to increase in number of MT bundles in *for3*Δ cells. A Chi-sqaure test was carried out to check statistical significance.P value 0.8 (not significant) Scale, 10 µm.

4.2.6 Type V myosin Myo-52 is involved in the actin cable-based nuclear movement in fission yeast

Next, I wanted to investigate how actin cables contact the nucleus in order to bring about nuclear movement. Actin-based motor proteins myosins are known to be involved in transport of a range of membrane-bound organelles (Woolner & Bement 2009). In wounded monolayers of serum-starved NIH3T3 fibroblasts treated with lysophosphatidic acid (LPA), nuclear movement depends on the force generated by the rearward-moving actin cables induced by the small GTPase Cdc42. This movement of actin cables is likely to be powered by myosin-II, as inhibition of myosin-II by blebbistatin prevents actin flow and rearward nuclear movement (Gomes et al. 2005; Gundersen & Worman 2013). Based on this, I hypothesized that myosins might be involved in actin-cable based nuclear movement. Fission yeast has five different myosin proteins: a single class-I myosin, Myo1; two class-II myosins, Myo2 and Myp2; and two class-V myosins, Myo51 and Myo52 (East & Mulvihill 2011). Class-I myosin Myo1 has been shown to be associated with actin patches, which are localized at the cell tips during interphase (Sirotkin et al. 2005). As such, it is highly unlikely that Myo1 is involved in nuclear movement in fission yeast. Class-II myosins Myo2 and Myp2 are both integral components of the cytokinetic machinery and localizes to the cytokinetic ring during mitosis, making either one a highly unlikely candidate for contributing to interphase nuclear movement. However, previous work carried out in our lab has shown that Myp2 was important for the eMTOC (equatorial Microtubule organizing centre) localization of Mto1 (Samejima et al. 2010). Mto1 is a centrosomin-related protein important for recruitment of gamma tubulin complex to the cytoplasmic MTOCs (Sawin et al. 2004). *mto1*Δ cells were previously shown to have aberrant MTs and also showed misplaced nuclear position (Lynch E.M Thesis)(Sawin et al. 2004). Similarly, in *mto1*Δ cells, unlike wild-type cells, the nucleus fails to re-centre after centrifugation (Daga et al. 2006). As a result I decided to check if Myp2 has a role in nuclear movement in fission yeast. I constructed a *myp2*Δ *CRIB-3xmcitrine* strain. Live-cell imaging was carried out with *myp2*Δ *CRIB-3xmcitrine* in the presence and absence of MBC. Kymographs obtained from live-cell imaging showed that nuclear movement was not affected in both the cases (Fig.4.6A). This suggests that Myp2 might not be involved in nuclear movement in fission yeast.

Class-V myosins Myo51 and Myo52 dimerize to transport cargoes along actin cables to discrete cellular locations (East & Mulvihill 2011). Myo51 was shown to be a component of cytokinetic ring, whereas Myo52 showed movement within the cell

and localizes to regions of growth (Win et al. 2001; Motegi et al. 2001; East & Mulvihill 2011). To investigate a role for Myo51 in nuclear movement, I constructed a *myo51*Δ *CRIB-3xmcitrine* strain. Kymographs from live-cell imaging of revealed nuclear movement in *myo51*Δ *CRIB-3xmcitrine* cells both in untreated and MBC-treated cells (Fig.4.6A). This suggests that Myo51 is not involved in actin cable-based nuclear movement in fission yeast.

Next I wanted to investigate if Myo52 is involved in actin cable-based nuclear movement. I constructed a *myo52*Δ *CRIB-3xmcitrine* strain. Consistent with previously published results, these cells grew slowly and showed altered morphology (Win et al. 2001). Live-cell imaging of MBC-treated *myo52*Δ *CRIB-3xmcitrine* cells revealed aberrant nuclear movement. Kymographs from these experiments showed the nucleus undergoing random and sudden movements, including movement away from the growing end (Fig.4.6B). By contrast, untreated *myo52*Δ *CRIB-3xmcitrine* cells showed normal nuclear movement. Interestingly, kymographs of these untreated cells revealed an increase in nuclear oscillations relative to wild-type cells, similar to that observed in *for3*Δ cells (Fig.4.6B). These results indicate that Myo52 is involved in actin cable-based nuclear movement in fission yeast.

The first, and most obvious, role for Myo52 in actin-based nuclear movement could be to directly link actin cables to the nucleus—for example, if Myo52 were associated with the nuclear surface. In this case, actin cables that is nucleated from the growing end of the cell contact the nucleus via Myo52, which is associated with the nuclear surface. As a result, in *myo52*Δ cells, actin cables failed to contact the nucleus and therefore, nuclear movement is affected. Myo52 would likely function in this context more as a “tether” rather than a “motor”, possibly because of the heavy mechanical load presented by the nucleus. A second possible role for Myo52 is suggested by recent results showing that in addition to functioning as a transport motor, Myo52 may also be involved in organization of actin cables, because *myo52*Δ cells showed curled and bundled actin cables (Lo Presti et al. 2012). Therefore, Myo52 might contribute to nuclear movement more indirectly, via its role in actin cable organization. Currently it is difficult to distinguish between these two possibilities, because the cytoplasmic tail region of Myo52, which is important for motility, is also important for actin cable organization (Mulvihill et al. 2006; Lo Presti et al. 2012). Therefore, any truncations or mutations in Myo52 that perturb motility will also affect the actin cable organization. In summary, actin cable-based nuclear movement in fission yeast is dependent on type V myosin, Myo52 and this role of Myo52 might be indirect due to its role in actin cable organization or direct where

Myo52 is linking the nucleus to the actin cables thereby helping in nuclear movement. However, this further needs to be carefully investigated.

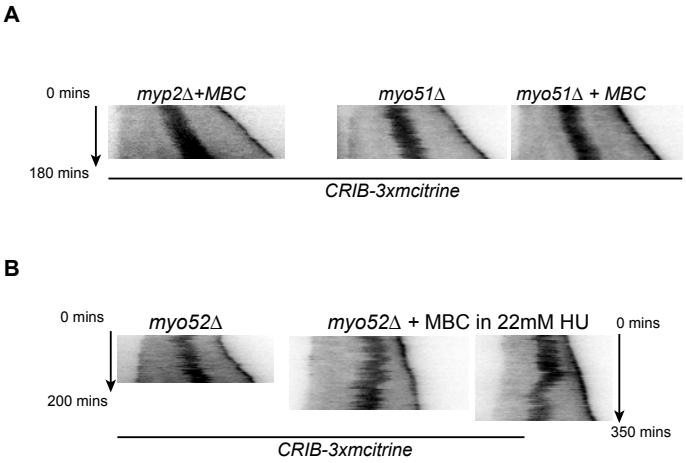

Figure 4.6. TypeV myosin, Myo52 is involved in actin cable-based nuclear movement in fission yeast. A) Kymographs plotted from live-cell imaging of *myp2*Δ cells treated with MBC shows that Myp2 is not involved in nuclear movement. Kymographs obtained from live-cell imaging of *myo51*Δ cells and *myo51* Δ cells treated with MBC continued to show nuclear movement suggesting Myo51 is not involved in nuclear movement. **B)** Kymographs plotted from live-cell imaging of *myo52*Δ cells treated with MBC shows aberrant nuclear movement suggesting that Myo52 is involved in nuclear movement in fission yeast. *myo52*Δ cells with intact MTs continue to show nuclear movement.

4.3 Discussion

In this chapter, I have shown a previously unknown role for actin cables in nuclear movement, which was previously thought to be exclusively MT-dependent. Previously, a role for MTs in nuclear movement was based on the observations that the nucleus was not maintained at the centre of the cell in conditions where MTs were depolymerized or not properly organized (e.g. MBC treatment, *mto1*Δ mutants, and tubulin mutants) (Hagan & Yanagida 1997; Tran et al. 2001; Sawin et al. 2004). For example, in *mto1*Δ cells, there are long abnormal stable MTs, and these could interact with the nucleus and lead to abnormal nuclear displacement that would normally not occur in a wild-type cell. Similarly, in tubulin mutants, MTs exists as short aberrant bundles, which could result in nuclear displacement leading to off-centred nucleus. However, even though this suggests MTs are important for nuclear positioning, it cannot rule out the possibility that nuclear movement is still continued in the absence of MTs. In this study, using optimized long-term live-cell imaging, drug perturbations and yeast mutants, I showed that indeed the nucleus is able to move in the absence of MTs, and this nuclear movement is dependent on actin cables and motor protein Myo52.

4.3.1 Microtubules and actin cables exert opposing forces on the nucleus

In fission yeast, precise central positioning of nucleus is important to define the future plane of cell division to ensure proper segregation of genetic material between daughter cells (Chang & Nurse 1996). Here, I have shown that in addition to the pushing forces on the nucleus, which are generated by MT bundles that are organized from the cell centre towards the cell tips, there are also pulling forces, which are dependent on actin cables that are nucleated from the cell tips towards the cell centre. This suggests that a net force exerted by these two pushing and pulling forces might be important for nuclear movement and subsequent central positioning. However, I have shown that nuclear off centring is much more pronounced in MBC-treated cells compared to *for3*Δ cells. Based on this I propose that MTs play a major role in nuclear centring in fission yeast by exerting pushing forces, whereas actin cables play a lesser role in nuclear centring. I have shown that in the absence of actin cables, the amplitude of nuclear oscillations due to pushing forces generated by MTs is much higher compared to wild-type cells. This led us to propose that pulling force generated by actin cables might be important for buffering the pushing forces

exerted by MTs. Additionally, actin cable-mediated nuclear positioning might be also important to position the nucleus in the centre of the cell especially in situations where cells are exposed to toxins or adverse environmental conditions, which might perturb the normal organization of MTs. In such situations actin cable-mediated nuclear movement might help to position the nucleus, thereby ensuring precise positioning of actomyosin ring and subsequently proper segregation of genetic material between the two daughter cells. Moreover, I have shown that in the absence of actin cables (*for3*Δ cells), cells are not able to precisely position the cytokinetic ring compared to control cells and this inaccurate positioning of septum leads to two unequal daughter cells. This suggests that actin cable-mediated nuclear movement might be important to produce two equal daughter cells after each cell division. However, the physiological significance of having two unequal daughter cells is still not clear and need more investigation.

4.3.2 Models for actin cable-based nuclear pulling

By artificially displacing the nucleus to the cell ends from the cell centre, I have shown that when the nucleus is very close to the growing tip, nucleus moves in the direction of the growing tip, whereas when nucleus is close to the non-growing tip, nucleus doesn't move at all. This suggests that actin cables, which are nucleated from the growing end of the cell might have to physically "reach" the nucleus in order to move the nucleus. Further, I have also shown that actin cable-based pulling of the nucleus involves class-V myosin Myo52. Here, I propose a model by which actin cables and Myo52 regulate nuclear movement. In this model, Myo52 might act as a "tether" or linker between the nucleus and actin cables, which are nucleated from the cell tip(s) towards the nucleus to pull the nucleus. In the model of actin cable nucleation proposed by Martin and Chang (Martin & Chang 2006), For3 is transiently recruited and activated at the cell tips followed by rapid actin cable assembly. For3 then moves inwards by retrograde flow with the elongating actin filament, which might lead to partial inactivation of For3. New For3 is recruited at the cell tips to nucleate more actin filaments, which will push the previous actin filaments further inwards. Once the actin filament depolymerizes, For3 recycles back to the cell tips and continues the cycle (Martin & Chang 2006; Kovar et al. 2011). In this way, actin cables undergo constant polymerization and depolymerization from the growing cell ends towards the cell centre. As a result, multiple actin cables are nucleated towards the cell nucleus and these cables might make transient contact with the nucleus via

Myo52 present on the nuclear membrane. Myo52 could then act to pull the nucleus towards the growing end of the cell.

In fission yeast, in vivo measurements of Myo52 showed two distinct types of movements –short, slow and erratic movement of ~0.25 μm/sec and fast, longer and directional movement (~0.5μm/sec) towards the cell pole or septum (Grallert et al. 2007). As mentioned before, Myo52 has been shown to be involved in transport of vesicles and different cell wall synthases such as Bgs1 (Mulvihill et al. 2006). It is possible that two separate pools of Myo52 exist in fission yeast where one pool of Myo52 is involved in transport of vesicles along the actin cables and hence exhibit the long, directional faster movements of Myo52, whereas the second pool of Myo52 might be associated with the nuclear surface. If this is the case, the short, slow and erratic movement of Myo52 might be due to MT-dependent pushing forces exerted on the nucleus causing nuclear oscillations and hence oscillation of Myo52 associated with the nuclear membrane. In order for this model to be true, Myo52 need to be localized on the nuclear membrane and therefore, this needs to be probed by imaging Myo52 to check if Myo52 localizes to the nuclear membrane. Additionally, slow and erratic movement of Myo52 might also be due to actin cables pulling on the nucleus via Myo52 present on the nuclear membrane. Since nucleus poses a heavy load, this movement of Myo52 associated with nucleus could be slow.

Previously, Lo Presti *et al.* (Lo Presti et al. 2012) showed that in addition to acting as a motor protein, Myo52 might also be involved in actin cable organization. They showed that by artificially tethering actin cables to nuclear envelope, actin cable organization defects observed in *myo52*Δ mutants were partially restored (Lo Presti et al. 2012). This supports our idea that Myo52 might be acting as a linker between the nucleus and actin cables enabling actin cables to pull the nucleus. Since the nucleus poses a heavy load, this might help to straighten up the actin cables, which are pulling the nucleus and thereby helping in actin cable organization. In addition, a kinesin 7-Myo52 tail chimera, which can deliver cargo on MTs, also partially restored the actin cable organization defects in *myo52*Δ cells (Lo Presti et al. 2012). This suggests that apart from possibly acting as a linker between nucleus and actin cables, Myo52 might be also contribute to actin cable organization by delivering different cargoes important for actin cable organization. However, it is difficult to differentiate between these two possibilities because any truncations or mutations in Myo52 that perturb motility will also affect the physical pulling-based actin cable organization (Grallert et al. 2007; Mulvihill et al. 2006).

A role for myosin motor proteins as a nucleocytoplasmic linker hasn't been reported in animal cells. However, in *Arabidposis thaliana,* a plant specific myosin

Myo XI-I localizes specifically to the nuclear membrane and physically interacts with outer nuclear membrane proteins WIT1 and WIT2, and this interaction is essential for nuclear movement (Tamura et al. 2013). In animal cells, a LINC (LInkers of Nucleoskeleton and Cytoskeleton) complex has been shown to link the nucleus with the cytoskeleton. This LINC complex includes an outer nuclear membrane protein such as nesprin 2G, which has a KASH domain, and an inner nuclear membrane protein such as SUN2 and forms a SUN-KASH bridge (Gundersen & Worman 2013; Luxton et al. 2010). Nesprin 2G and SUN2 form linear assemblies termed transmembrane actin-associated nuclear (TAN) lines, which provide a direct linkage between the nucleus and retrograde moving dorsal actin cables (Luxton et al. 2011). Additionally Samp1, a component of TAN lines, has also been shown to provide additional anchorage by binding to SUN2 (Borrego-Pinto et al. 2012). In fission yeast, two KASH domain proteins Kms1 and Kms2 and Samp1 homolog Ima1 have been reported (Miki et al. 2004; King et al. 2008). In order to investigate if Kms1 and Ima1 have a role in actin cable-based nuclear movement in fission yeast, I constructed and imaged *ima1*Δ*CRIB-3xmcitrine* and *kms1*Δ*CRIB-3xmcitrine* cells and treated them with MBC. In both *ima1*Δ and *kms1*Δ cells, nucleus continue to move suggesting that these proteins are not involved in actin cable-based nuclear movement in fission yeast (Data not shown).

Experiments carried out in this chapter show that perturbation of actin cables (*for3*Δ) or myo52 (*myo52*Δ) in the presence of MBC results in loss of nuclear movement or aberrant nuclear movement. Further, artificially displacing nucleus away from the actin cable-nucleating end in MBC-treated cells also results in loss of nuclear movement. Although, these experiments show that actin cables and myo52 are involved in nuclear movement, in future I would like to investigate how an increase in number of actin cables or Myo52 might affect nuclear movement. This will provide a positive evidence for how affecting actin cables and Myo52 have a direct consequence of nuclear movement. Both For3 and Myo52 can be overexpressed to increase the number of actin cables and Myo52 and I would like to investigate nuclear movement in these overexpressed cells. Additionally, I can also use CK-666, a drug that specifically depolymerize actin patches without affecting actin cables. It was previously reported that 25µg/ml of CK-666 depolymerizes actin patches and as a result more monomeric actin is available to make actin cables resulting an increase in actin cables (Burke et al. 2014). I would like to study nuclear movement under these conditions as well.

Additional possible mechanisms for nuclear movement in fission yeast

Although I have shown that actin cables and Myo52 are involved in nuclear movement, it is possible that the role-played by actin and Myo52 in nuclear movement is indirect and/or additional players/mechanisms are also involved in MT-independent nuclear movement in fission yeast.

In eukaryotic cells, Endoplasmic reticulum (ER) exists as a large membrane bound organelle with different structural domains and is involved in synthesis of lipids, storage and release of calcium and protein synthesis. The largest domain of the endoplasmic reticulum (ER) is associated with the nuclear envelope, whereas the peripheral ER, which consists of network of tubules and cisternae make contacts with plasma membrane and other organelles such as mitochondria, endosomes, Golgi and lysosomes (Phillips & Voeltz 2015). In fission yeast, similar to higher eukaryotes, the ER is made up on an extensive network of tubules and cisternae continuous with the nuclear envelope and make contacts with the plasma membrane (Zhang et al. 2010; Zhang et al. 2012). Previously it was shown that vesicle-associated membrane protein-associated proteins (VAPs) Scs2 and Scs22 are important for ER-plasma membrane attachment. Interestingly, it was previously shown that ER is actively delivered to the cell tips on actin cables in a myo52-dependet manner (Zhang et al. 2012). This suggests the possibility that loss of nuclear movement in *for3*Δ MBC-treated cells treated could potentially be due to role of actin cables and Myo52 in transport of ER components. Indeed, in *scs2*Δ*scs22*Δ cells, percentage of cells showing off-centred septa was higher compared to wild-type cells similar to what I have observed in *for3*Δ cells (Zhang et al. 2012). In future, it will be interesting to investigate what happens to nuclear movement in *scs2*Δ*scs22*Δ cells treated with MBC. If these cells show loss of nuclear movement, this will indicate a novel role for ER in nuclear movement in fission yeast.

Another possible mechanism for nuclear movement consistent with my observation is cytoplasmic streaming. Cytoplasmic streaming is a process in which objects are moved inside the cell due to the flow of cytoplasm (Quinlan 2016). Cytoplasmic streaming is generally observed in large cells such as plant cell and oocytes of many metazoan species. A direct role for cytoplasmic streaming in yeast has not been reported. Both actin and myosin have been implicated in cytoplasmic streaming. For example, during meiotic spindle positioning, an actin meshwork and myosin V is important for active diffusion of vesicles (Almonacid et al. 2015).

In summary, I have shown that nuclear movement in fission yeast involves both MTs and actin cables. MT-based pushing position the nucleus at the centre,

whereas actin cable-based pulling might buffer the pushing force exerted by MTs. This actin cable-based pulling also involves Myo52, which might act as a linker between actin cables and nucleus and this tethering might be important for proper organization of actin cables. Previously I have shown that myo52Δ cells when treated with MBC showed aberrant nuclear movement. If nuclear movement is dependent on force generated by cytoplasmic streaming due to transport of vesicles by Myo52, this does not explain how nucleus show aberrant movement in the absence of Myo52. Therefore, nuclear movement in fission yeast due to cytoplasmic streaming is highly unlikely.

Chapter 5: Multiple internal cues cooperate and compete to establish polarized growth in fission yeast

5.1 Introduction

Fission yeast cells grow in a highly polarized fashion in a cell cycle-dependent manner (Martin & Chang 2005). Initially, upon cell division, the two new daughter cells only grow from their old ends (inherited from their mother cell) and later when cells enter G2 phase, cells establish new end growth - a process termed as NETO (Mitchison & Nurse 1985). This suggests that polarized growth in fission yeast is highly regulated in space and time.

Previously, Tea1 was identified as an important polarity landmark transported on the plus end of the MTs to mark the cell tips for active growth (Mata & Nurse 1997; Verde et al. 1995). Indeed, *tea1*Δ cells failed to show normal growth pattern of fission yeast cells and instead grow strictly monopolar with one daughter cell growing exclusively from the old end, whereas the other daughter cell growing exclusively from the new end (Mata & Nurse 1997). This growth pattern of Tea1 suggests that even though Tea1 is important for normal polarized growth in the fission yeast, in the absence of Tea1 other landmarks might be involved in establishment of polarized growth. More interestingly, multiple cues might be involved in establishing polarized growth in *tea1*Δ cells because the two daughter cells of *tea1*Δ cells grow from different cell ends.

An SH3 domain protein Tea4 links Tea1 with the actin cable nucleating protein For3 and recruits For3 to the growing cell tips (Martin et al. 2005). These cables act as tracks for myosin-V mediated transport of secretory vesicles and cell wall synthases in order to promote polarized growth (Martin et al. 2005; Win et al. 2001; Motegi et al. 2001). However, this is a rather simplified model because *for3*Δ cells do not show the monopolar growth pattern of *tea1*Δ cells and moreover For3 is still recruited to the old ends in *tea1*Δ cells (Feierbach et al. 2004; Martin et al. 2005). All these results indicate that multiple redundant pathways involving spatial landmarks, MTs and actin cables might be involved in regulation of polarized growth in fission yeast. However, the redundancy of these pathways made it difficult to understand how different cues are involved in this polarized growth.

In this chapter, using a combination of optimized live-cell imaging, polarity mutants and drug perturbations, I address how polarized growth is established by cooperation and competition between multiple internal polarity cues.

5.2 Results

5.2.1 Microtubules are important for establishment of bipolar growth in fission yeast

Although MTs are known to transport polarity proteins Tea1 and Tea4, which are important to establish bipolar growth, a direct role for MTs in establishment of bipolar growth was never studied before. Therefore, I decided to investigate if MTs are required for establishment of bipolar growth in fission yeast. In order to address this, I depolymerized MTs using the drug MBC in *CRIB-3xmcitrine* cells. CRIB binds to GTP-bound form of Cdc42 and can be used as a reporter for active Cdc42, which is present only on the growing end of the cell, making it easy to distinguish between monopolar and bipolar growing cells (Tatebe et al. 2008) (Mutavchiev *et al.*, submitted).

Previously Sawin *et al.* showed that once an axis of polarity is established, MTs are not required to maintain polarized growth at the cell tips (Sawin & Snaith 2004). As a result, depolymerization of MTs in an asynchronously growing population of cells gave a mixture of both monopolar and bipolar cells, making it difficult to interpret the effect of MT depolymerization on establishment of bipolar growth. In order to overcome this problem, I devised a simple imaging criterion that could check the effect of MT depolymerization on transition from monopolar to bipolar growth. *CRIB-3xmcitrine* cells were treated with 25µg/ml MBC to depolymerize the MTs. MTs were completely depolymerized within 15 minutes at 25˚C (Fig.5.1A). Live-cell imaging was carried out on these asynchronously growing MBC-treated *CRIB-3xmcitrine* cells. During analysis, in order to avoid cells that already established bipolar growth before addition of MBC and to differentiate between whether depolymerization of MTs results in delayed NETO vs. failure to establish NETO, I only considered those cells that I can track from the start of the cell cycle to end of the cell cycle (Fig. 5.1B). In control *CRIB-3xmcitrine* cells imaged in conditioned minimal medium (C-SGALU), approximately 60% of the cells established bipolar growth, whereas 40% of the cells remained monopolar throughout the cell cycle (Fig. 5.1C). However, in MBC-treated *CRIB-3xmcitrine* cells imaged in C-SGALU, almost all the cells failed to establish bipolar growth (Fig. 5.1C). This shows that MTs are important for the establishment of bipolar growth in fission yeast. While this work was being written up, Das *et al.* independently showed that depolymerization of MTs results in failure to establish bipolar growth (Das et al. 2015).

5.2.2 NETO failure upon depolymerization of MTs is severe in minimal medium compared to rich medium

Next, I wanted to investigate if role-played by MTs in establishment of bipolar growth is dependent on the growth medium in which cells are imaged. In fission yeast, key cellular processes including cell growth, division, cytoskeletal organization and protein synthesis are dependent on different stress pathways such as Sty1 MAPK stress response and target of rapamycin (TOR) pathways (Shiozaki & Russell 1995; Petersen & Nurse 2007; Petersen & Russell 2016). These pathways respond differently to different external environments, including growth medium (Petersen & Russell 2016). Fission yeast cells are generally grown in complex rich medium or synthetic minimal medium (see materials and methods). Previously Mitchison and Nurse (Mitchison & Nurse 1985) reported that depending on the growth medium, fission yeast cells show different growth rates and times in the cell cycle at which NETO takes place. In minimal medium with ammonia as nitrogen source, NETO takes place at 0.49 of a cell cycle (that is, within a 4h generation time), whereas in rich medium, NETO takes place at 0.34 of a cell cycle (within a 2 h 10 min generation time).

In order to investigate this, I depolymerized MTs in *CRIB-3xmcitrine* cells imaged in rich medium. While DMSO-treated cells imaged in C-SGALU cells showed 60% bipolar growth and 40% monopolar growth, DMSO-treated cells imaged in rich medium showed 100% bipolar growth (Fig. 5.1D). Similarly, while almost all the MBC-treated cells failed to establish bipolar growth in C-SGALU, only 60% of the MBC-treated cells failed to establish bipolar growth in rich medium (Fig. 5.1D). This shows that similar to other cellular processes influenced by growth media, role-played by MTs in establishment of bipolar growth is also dependent on the growth media in which cells are imaged. This difference in number of cells showing NETO failure in minimal medium vs. rich medium suggests that MTs might be essential for establishment of bipolar growth in minimal medium, whereas MT-independent factors might contribute to establishment of bipolar growth in rich medium.

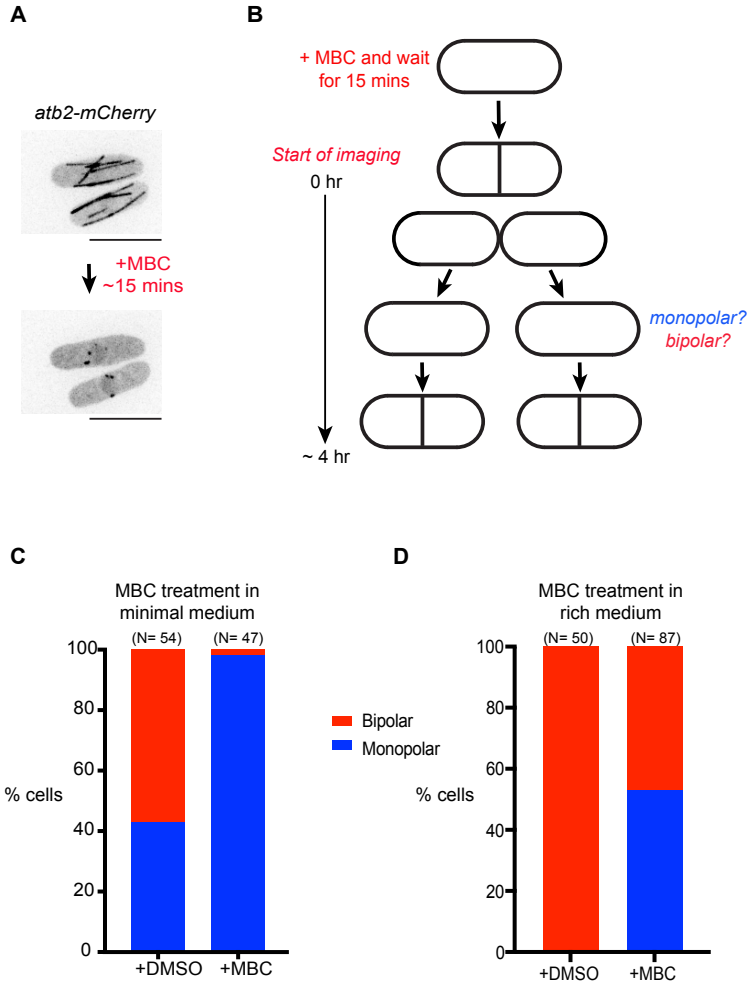

Figure 5.1 Microtubules are important for establishment of bipolar growth. **A)** MTs labelled by *atb2-mCherry* are depolymerized in ~15 mins after MBC addition. **B)** Schematic representation of the criteria used for scoring growth polarity after MT depolymerization. 25µg/ml of MBC is added to depolymerize the MTs, followed by live-cell imaging for 4 hours to study the growth patterns. After MBC addition, I considered only those cells that I can track from the start of the cell cycle to end of the cell cycle. **C)** In minimal medium, 60% of control cells establish bipolar growth and upon depolymerization of MTs, almost all cells fail to establish bipolar growth. **D)** In rich medium, all control cells establish bipolar growth and upon depolymerization of MTs, approximately 50% of cells fail to establish bipolar growth.This shows that MTs are essential for NETO in minimal medium, whereas MT-indepndent establishment of NETO can occur in rich medium. Scale, 10µm

5.2.3 Depolymerization of MTs at different stages of cell cycle gives two different growth patterns of polarized growth

I have shown that depolymerization of MTs results in failure to establish bipolar growth or NETO. Surprisingly, upon depolymerization of MTs in the mother cells, two different patterns of polarized growth were observed in the daughter pairs. In a subset of daughter pairs, both the daughter cells grew monopolarly from their old ends inherited from their mother cell from the previous cell cycle. This growth pattern is similar to the growth pattern of wild type cells before NETO and is hereafter referred to as “anti” pattern (Fig. 5.2B). In the second subset of daughter pairs, one daughter cell grew from the old end, whereas the other daughter cell grew from the new end or the end generated by septation (Fig. 5.2B). This growth pattern of daughter pair is similar to previously reported growth pattern observed in polarity mutants such as *tea1*Δ, *tea4*Δ, *tea3*Δ and *pom1*Δ and hereafter referred to as “syn” pattern (Niccoli et al. 2003; Mata & Nurse 1997; Martin et al. 2005; Tatebe et al. 2005). Therefore, I wanted to investigate why depolymerization of MTs gave these two different growth patterns. Since MBC was added into asynchronously growing cells, I hypothesized that these two growth patterns might be dependent on the time in the cell cycle at which MTs were depolymerized.

In order to check this hypothesis, I depolymerized MTs in *CRIB-3xmcitrine* cells during live-cell imaging. MBC was added to *CRIB-3xmcitrine* cells under the microscope after imaging for 2.5 hours and continued imaging after MBC addition for 4 more hours (Fig. 5.2A). In this way I could observe MTs being depolymerized at different stages of cell cycle and could track the growth patterns of the resulting daughter pairs. When MBC was added after disassembly of the septum in the mother cell, 82% of the daughter pairs grew in an anti pattern (Fig. 5.2C). On the other hand, when MBC was added before disassembly of the septum in the mother cell, 78% of the daughter pairs grew in a syn pattern (Fig. 5.2C). This suggest that MTs might be regulating polarized growth at different stages of the cell cycle and therefore, depolymerization of MTs before or after disassembly of the septum in the mother cell give rise to different growth patterns in the daughter pairs.

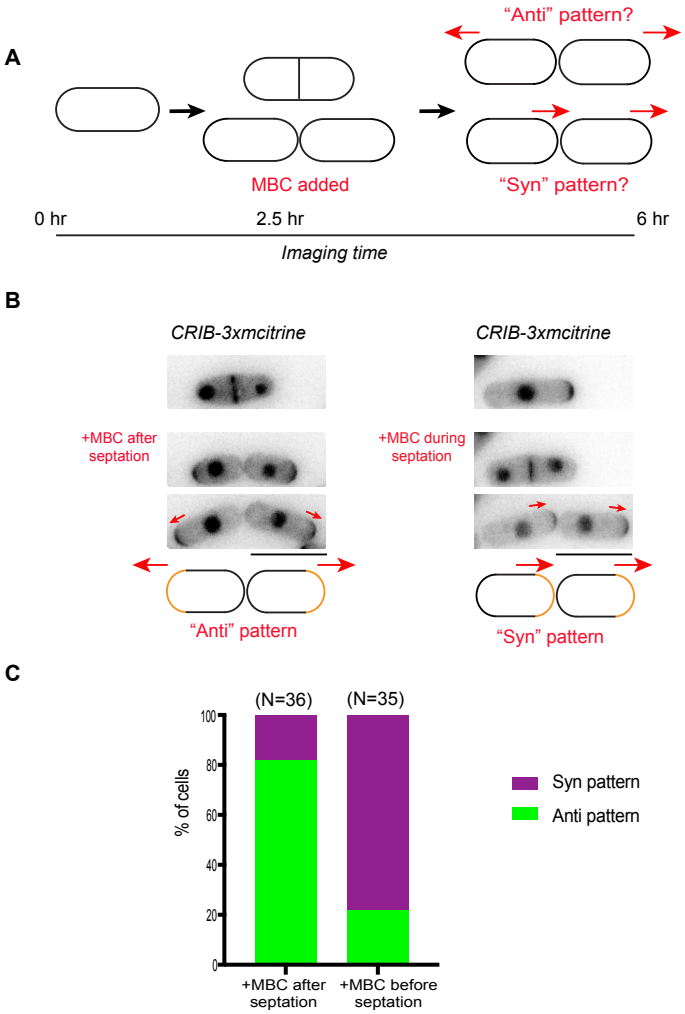

Figure 5.2. Depolymerization of MTs before and after disassembly of the septum gives two different growth patterns. A) Imaging strategy to investigate the two growth patterns. *CRIB-3xmcitrine* cells were imaged for 2.5 hours, followed by addition of 25µg/ml MBC under the microscope to depolymerize the MTs and continued imaging to investigate the growth patterns of daughter pairs. **B)** Depolymerization of MTs after disassembly of the septum in *CRIB-3xmcitrine* cells imaged in minimal medium mostly gave an anti growth pattern, whereas depolymerization of MTs before disassembly of the septum mostly gave a syn growth pattern. **C)** Percentage of cells showing anti and syn growth pattern upon depolymerization of MTs after and before disassembly of the septum respectively. Scale, 10µm.

5.2.4 Post anaphase arrays are not required for the syn growth pattern

Next, I wanted to investigate why depolymerization of MTs before and after disassembly of the septum results in syn vs. anti growth pattern. I first hypothesized that this different growth patterns might depend on the post anaphase array (PAA) of MTs that forms during cell division. In fission yeast, MTs undergo dramatic changes in their organization during different stages of cell cycle (Sawin & Tran 2006). During interphase, MTs exists as anti-parallel bundles spanning the long axis of the cell. When cells enter mitosis, MTs reorganize into mitotic spindle and astral MTs. Finally, at the close of mitosis during cell division, MTs organize into a post anaphase array (PAA) (Fig. 5.3A) (Sawin & Tran 2006; Tran et al. 2001). Nucleation of PAA MTs depends on the prior formation of the cytokinetic actin ring (CAR) and the PAA MTs in turn stabilize the position of the CAR during delayed cytokinesis. Even though the precise function of the PAA MTs are not known, PAA MTs are thought to play a role in setting up the initial state of MT organization for the next interphase and to keep the daughter nuclei away from each other and from the division site during mitosis (Sawin & Tran 2006).

I proposed that PAA MTs of the mother cell might be important for reinitiating polarized growth at the old ends of the daughter pairs and therefore, depolymerization of MTs before disassembly of the septum failed to give anti growth pattern. In fission yeast, during mitosis, cell growth ceases at the cell tips and is redirected to the cell septum. Moreover, MTs that are important for transport of different polarity proteins to the cell tips are no longer organized into long anti-parallel bundles spanning the long axis of the cell. As a result, during septation, PAA MTs of the mother cell might be important to redirect polarity proteins from the septum to the cell tips to reinitiate polarized growth.

In order to determine whether the PAA MTs are required for generating anti growth pattern or to reinitiate growth at the old ends, I used an *mto1-427* strain, which fails to nucleate PAA but can nucleate all other MT structures (Samejima et al. 2010). In fission yeast, Mto1/Mto2 protein complex localizes to different MTOCs and recruits the γ-tubulin complex in order to nucleate cytoplasmic MTs (Sawin et al. 2004; Samejima et al. 2010) This targeting of Mto1 to different MTOCs is dependent on the conserved C-terminal region of Mto1. A triple point mutation in the C-terminal region of Mto1 (*mto1-427*) failed to localize Mto1 to eMTOCs (equatorial), which are important to nucleate PAA MTs (Samejima et al. 2010). First, I constructed an *mto1-427 CRIB-3xmcitrine* strain. Live-cell imaging of *mto1-427 CRIB-3xmcitrine* cells showed growth patterns similar to wild type cells and did not show any increase in

“syn” growth pattern (Fig. 5.3B). This refutes my hypothesis of PAA MTs requirement to reinitiate growth at the old ends or grow in an “anti” pattern and suggests that a different mechanism might be responsible for generating the syn growth pattern.

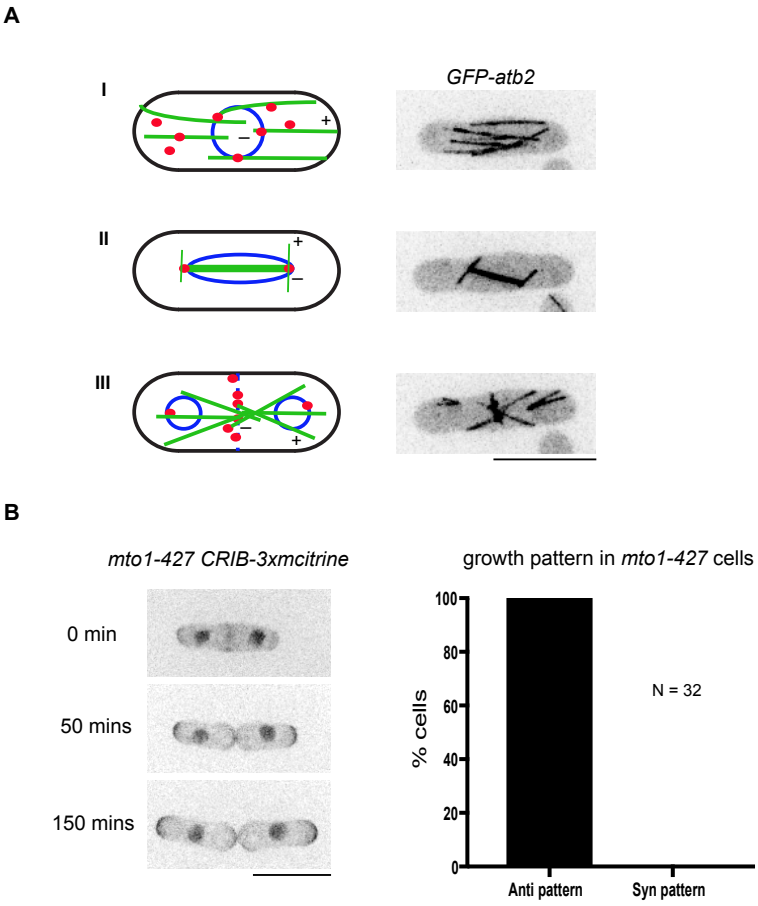

Figure 5.3. Post anaphase array (PAA) MTs are not required for establishment of polarized growth at the old ends. A) Left panel shows schematic representation of cell cycle-dependent organization of MTs in fission yeast (adapted from Sawin and Tran, 2006). (I) Interphase MTs (green) nucleated from iMTOCs (red) associated with the nuclear envelope (blue), cytoplasm and MTs themselves. (II) Mitotic astral MTs nucleated from SPBs on the nuclear envelope. (III) PAA nucleated from the eMTOCs. Right panel shows MTs labelled by *GFP-atb2* at different stages in cell cycle. **B)** *mto1-427 CRIB-3xmcitrine* cells establish polarized growth at the old ends of the daughter pairs similar to wild-type cells showing that PAA MTs are not required for anti growth pattern and syn pattern is not generated due to depolymerization of PAA MTs. Graph showing percentage of cells showing anti and syn growth pattern in *mto1-427 CRIB-3xmEcitrine* cells. Scale, 10µm.

5.2.5 Differential Tea1 localization upon MT depolymerization might be responsible for syn growth pattern

I have shown that depolymerization of MTs in the mother cell before disassembly of the septum results in syn growth pattern in the daughter pairs. This growth pattern as mentioned before is similar to growth pattern observed in *tea1*Δ daughter pairs (Mata & Nurse 1997). Therefore, I hypothesized that the syn growth pattern I observed in wild-type cells might be dependent on behaviour of Tea1 in response to MT depolymerization. Tea1 was identified as an important polarity cue that is transported on the plus end of the microtubules to reach the cell tips and regulate polarized growth (Mata & Nurse 1997). Similar to MBC-treated wild-type cells, *tea1*Δ cells failed to establish bipolar growth suggesting that syn and anti patterns generated in MBC-treated wild-type cells might be due to Tea1 behaviour upon MT depolymerization. Previously it was shown that Tea1 localizes to both growing and non-growing ends of the cell, and upon septation, Tea1 also localizes to the cell septum (Mata & Nurse 1998). In order to investigate how Tea1 localization is affected by MT depolymerization, I did live-cell imaging of *tea1-GFP* cells. In wild type interphase cells, consistent with previous observations, Tea1 localized to both growing and non-growing ends, and during cell division, Tea1 localized both to cell tips and to the cell septum (Fig. 5.4A).

In order to investigate the behaviour of Tea1 upon depolymerization of MTs, I added MBC (25µg/ml) to *tea1-GFP* cells under the microscope during imaging. In this way I could check the behaviour of Tea1 in the same cells both before and after depolymerization of MTs. Kymographs plotted from live-cell imaging of *tea1-GFP* cells showed that in bipolar-growing cells, Tea1 remained at the cell tips after depolymerization of MTs, although the tea1 signal at the cell tips was decreased (Fig. 5.4B). Surprisingly, in monopolar-growing cells, upon depolymerization of MTs, Tea1 remained on the growing cell tip albeit with decreased signal, but disappeared from the non-growing tip within ~15 mins (Fig. 5.4B). This indicates that Tea1 shows different stability at growing and non-growing ends upon depolymerization of MTs.

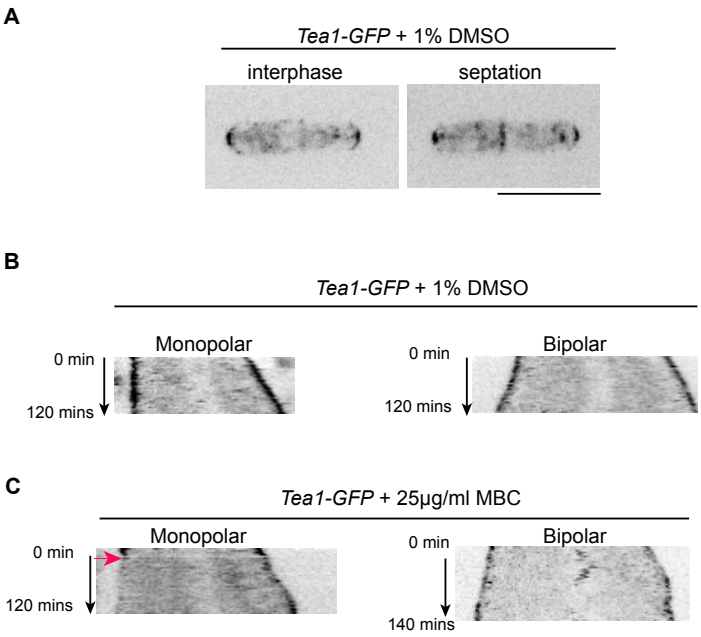

Figure 5.4. Tea1 shows differential stability at the growing end vs. non-growing end after depolymerization of MTs. A) Localization of Tea1 during interphase and septation. Tea1 localizes to the cell tips during interphase and localizes to the septum during septation. B) Tea1 localizes to both growing and non-growing ends in wild-type cells. Kymogrpahs obtained from live-cell imaging of control monopolar and bipolar cells show Tea1 localized to both growing and non-growing ends. **C)** Kymographs obtained from live-cell imaging of MBC-treated cells show Tea1 localizes to both the the ends in bipolar cells, whereas Tea1 falls off from the non-growing end in monopolar cells. This shows that Tea1 exhibits different stability at the cell tips upon depolymerization of MTs Scale, 10 µm.

5.2.6 Differential Tea1 stability at growing vs. non-growing end upon MT depolymerization might be responsible for syn and anti growth patterns

Having shown that Tea1 exhibits differential stability at growing and non-growing ends upon depolymerization of MTs, I hypothesized that syn and anti growth patterns in daughter pairs might be dependent on this differential Tea1 stability at the cell tips after MT depolymerization (Fig. 5.5A-B). According to my hypothesis, if MTs are depolymerized after disassembly of septum, Tea1 will have already been transported to the old ends of the daughter pairs to initiate cell growth, and hence Tea1 would remain at the growing old ends. However, in the case of Tea1 present at the non-growing ends of the daughter pair, Tea1 will disappear immediately in the absence of MTs. As a result, the daughter pair would fail to establish bipolar growth and instead grow in an anti pattern (Fig. 5.5A). By contrast, if MTs were depolymerized before disassembly of septum in the mother cell, Tea1 would fall off from the non-growing cell tips of the mother cell. This is because during septation, all "growth" is at the septum instead of cell tips. Therefore, immediately after cell division, one daughter cell would fail to establish polarized growth at the old end due to lack of Tea1 landmark and instead grow from the new end, probably using cues generated by septation. The other daughter cell, however, would still grow from the old end, and this growth would be therefore expected to be dependent on a cue that is independent of MTs and Tea1 (Fig. 5.5B). This MT and Tea1-independent cue might be the same cue that establishes polarized growth at old end in a *tea1*∆ cell.

In order to investigate this hypothesis, I constructed a *tea1-mEcitrine bgs4-Cherry* strain. Because Tea1 is tagged with mEcitrine I could not use CRIB-3xmcitrine as a growth reporter. Bgs4 is one of the catalytic subunits of (1,3) β-D-glucan synthase, an enzyme complex involved in the synthesis of major cell wall component (1,3) β-D-glucan (Cortés et al. 2005). Bgs4 is an essential gene important for polarized growth and cytokinesis (Cortés et al. 2005). Similar to CRIB, Bgs4 is localized to the growing cell tips only during interphase and to the septum only during septation (Fig. 5.6A). Live-cell imaging of *bgs4-cherry CRIB-3xmcitrine* cells showed that *CRIB-3xmcitrine* and *bgs4-cherry* colocalize to the cell tips and septum, and hence Bgs4 can be used as a growth reporter similar to CRIB-3xmcitrine (Fig. 5.6A). I did live-cell imaging of *tea1-mEcitrine bgs4-Cherry* and depolymerized MTs during imaging to study the localization of Tea1 in relation to syn and anti growth patterns. However, unlike cells with untagged Tea1 (*CRIB-3xmcitrine* cells), *tea1-mEcitrine bgs4-cherry* cells failed to show a syn pattern when MTs are depolymerized before disassembly of septum (Fig. 5.6B). This failure to show syn pattern is not due to

tagging of Bgs4 because *bgs4-Cherry* (untagged Tea1) cells show syn pattern of growth upon depolymerization of MTs before disassembly of septum (Fig. 5.6B). This suggests that C-terminal tagging of Tea1 with mEcitrine might be making Tea1 more stable or "sticky" at the cell tips (i.e. a longer residence time) and therefore the rate of decay of Tea1 from the cell tips might be slower. As a result, if MTs are depolymerized before disassembly of septum, Tea1 might still remain at the non-growing ends of mother cell and hence can initiate growth at the old ends of the daughter pairs resulting in an anti pattern of growth. This further provides indirect evidence for the hypothesis that rate of decay of Tea1 from the cell tips upon depolymerization of MTs might be responsible for syn and anti growth patterns. However, it is important to bear in mind that how Tea1 behaviour upon depolymerization of MTs affects growth patterns of daughter pairs need to be further investigated.

I also constructed *tea1-GFP bgs4-cherry* and *tea1-mCherry CRIB-3xmcitrine* strains to study the behaviour of Tea1. Similar to *tea1-mEcitrine* cells, both *tea1-GFP* and *tea1-mCherry* cells also failed to show syn growth pattern upon depolymerization of MTs during septation (Fig. 5.6B). These results indicate that tagging of Tea1 likely affects dynamics of Tea1 and therefore might not be suitable for studying patterns of daughter cell growth. In order to explore other tagged versions of Tea1; I also constructed *tea1-3xmEcitrine bgs4-cherry* and *tea1-3xmCherry CRIB-3xmcitrine* strains. In both these strains, cell growth seems to be affected even in the absence, of MBC, as both *CRIB-3xmcitrine* and *bgs4-cherry* were displaced from the cell tips to the cell sides intermittently at random times (data not shown). This clearly suggests that C-terminal tagging of Tea1 alters the stability of Tea1 and therefore it may not be possible to directly demonstrate whether Tea1 stability after depolymerization of MTs is responsible for syn and anti growth patterns.

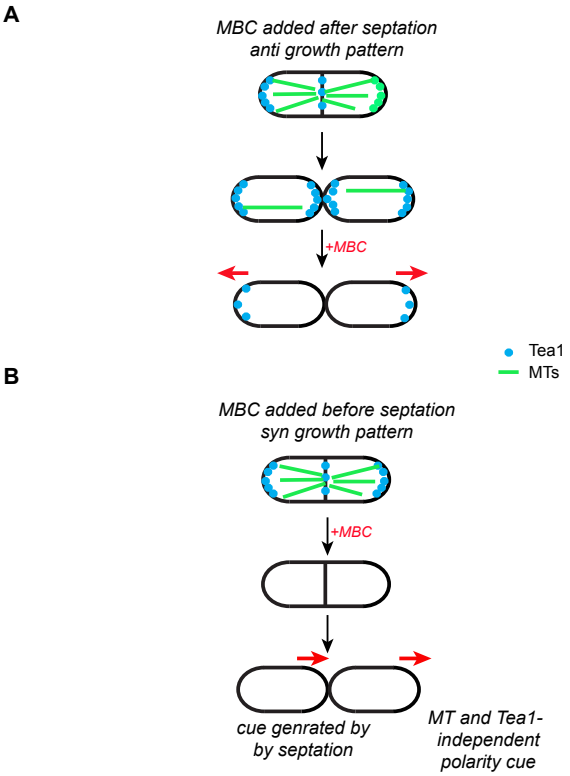

Figure 5.5. Model for differential Tea1 stability upon MT depolymerization resulting in syn and anti growth patterns. A) According to the model, if MTs (green) are depolymerized after disassembly of the septum , Tea1 (blue) will have already been transported to the old ends of the daughter pair and therefore, grow in an anti pattern (similar to wild-type pre-NETO cells). **B)** If MTs are depolymerized before disassembly of the septum, Tea1 will fall-off from the non-growing cells ends and cells will grow in a syn pattern where one daughter cell grow from the old end, probably using a MT and Tea1-independent cue and the other daughter cell grow from the new end, probably using a cue generated by septation.

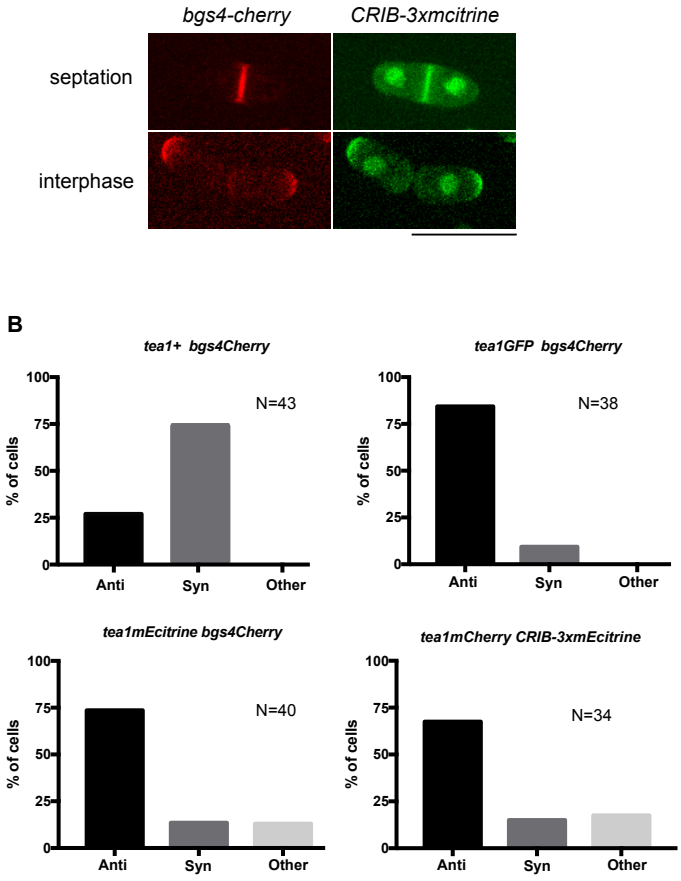

Figure 5.6. C-terminal tagging of Tea1 affects the stability of Tea1 at the cell tips. A) Bgs4 and CRIB-3xmcitrine colocalize at the growing cell tips and cell septum, making Bgs4 a suitable polarity marker similar to CRIB-3xmcitrine **B)** Growth pattern of daughter pairs in which MTs are depolymerized before disassembly of the septum. In *tea1mEcitrine*, *tea1GFP* and *tea1mCherry* cells, majority of daughter pairs grow in an anti pattern instead of syn pattern observed in *tea1+bgs4-cherry* cells suggesting C-terminal tagging of Tea1 might be affecting the stability of Tea1 at the cell tips. Scale, 10 µm.

5.2.7 what are the microtubule and Tea1-independent polarity cues?

Next, I wanted to investigate how polarized growth is established in syn-growing daughter pairs observed in *tea1*∆ mutants and wild-type cells treated with MBC before septum disassembly. What is remarkable is that in syn growing daughter pairs, the two daughter cells have different fates i.e. one daughter cell grow only from the old end while the other daughter cell grow only from the new end. This suggests that there might be different mechanisms or cues regulating polarized growth in these syn-growing daughter pairs. Previously, it was reported that in syn-growing daughter pairs of *tea1*∆ cells, the daughter cell growing from the old end always inherited the old growing-end of the mother cell, whereas the daughter cell growing from the new end grew from the end generated from septation (Niccoli et al. 2003; Mata & Nurse 1997)(Fig. 5.7A) (96% cells, n = 158). Therefore, I hypothesized that in a syn-growing daughter pair generated by depolymerization of MTs, the daughter cell growing from the old end might inherit the old growing end of the mother cell. Indeed, live-cell imaging of *CRIB-3xmcitrine* cells treated with MBC showed that in 98% of the daughter pairs (n=45), the daughter cell growing from the old end always inherited the old growing end of the mother cell. This suggests that the growth orientation of mother cell somehow seems to dictate the growth pattern of the daughter pairs (Fig. 5.7A).

I propose that this inheritance of growth orientation from the mother to the daughter cell might be dependent on a “memory” cue because even though cell growth is stopped at the cell tips during septation, the old-end of the mother cell seems to “remember” that it used to be the growing end and reinitiate growth again at the same end in the daughter cell in the next cell cycle. Hence, I refer to this as growth “memory-based” polarity cue. However, In the case of the daughter cell growing from the new end it might depend on a “default” cue generated from what is remained from septation (Fig. 5.7B). This poses two important questions – 1) why does the daughter that inherit the old growing end of the mother cell only grow at its old end and not the new end? 2) Why does the daughter that inherits the non-growing end of the mother grow only at its new end and not the old end?

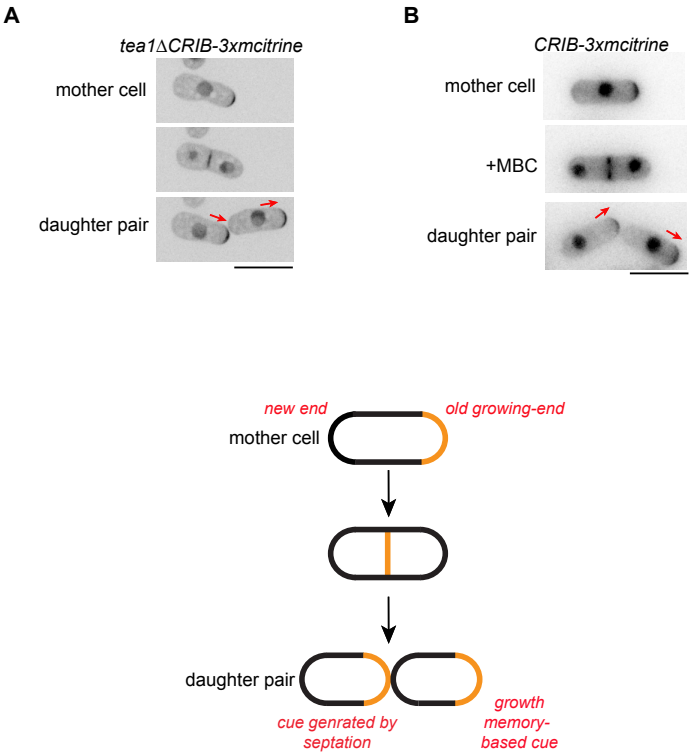

Figure 5.7. A model in which, in the absence of Tea1 and MT-based cue, cell polarity follows a growth memory-based cue and cue generated by septation. A) *tea1Δ CRIB-3xmcitrine* cells grow in a syn pattern where daughter cell growing from the old end inherit the old-growing end of the mother cell. The daughter cell growing from the new end might depend on a cue generated by septation. **B)** *CRIB-3xmcitrine* cells treated with MBC before disassembly of the septum in the mother cell show syn pattern. The daughter cell growing from the old end always inherit the old-growing end of the mother cell and the other daughter cell grow from the new end. **C)** Model for Tea1 and MT-independent polarity cue-based establishment of polarized growth. In the absence of Tea1 and MT-based cues (*tea1Δ* and MBC-treated cells), cells will depend on a growth memory-based cue inherited from the old-growing end of the mother cell to the old end of the daughter cell and a cue generated by septation to establish polarized growth at the new end in the daughter cell that did not inherit the old-growing end of the mother cell. Scale, 10μm.

5.2.8 Actin cable-based transport clears growth cues from the new end thereby reinforcing old-end growth

Next, I wanted to investigate why the daughter cell growing from the old end does not grow from the new end or use the cue generated by septation in a syn-growing daughter pair? I hypothesized that since syn pattern is generated upon depolymerization of MTs, polarized growth initiated by the growth "memory"-based cue promotes actin cable nucleation from the old end towards the new end and this cables might clear cues generated by septation with the help of actin cable-based transporter such as Myo52. I propose that this actin cable-based clearance of septation cues might also exist in wild type cells to ensure that immediately after cell division, daughter pairs only grow from their old ends and not from their new ends.

In order to determine whether actin cable-based transport is involved in clearing cues generated by septation from the new ends, I constructed *for3∆CRIB-3xmcitrine* and *myo52∆CRIB-3xmcitrine* strains. As mentioned before, in fission yeast, actin cables are nucleated by formin For3 and these cables are used as a track for transport of different cargo by motor protein Myo52 (Feierbach & Chang 2001; Win et al. 2001; Motegi et al. 2001; Nakano et al. 2002) From live-cell imaging of *for3∆CRIB-3xmcitrine* and *myo52∆CRIB-3xmcitrine* cells I found that these cells grow in a premature bipolar fashion. In these cells, after cell division, the daughter pairs initiated growth from their new ends immediately instead of initially growing monopolar and then switching to bipolar growth (n= 12 daughter pairs) (Fig. 5.8A-B). By contrast (and as expected), in control *CRIB-3xmcitrine* cells, upon cell division, the daughter cells initially grow only from their old ends and initiated new end growth only at a later stage in cell cycle (Fig. 5.8A-B). This is consistent with my hypothesis that actin cable-based transport might be involved in clearing cue generated by septation from the new ends. Further, this suggests that failure of new end growth in the daughter cell inheriting the old end of the mother in a syn pattern might be due actin-based clearance of cues generated by septation. Previously Feierbach *et al.* showed that *for3∆* cells show an asymmetric growth pattern where one daughter cell grows monopolar while the other daughter cell grows bipolar (Feierbach & Chang 2001). The difference in growth pattern here I believe might be due to difference in the way imaging was carried out. Feierbach *et al*. carried out imaging of *for3∆* cells on agarose pads, which I have previously shown to cause stress to the cells.

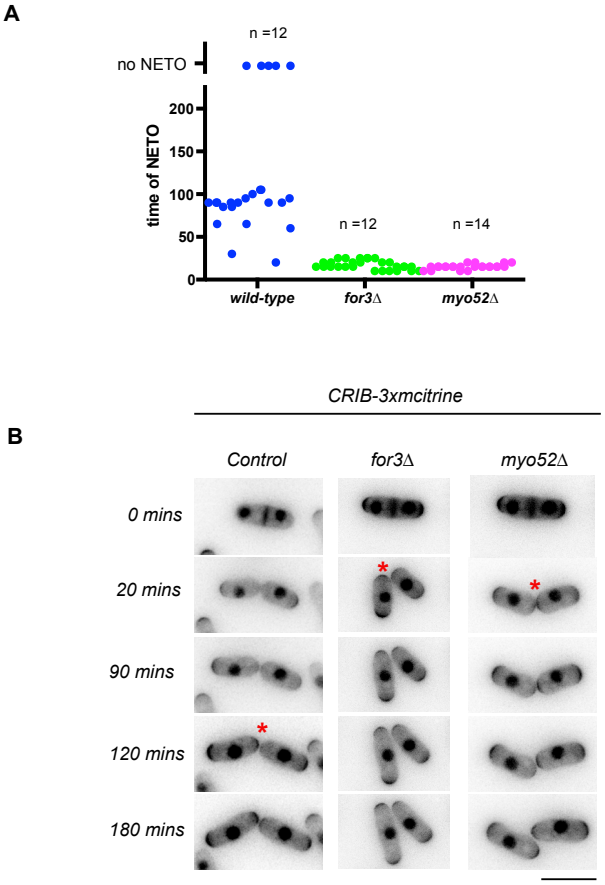

Figure 5.8. Actin cable-based transport is important to remove cues generated by septation from the new ends to reinforce old-end growth in pre-NETO wild-type cells. A) Time of NETO in wild-type (blue), *for3*Δ (green) and *myo52*Δ (purple) cells. In both *for3*Δ and *myo52*Δ cells, both the daughter cells establish NETO prematurely. (n = number of daughter pairs; no NETO = cells that failed to establish NETO) **B)** NETO in wild-type, *for3*Δ and *myo52*Δ cells. Still images from live-cell imaging of *for3*Δ*CRIB-3xmcitrine* and *myo52*Δ *CRIB-3xmcitrine* cells undergo NETO premturely (~15 mins) compared to wild-type *CRIB-3xmcitrine* cells (~90 mins). Time zero is the time at which septum disassembles. Scale, 10μm..

5.2.9 Memory-based growth polarity cue is cumulative

Having shown that a memory-based cue might be involved in establishment of polarized growth at the old end in a syn-growing daughter pair. Next, I wanted to investigate why the daughter cell growing from the new end did not inherit this memory-based cue. I hypothesized that since old end of the mother cell grew for a longer period of time compared to the new end of the mother cell, this memory-cue might be cumulative and hence the cell end need to grow for a particular amount of time to accumulate this cue to inherit it to the daughter cell. Therefore, I propose that if both the cell ends of the mother cell grew for the same amount of time, upon depolymerization of MTs before disassembly of septum, both the daughter cells will be able to inherit the memory cue and grow from their old ends in an anti pattern.

I checked this hypothesis in two different ways. Firstly, I depolymerized MTs in wild-type cells imaged in rich medium. Previously, it was reported that that the time taken to establish NETO is much shorter in rich medium vs. minimal medium (Mitchison & Nurse 1985). Therefore, in rich medium, by the time of cell division, both ends of a mother cell will have grown for a long time compared to in minimal medium, in which only one end will have grown for a long time, while the other end will have grown for a short period of time. I therefore wanted to determine if the duration of growth in the two cell ends of a mother cell could influence the growth patterns of the daughter-cell pair. I carried out live-cell imaging of *CRIB-3xmEcitrine* cells in rich medium for 2.5 hrs and depolymerized MTs (25µl/ml MBC) under the microscope and continued imaging for 4 hrs to track the growth pattern of daughter pairs. I found that unlike in minimal medium, in the cells imaged in rich medium, upon depolymerization of MTs before disassembly of septum in the mother cell, the daughter pairs grow in an anti pattern (Fig. 5.9A-B). This is consistent with my hypothesis that when both cell ends grow for a long period of time, both ends can accumulate a “growth memory” cue, which therefore can be inherited to both the daughter cells.

Secondly, I used *for3*Δ cells, which, as I previously showed, grow in a premature bipolar fashion. As a result, both the ends in *for3*Δ cells grow for the same amount of time, and therefore both ends could potentially accumulate the memory cue to the same extent. I carried out live-cell imaging of *for3*Δ cells in conditioned minimal medium for 2.5 hrs and depolymerized MTs (25µl/ml MBC) under the microscope and continued imaging for 4 hrs to track the growth pattern of daughter pairs. I found that similar to wild-type cells treated with MBC before disassembly of septum, in *for3*Δ cells treated with MBC before disassembly of septum in the mother

cell, the daughter pairs grow in an anti pattern (Fig. 5.9C-D). These two results suggest that consistent with my hypothesis, the growth memory-based cue inherited from the mother cell to the daughter cell might be cumulative.

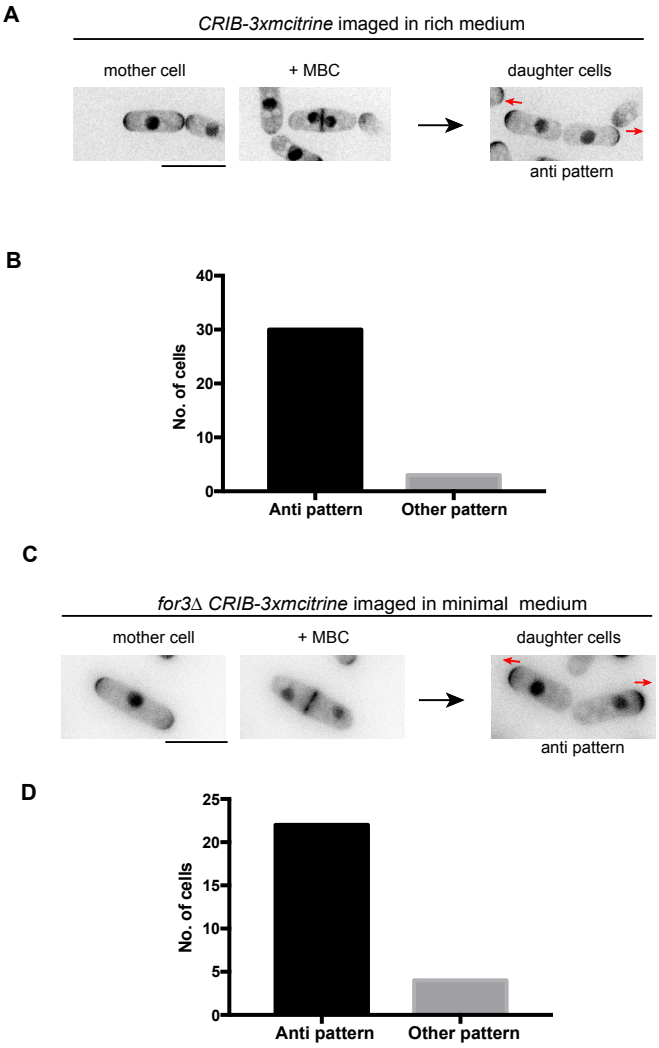

Figure 5.9. The proposed growth memory-based polarity cue may be cumulative. A) Depolymerization of MTs in *CRIB-3xmcitrine* cells imaged in rich medium before disassembly of septum gives an anti growth pattern instead of the syn pattern observed in same cells imaged in minimal medium. **B)** Approximately 90% of the MBC-treated cells imaged in rich medium grow in an anti pattern, whereas about 10% of the cells show other pattern (one daughter grows monopolar and other grows bipolar). **C)** Premature bipolar growing *for3*Δ cells show the anti growth pattern instead of the syn pattern after depolymerization of MTs before disassembly of the septum. **D)** Approximately 85% of MBC-treated *for3*Δ cells grow in an anti pattern whereas about 15% of the cells show other pattern. Scale, 10µm.

5.3 Discussion

In this chapter using a combination of live-cell imaging, drug perturbations and polarity mutants, I have shown that establishment of polarized growth in fission yeast depends on three redundant and independent cues. 1) A MT and Tea1-based cue, 2) a cue generated by septation, and 3) a growth memory-based cue, which is inherited from the mother cell to the daughter cell.

5.3.1 MT and Tea1-based polarity cue

Tea1 has been identified as an important landmark transported on the plus end of the MTs along with SH3 domain protein Tea4 in establishment of polarized in fission yeast (Mata & Nurse 1997; Sawin & Snaith 2004). Indeed, *tea1*Δ and *tea4*Δ cells failed to establish bipolar growth indicating its role in polarized growth (Mata & Nurse 1997; Martin et al. 2005; Tatebe et al. 2005). However, whether MTs are involved in the establishment of bipolar growth was never directly demonstrated. In this study, I have shown that similar to Tea1, MTs are also important to establish bipolar growth and this role of MTs most likely is to transport polarity proteins from the old end to the new end.

Interestingly, I have shown that timing of addition of MBC in the mother cell seems to dictate the growth patterns of the daughter pairs. When MTs are depolymerized after disassembly of the septum in the mother cell, the daughter pairs grow only from their old ends (anti pattern) similar to pre-NETO wild-type cells. Surprisingly, When MTs are depolymerized before septum disassembly, one daughter cell failed to grow from the old end and instead grow from the new end and the other daughter grow from their old end similar to a *tea1*Δ mutant (syn pattern). This suggests that immediately after septation, MTs are important to initiate polarized growth at the old ends of the daughter pair. Based on this, I proposed a simple model for MT-based regulation of polarized growth. Initially, immediately after septation, MTs establish polarized growth at the old ends and later in G2 phase, MTs establish polarized growth at the new end. Therefore, depolymerization of MTs before and after septation gave syn and anti growth patterns respectively (Fig. 5.10).

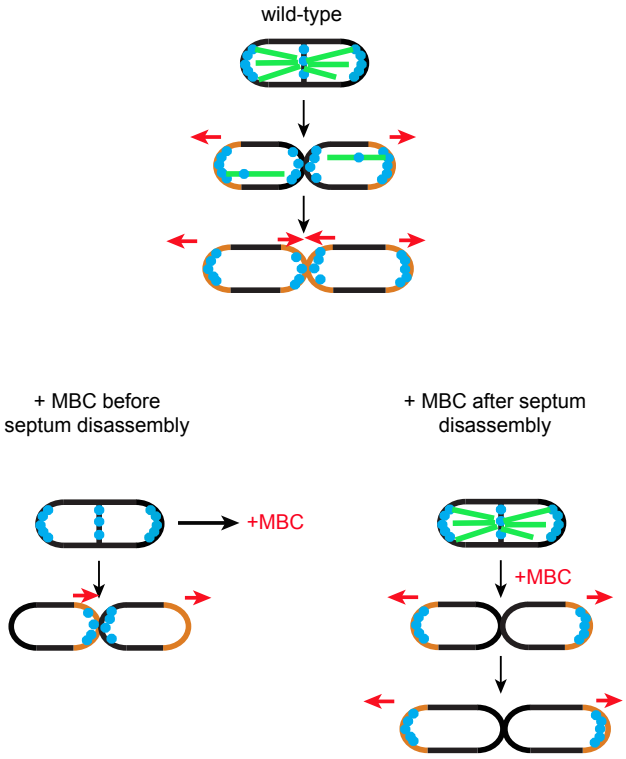

Figure 5.10. Model for MT and Tea1-based regulation of polarized growth in fission yeast. During septation, Tea1/Tea4 proteins are localized to the cell septum and are transported to the old ends of the daughter cells immediately after cytokinesis to initiate monopolar growth from the old ends of the daughter pair. Later, once cells enter G2 phase, MTs transport Tea1-Tea4 proteins to estbalish bipolar growth at the new ends of the daughter cells. Depolymerization of MTs before disassembly of the septum results in syn pattern (similar to growth pattern in *tea1Δ/tea4Δ* mutants) becuase MTs are already depolymerized before transporting Tea1/Tea4 to the old ends and therefore, depend on growth memory-based cue and septation-based cue. Depolymerization of MTs after disassembly of the septum results in anti growth pattern becuase Tea1 and Tea4 cues are already transported to the old ends and hence grow from old ends. However, since MTs are depolymerized before transporting Tea1 and Tea4 cues to the new end, these cells fail to establish NETO.

In this chapter, I have shown that differential Tea1 stability at the cell tips upon depolymerization of MTs might be responsible for the syn and anti growth patterns in wild-type cells. As mentioned before, Tea1 is transported on the plus end of MTs and is anchored at the cell tips with the help of a prenylated protein Mod5 (Snaith & Sawin 2003; Mata & Nurse 1997). Previously, it was reported that once Tea1 is deposited at the cell tips, MTs are no longer required to maintain the tip localization of Tea1 and hence along with Mod5, Tea1 can generate a polarity landmark that is robust to MT perturbation (Bicho et al. 2010; Sawin & Snaith 2004). Here, I have shown that although this is true at the growing end of a cell, stability of Tea1 is different at the non-growing end compared to the growing end upon depolymerization of MTs. Upon depolymerization of MTs, Tea1 completely falls off immediately from the non-growing end in comparison to the growing end, where Tea1 remains for a longer time. Based on this, I proposed a simple model to explain syn and anti growth pattern based on Tea1 stability upon depolymerization of MTs. When MTs are depolymerized during septation, Tea1 would disappear from the non-growing cell tips of the mother cell and remain at the septum. As a result, upon cell division, one daughter cell would fail to establish polarized growth at the old end due to lack of Tea1 landmark and instead grow from the new end. The other daughter cell, however, would still grow from the old end, and this growth would be therefore expected to be dependent on a cue that is independent of MTs and Tea1. On the other hand, if MTs are depolymerized after disassembly of septum Tea1 will have already been transported to the old ends of the daughter pairs to initiate cell growth, and hence Tea1 would remain at the growing old ends. However, a direct demonstration of differential Tea1 stability upon MT depolymerization leading to syn and anti growth pattern have been difficult because C-terminal tagging of Tea1 seems to affect the stability and dynamics of Tea1.

An important unanswered question is why Tea1 shows different stability at growing vs. non-growing ends? One possible explanation is stability and dynamics of Tea1 at the cell tips are somehow regulated by posttranslational modifications such as phosphorylation. Indeed, in anti-Tea1 western blots Tea1 shows a band shift that is eliminated upon treatment with lambda phosphatase (Niccoli & Nurse 2002). Similarly, *in vitro* studies showed that Tea1 is a substrate for protein kinase Shk1/Orb2 (Kim et al. 2003). In addition, previous unpublished work from Sawin lab has identified different phosphorylation sites in Tea1 by NetPhos analysis and mass spectrometry (24 phospho-serines and one phospho-threonine). Nearly all the phosphorylation sites identified (20 out of 25 phosphorylated residues) are present in the Tea1 central unstructured region, whose function is not known (Bicho PhD thesis,

2011). Based on this phosphomapping, an internal deletion (Tea1 central region) and non-phosphorylatable mutants were constructed (Bicho PhD thesis, 2011 and Snaith, Pilkington and Sawin unpublished results). Live-cell imaging with these strains showed that internal deletion strain and non-phosphorylatable mutant strains showed higher Tea1 stabilty at the cell tips comapared to wild-type Tea1 strains, suggesting phosphorylation of Tea1 might be important for dissociation of Tea1 from the cell tips and hence regulate the turnover of Tea1 (data not shown). However, this needs to be tested further by looking at the dynamics of Tea1 in different Tea1 phosphomutants upon depolymerization of MTs.

In fission yeast, different protein kinases and phosphatases are present at the cell tips and are involved in polarized growth(Das et al. 2009; Tatebe et al. 2008; Hachet et al. 2011). For example, the p-21 activated kinase (PAK) Shk1/Orb2, which has been shown to phophorylate Tea1 *in vitro*, shows reduced kinase activity upon depolymerization of MTs using a cold-sensitive mutation in the β-tubulin gene nda3 (Qyang et al. 2002). This suggests depolymerization of MTs could potentially affect different kinases, which in turn could regulate the dynamics and stability of Tea1. Another important kinase at the cell tip involved in polarized growth is the DYRK family kinase, Pom1. Polarity proteins Tea1 and Tea4 moving on the plus end of microtubules are necessary and sufficient for the tip localization of Pom1 (Hachet et al. 2011). At the cell tips, Pom1 associates and dissociates with the plasma membrane by dephosphorylation and auto-phosphorylation respectively to form a concentration gradient and are involved in establishment of bipolar growth, cell morphogenesis and septum positioning (Bähler & Pringle 1998; Padte et al. 2006; Hachet et al. 2011). Hence, depolymerization of MTs might affect the localization of Pom1, which in turn might affect Tea1 stability at the cell tips through its phosphoregulation.

It is important to note that the role-played by MTs in establishment of polarized growth seems to be dependent on the growth medium. MTs are essential for the establishment of bipolar growth in synthetic minimal medium (SGALU), whereas MT-independent establishment of bipolar growth exists in complex rich medium (YE5S). Similarly, syn pattern is only observed in SGALU, whereas cells grow in an anti pattern upon depolymerization of MTs during septation in rich medium. In fission yeast, key cellular processes including cell growth, division, cytoskeletal organization and protein synthesis are dependent on different stress pathways such as Sty1 MAPK stress response and target of rapamycin (TOR) pathways (Shiozaki & Russell 1995; Petersen & Nurse 2007; Petersen & Russell 2016). These pathways respond differently to different external environments,

including growth medium. Complex rich medium (explained in materials and methods) has different composition to simple synthetic medium, which is evident from the generation time in these two mediums (YE5S = 2.5hrs, SGALU = 4hrs). Therefore, it is not surprising that MT-based regulation of polarized growth is differently regulated in rich medium vs. minimal medium.

5.3.2 Septation-based polarity cue

Depolymerization of MTs in the mother cell before disassembly of septum and mutants of *tea1* show syn pattern of growth in their daughter pairs. This suggested that MT and Tea1-independent cue(s) might be involved in establishment of polarized growth in these daughter pairs. In this study, I propose that the daughter cell growing from the new end depends on a cue generated by septation. This poses an important question of why cue generated by septation initiate new end growth immediately after cell division in wild-type cells. Here, I have shown that actin cable-based transport “clears” cue generated by septation from the new ends immediately after cell division thereby further reinforcing old end growth. Indeed, *for3*Δ and *myo52*Δ cells showed premature bipolar growth.

One possible candidate protein(s) to be cleared from the new end immediately after cytokinesis might be β glucan synthases such as Bgs1 and Bgs4. Bgs1 and Bgs4 are catalytic subunits of (1,3) β-D-glucan synthase, an enzyme complex involved in the synthesis of major cell wall component (1,3) β-D-glucan (Cortés et al. 2005). Bgs4 is localized to the growing cell tips during interphase and cell septum during septation (Cortés et al. 2005). Previously it was reported that actin cytoskeleton and Myo52 are involved in relocalization of Bgs4 from cell tip to septum and *vice versa* (Mulvihill et al. 2006; Cortés et al. 2005).Therefore, perturbation of actin cable-mediated transport might fail to “clear” Bgs4 from the new ends, which might then lead to initiation of new end growth. Indeed, Bgs4 was shown to be localized to the new ends for an extended period of time even after growth is initiated at old ends (Cortés et al. 2005).

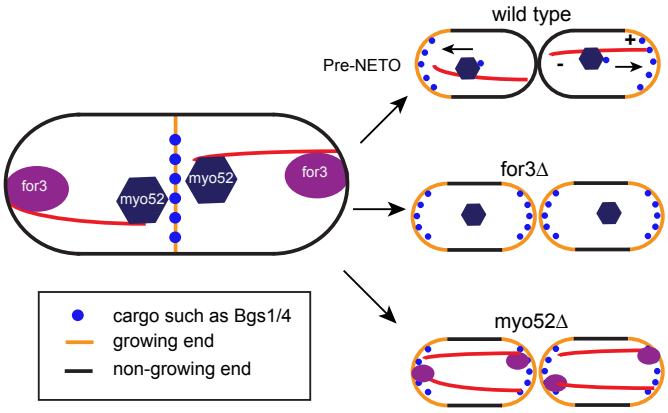

Figure 5.11. Proposed model for actin cable-based negative regulation of septum-derived cue in regulation of polarized growth. In wild-type cells, actin cable nucleator For3 is relocalized to the old ends after cytokinesis and nucleates actin cables. These cables act as a track for motor protein Myo52 to clear cues generated by septation from the new ends of the daughter pair towards the old ends to reinforce old end growth. Perturbation of actin cable-based transport (*for3*Δ and *myo52*Δ) results in failure to clear cues from the new end immediately after cytokinesis and therefore, these cells initiate premature bipolar growth.

5.3.3 A growth memory-based polarity cue

In this study, I have shown that in a syn-growing daughter pair of MBC treated wild-type cell and polarity mutants such as *tea1*Δ, a growth memory-based cue is inherited from the mother cell to the daughter cell to establish polarized growth. Further, since this memory-based cue is inherited only to one daughter cell in a bipolar growing wild-type cell, I predicted that end of the mother cell need to grow for a particular amount of time in order to accumulate this cue to inherit it to the daughter pairs. Indeed, in situations where both the ends of the mother cell grow for a longer period of time such as *for3*Δ or wild-type cells imaged in rich medium, depolymerization of MTs before disassembly of septum resulted in anti growth pattern. This suggests that the growth memory-cue is cumulative and need to be accumulated to a particular level in order to be inherited to the daughter pair.

It is remarkable that in the absence of cues regulated by cytoskeleton (Tea1 cue and cues generated by septation), cells depend on a memory cue, which is accumulated in the previous cell cycle and can be used in the next cell cycle. It is possible that such a cue might be very important under situations such as starvation or other unfavourable conditions, which might affect the organization of cytoskeleton and thereby positioning of cytoskeleton-dependent cues. Under such conditions growth memory cue might be crucial to “remember” the previous growing ends and reinitiate polarized growth.

5.3.4 Cooperation and competition between multiple internal cues might be important for regulating the wild-type growth pattern of fission yeast cells

Polarized growth in fission yeast is highly regulated in space and time such that initially daughter cells only grow from their old ends and establish new end growth only at a later stage in the cell cycle (Mitchison & Nurse 1985). Even though this growth pattern of fission yeast is known for a very long time, how cells regulate this growth pattern is not clear. I have shown that three independent polarity cues are involved in regulation of polarized growth in fission yeast. Here, I propose that cooperation and competition among these redundant cues might be important for maintaining the wild-type growth pattern of fission yeast (Fig. 5.12). At the beginning of the cell cycle, both MT-based Tea1 cue and growth memory-based cue inherited from the mother cell establish polarized growth at the old ends of the daughter cell.

This growth at the old end helps to organize actin cables towards the new end and can "clear" cue generated by septation and prevent new end growth. Further, even though Tea1 cue is present at both old and new ends at the beginning of cell cycle, since old end has two independent cues (i.e., Tea1 and growth memory cue), these two cues cooperate and compete against the Tea1 cue present at the new end to initiate old end growth. Later, when cells enter G2 phase of cell cycle, MTs and Tea1 cue helps to establish bipolar growth.

In order to test this model of polarity regulation involving multiple redundant cues, I can predict fate of growth patterns of daughter pairs in the absence of different polarity cues and test this predictions using drug perturbations and polarity mutants (Fig. 5.13). For instance, If MTs and Tea1-based cue is important to establish polarized growth initially at the old end and later at the new end, I predicted that in the absence of Tea1 and MTs cell would fail to establish old end growth and bipolar growth. Indeed, *tea1*Δ cells and MBC-treated wild-type cells failed to establish old end growth (syn pattern) and bipolar growth. Further, I predicted that cells could use a cue generated by septation to initiate polarized growth at the new end. Indeed, in *tea1*Δ cells and MBC-treated wild-type cells, one daughter cell grows from their new end. I predicted that in wild-type cells, this cue generated by septation might be cleared by actin cable-based transport. Indeed, perturbation of actin cable-based transport (*for3*Δ and *myo52*Δ) failed to clear this cue and initiated growth at the new end using the cue generated by septation. Finally, I predicted that a growth memory-based cue is inherited from the mother cell to the daughter cell to establish polarized growth at the old end. Indeed, by making new ends of the mother cell grow for the longer amount of time similar to the old end, I could show that daughter cell inheriting the new end could also inherit the growth memory cue.

In summary, I have shown that establishment of polarized growth in fission yeast involves multiple redundant cues making polarized growth in fission yeast robust to various perturbations. In the next chapter, I will focus on identifying the key player(s) involved in the memory-based cue and how is it regulated.

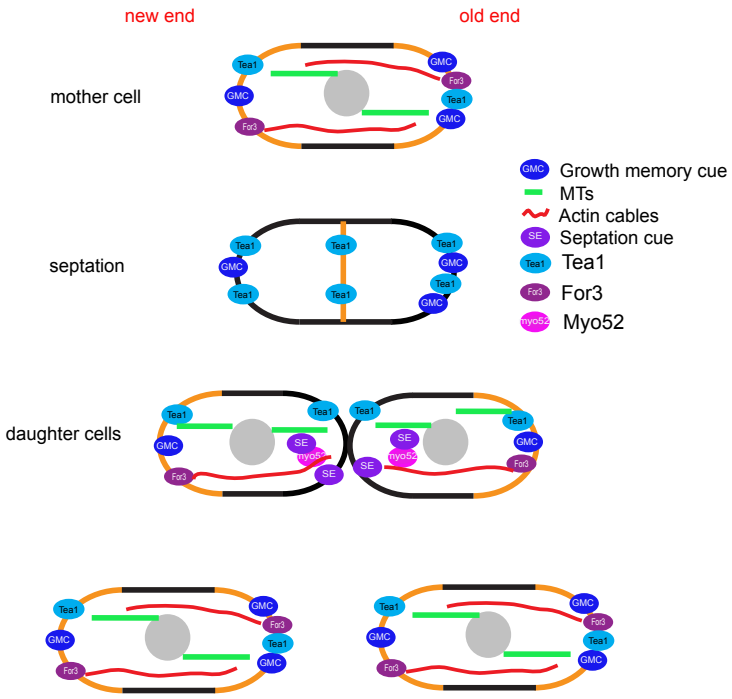

Figure. 5.12. Model for competition and cooperation between multiple internal cues regulating the wild-type growth pattern in fission yeast. Three internal, redundant cues are involved in establishment of polarized growth. After cytokinesis, MT and Tea1 along with the growth memory cue (GME) inherited from the mother cell coperate to establish polarized growth. Further, establishment of polarized growth at the old end organizes actin cables, which clears septation cues (SE) at the new end with the help of Myo52 therby reinforcing old end growth. Finally, when cells enter G2 phase of cell cycle, MTs and Tea1 establish bipolar growth.

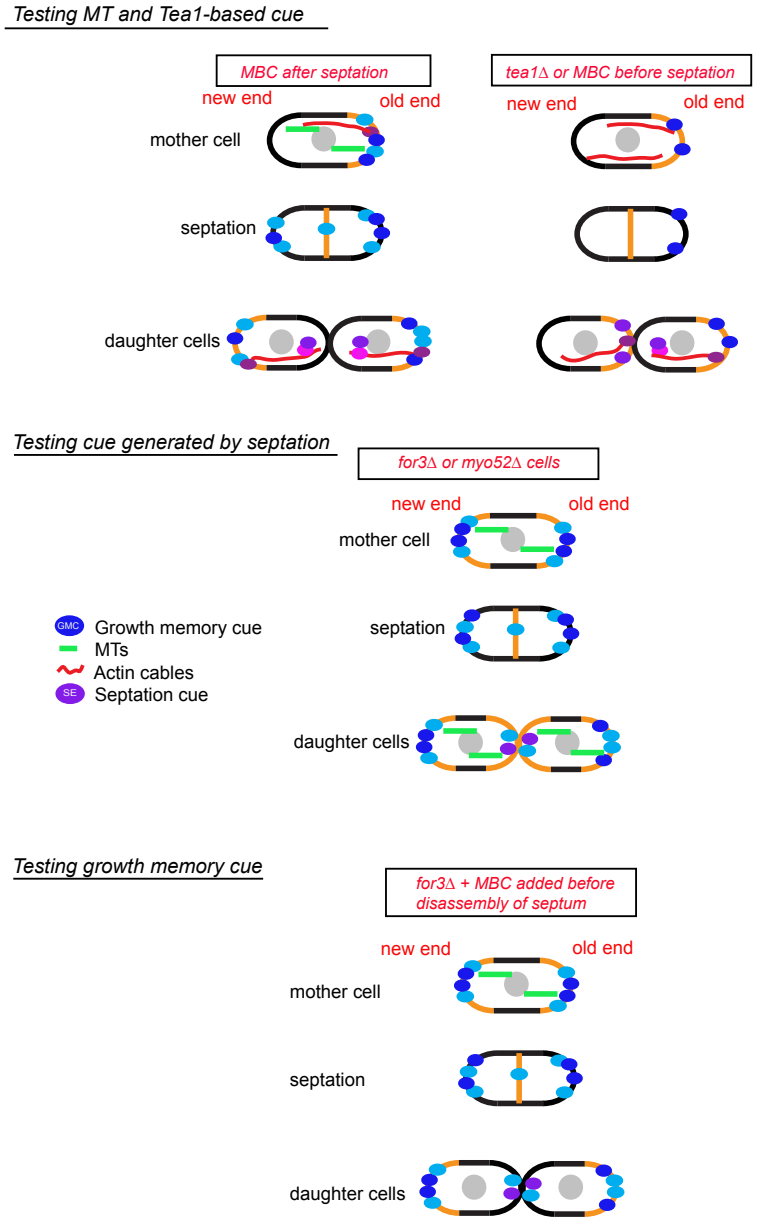
Testing MT and Tea1-based cue
MBC after septation
new end
old end
mother cell
septation
daughter cells
tea1Δ or MBC before septation
new end
old end
Testing cue generated by septation
for3Δ or myo52Δ cells
new end
old end
mother cell
septation
daughter cells
GMC
Growth memory cue
MTs
Actin cables
SE
Septation cue
Testing growth memory cue
for3Δ + MBC added before disassembly of septum
new end
old end
mother cell
septation
daughter cells

Figure 5.13. Testing the model for multiple internal cues involved in regulation of polarized growth. 1)Testing MT and Tea1-based cue by using *tea1*Δ and MBC treatment. MBC treatment and results in failure to establish bipolar growth and two seperate monopolar patterns. 2) Testing cue generated by septation by perturbing actin cable-based transport (*for3*Δ and *myo52*Δ). Perturbation of actin cable-based transport results in immediate new end growth by septation cues, which are genrally cleared by actin cable-medited transport in wild-type cells. 3) Testing growth memeory cue by using a mutant (*for3*Δ*)* where both old eand new end of the mother cell grow for a longer period of time. Upon MT depolymerization cells depend on growth memory cue inherited from the mother cell and establish polarized growth in an anti pattern instead of syn pattern observed in wild-type cells treated with MBC before septation.

Chapter 6: Rax2-Rax1 proteins are involved in the growth memory-based establishment of polarized growth

6.1 Introduction

In the previous chapter, I have shown that a growth memory-based polarity cue along with a cue generated by septation are involved in establishment of polarized growth in a syn-growing *tea1*Δ cells and MBC-treated wild-type cells. Further, I showed that this growth memory cue is cumulative and is inherited from the mother cell to the daughter cell to establish polarized growth. In this chapter, I want to investigate what are the key players or proteins involved in this growth memory-based polarity establishment.

In budding yeast *Saccharomyces cerevisiae,* ScRax2 (Revert to Axial), a transmembrane protein was shown to behave as a stable cortical landmark important for bipolar budding pattern (Chen 2000). Depending on cell type, budding yeast cells forms buds in one of two distinct spatial patterns. In haploid a and α cells, both the mother cell and the daughter cell form buds directly adjacent to the previous site of cell division, whereas in diploid a/α cells, the mother and the daughter cell form buds either from the proximal or distal poles relative to the previous cell division site (Fig. 6.1) (Chant 1999; Chen 2000). Three different classes of genes are reported to play an important role for these budding patterns. ScAxl1, ScBud10/Axl2, ScBud3, and ScBud4 are required for the axial budding pattern, whereas ScBud8 and ScBud9 are important for the bipolar pattern and the third class, consisting of ScBud1, ScBud2 and ScBud5, is required for both axial and bipolar budding pattern (Chant 1999; Chant & Herskowitz 1991; Zahner et al. 1996; Sanders & Herskowitz 1996). Chen *et al.* (Chen 2000) identified ScRax2 through a mutant search by mutagenizing a bipolar budding *axl1* strain and examining isolates defective for the bipolar budding pattern. They showed that *rax2*Δ disrupts the bipolar pattern of *axl1*Δ cells without affecting the axial pattern of otherwise wild type cells. Similarly, *rax2*Δ cells failed to show bipolar budding pattern in diploid cells (Chen 2000). In diploid cells, Rax2-GFP localized to the previous division sites and is inherited for multiple generations (Chen 2000). Time-course experiments using Rax2-myc repressed for 18 hours under *GAL1* promoter showed that the insoluble pools of Rax2 were very stable, with a half-life of about 6 hours whereas, Bud10, another protein important for bipolar pattern disappeared rapidly after repression (Chen 2000). All these and other results

suggest that Rax2 is a stable cortical landmark inherited over multiple generations and is required for bipolar pattern of budding.

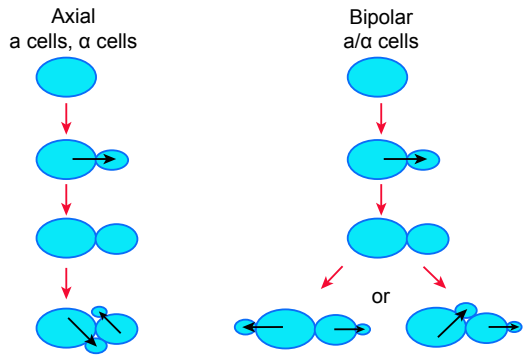

Figure 6.1. Patterns of budding in budding yeast cells. Budding yeast cells divide in two different spatial patterns. Haploid a and α cells divide in the axial pattern in which both the mother and the daughter cells forms bud immediately near to the previous site of cell division. In the case of diploid a/α cells, the mother and the daughter cell divide either from the proximal or distal poles with respect to the previous cell division site.

A homolog of *S. cerevisiae* Rax2 was identified in fission yeast (SPAC6F6.06c) (Chen et al. 2000). Based on the work carried out in budding yeast, I hypothesized that Rax2 might be part of the growth memory-based cue involved in establishment of polarized growth in fission yeast. Previously, preliminary work to characterize Rax2 was carried out in fission yeast and this study was consistent with our hypothesis of Rax2 having a role in establishment of polarized growth in fission yeast (Choi et al. 2006). Therefore, I decided to investigate if Rax2 is a part of growth memory-based polarity establishment in fission yeast.

In this chapter, I will focus on how I established Rax2 along with Rax1 as important proteins involved in growth memory-based establishment of polarized growth in fission yeast using live-cell imaging, yeast genetics, and Fluorescence Recovery After Photobleaching (FRAP).

6.2 Results

6.2.1 Transmembrane protein Rax2 is a potential memory-based cue for establishment of polarized growth in the fission yeast

In the preceding chapter I showed that depolymerization of MTs before disassembly of the septum results in a "syn" growth pattern. Further my experiments suggested that this might involve a stable, cumulative, microtubule-independent cue or landmark that is based on "growth memory", inherited from the mother cell. This syn growth pattern is also observed in polarity mutants such as *tea1*∆ and *tea4*∆*,* suggesting that this MT-independent cue is also independent of polarity proteins Tea1 and Tea4. I hypothesized that this growth memory-based cue might be dependent on Rax2, a stable, cortical landmark identified in budding yeast, which is required for bipolar budding (Chen et al. 2000).

A fission yeast homolog of Rax2 was previously reported (Chen et al. 2000; Choi et al. 2006). Fission yeast Rax2 is an 1155 amino acid long protein with a molecular weight of 128.33 KDa. I hypothesized that in order to be a growth memory cue, a protein should have certain attributes. Firstly, since polarized growth is restricted to cell tips, this cue must be localized to cell tips. In order to investigate this I constructed a *Rax2-3xmcitrine* strain and found that Rax2 was enriched at the cell tips – that is, regions of polarized growth (Fig.6.2A). Secondly, since syn pattern of daughter pairs are observed upon depolymerization of MTs before septum disassembly in the mother cell, I proposed that this growth memory cue must be stable to MT depolymerization. Indeed, in MBC-treated *Rax2-3xmcitrine* cells, Rax2 was still localized at the cell tips suggesting MTs are not required for maintaining Rax2 at the cell tips (Fig.6.2B). Finally, previously I have shown that in premature bipolar growing *for3*∆ cells, when MTs are depolymerized before disassembly of the septum, the growth memory cue is inherited to both the daughter cells. This suggests that this growth memory cue must be stable to depolymerization of MTs as well as actin cables. In order to investigate this I treated *Rax2-3xmcitrine* cells with 50µM LatA. Indeed, Rax2 was maintained at the cell tips suggesting that actin cables are not required for stable maintenance of Rax2 at the cell tips (Fig.6.2C). These results suggest that Rax2 could be a potential growth memory-based landmark involved in the establishment of polarized growth in fission yeast.

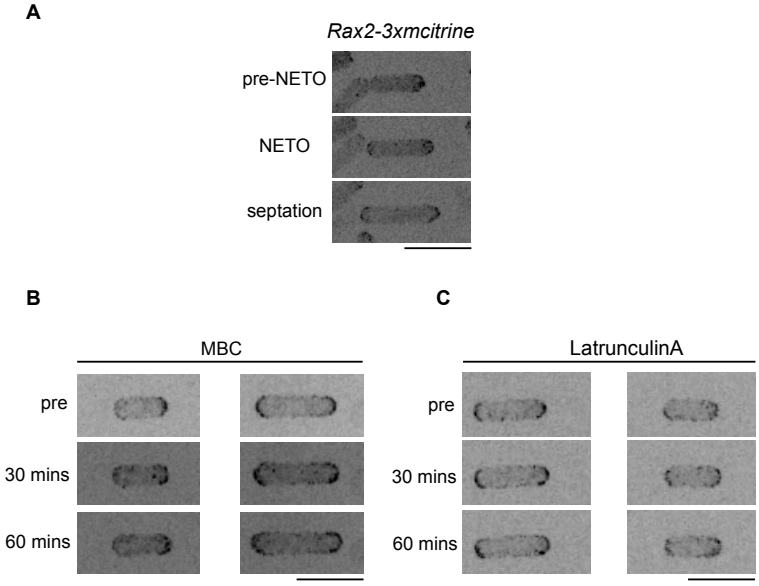

Figure 6.2 Rax2 is a potential growth memory-based landmark in fission yeast. A) Rax2-3xmcitrine localizes to the cell tips, regions of polarized growth. In pre-NETO cells, Rax2 is localized only to the monopolar growing end and after NETO, Rax2 is localized to both the ends. During septation, Rax2 remains at the cell tips and didn't localize to the cell septum (discussed in section 6.2.4) . **B)** Rax2 localization at the cell tips are stable to MT perturbation. Rax2-3xcitrine remains localized to the cell tips after 1 hour MBC treatment. **C)** Actin cytoskeleton is not required for the maintenance of Rax2 at the cell tips. Rax2 remains at the cell tips of 50μM LatA treated cells. Note that cells continue to grow in MBC-treated cells, whereas stop growth in LatA treated cells. Scale, 10μm.

6.2.2 Rax2 is involved in the growth memory cue-based establishment of polarized growth

Next I wanted to investigate if Rax2 is involved in the proposed growth memory-based establishment of polarized growth in fission yeast. Previously it was shown that *tea1*Δ cells grow in a syn pattern (Mata & Nurse 1997; Niccoli et al. 2003). In order to confirm this I constructed a *tea1*Δ *CRIB-3xmcitrine* strain. Live-cell imaging showed that indeed more than 90% of the *tea1*Δ cells imaged in rich medium grow in a syn pattern (n=110) (Fig. 6.3A-B). I predicted that if Rax2 were involved in a growth memory-based establishment of polarized growth at the old end of the daughter cell inherited from previously growing old end of the mother cell in a syn-growing *tea1*Δ daughter pair, then *tea1*Δ*rax2*Δ cells would fail to establish polarized growth at the old end of the daughter cell. In order to check this, I constructed and imaged a *tea1*Δ*rax2*Δ *CRIB-3xmcitrine* strain. I found that *tea1*Δ*rax2*Δ *CRIB-3xmcitrine* cells are viable, monopolar and indeed failed to grow at the old end of the daughter cell inherited from the growing old end of the mother cell and instead established growth exclusively at the new ends generated by septation (Fig. 6.3A-B). This strongly suggests that Rax2 is part of the growth memory-based cue involved in establishment of polarized growth in fission yeast. Moreover, in the absence of Tea1 and Rax2 cues, cells use previously explained cues generated by septation in order to establish polarized growth.

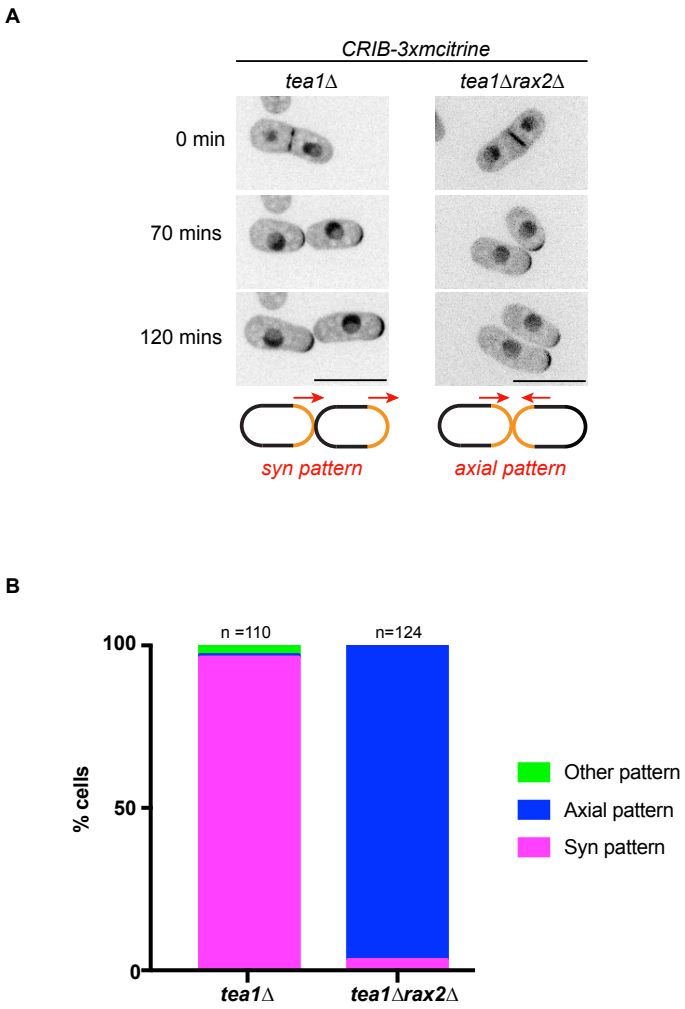

Figure 6.3. Patterns of daughter-cell growth in *rax2Δtea1Δ* are consistent with Rax2 functioning as part of a "growth memory cue". A) Stills from time-lapse movies of *tea1Δ CRIB-3xmcitrine* cells show syn growth pattern, whereas *tea1Δrax2Δ* cells can no longer grow at the old ends and instead grow exclusively at the ends generated by septation. I refer to this as an "axial" growth pattern. **B)** Graph showing percentage of cells growing in syn and axial patterns. 96% of *tea1Δ* cells show syn pattern and *96%* of *tea1Δrax2Δ* cells grow exclusively at the new ends - axial pattern. All movies are imaged in rich medium. (other = 1 monopolar, 1 bipolar). Scale, 10μm.

6.2.3 Rax1 is also involved in the Rax2-mediated establishment of polarized growth in fission yeast

Previously in the budding yeast *S. cerevisiae,* a second protein ScRax1 was also reported to be required for bipolar budding pattern (Fujita et al. 2004). In budding yeast, *rax1*Δ cells alter the bipolar pattern of mutant *axl1* haploids, resulting in reversion to an axial growth pattern. Similarly, *rax1*Δ also reverts the bipolar budding pattern of *bud3*Δ and *bud4*Δ haploids into axial budding pattern (Fujita et al. 2004). A budding yeast homolog of Rax1 was reported in fission yeast (SPAC23G3.05c) (Fujita et al. 2004). Previously in the budding yeast it was shown that localization of Rax2 and Rax1 are interdependent and GST-Rax1 could be copurified with Rax2-HA in yeast cells (Kang et al. 2004). Therefore, I wanted to investigate if Rax1 is also involved in the growth memory-based establishment of polarized growth in fission yeast. I constructed a *rax1*Δ*tea1*Δ*CRIB-3xmcitrine* strain. *rax1*Δ and *tea1*Δ were confirmed by colony PCR. Live-cell imaging showed that, as in *rax2*Δ*tea1*Δ *CRIB-3xmcitrine* cells, more than 90% of *rax1*Δ*tea1*Δ *CRIB-3xmcitrine* cells grow in an axial pattern, in which both of the two daughter cells establish polarized growth exclusively at the new ends (Fig. 6.4A-B) (n=108). This indicates that similar to Rax2, Rax1 is also involved in the growth memory-based polarity establishment. I also constructed a *rax1*Δ*rax2*Δ*tea1*Δ *CRIB-3xmcitrine* strain in order to investigate if both Rax2 and Rax1 are involved in the same pathway. Live-cell imaging of *rax1*Δ*rax2*Δ*tea1*Δ *CRIB-3xmcitrine* cells showed cells growing in axial growth pattern similar to that in single *rax1*Δ and *rax2*Δ cells. This suggests that Rax2 and Rax1 might be working in a linear pathway (Fig. 6.4A-B).

As mentioned before, in budding yeast localization of ScRax2 and ScRax1 was shown to be interdependent. In wild-type cells, both ScRax2 and ScRax1 are localized at the mother bud neck and previous site of cell division (Chen 2000; Kang et al. 2004). However, In Sc*rax2*Δ cells, ScRax1 was no longer localized to the normal sites instead were localized in small vesicles and patches or in structures that appeared to be vacuoles (Kang et al. 2004). Similarly in Sc*rax1*Δ cells, ScRax2 was localized in structures that appeared to be vacuoles (Kang et al. 2004). Also, recently it was shown that in budding yeast, the C-terminal region of ScRax2, which is predicted to be in the cytoplasm, is required for the proper cortical localization of ScRax1 and ScRax2 (Meitinger et al. 2014). Based on these results I wanted to investigate if localization of Rax2 and Rax1 are interdependent in fission yeast, which could explain why they both are involved in the same pathway. In order to check if Rax1 is required for localization of Rax2, I constructed a *rax1*Δ *rax2-3xmcitrine*

strain. Live-cell imaging showed that Rax2 in this strain failed to localize to the cell tips and instead appeared to be scattered in the cytoplasm (Fig. 6.5A). This shows that Rax1 is required for the proper localization of Rax2 in fission yeast. Similarly, a 26 amino acid (Δ26C) C-terminal truncation of Rax2 also failed to show proper tip localization of Rax2, suggesting that C-terminal region of Rax2 is important for tip localization of Rax2 (Fig. 6.5A). I could not determine whether Rax2 is required for the localization of Rax1 because attempts to C-terminally or N-terminally tag Rax1 seems to affect the localization of Rax1 since I could not see any signal under the microscope. These results indicate that, similar to budding yeast, Rax2 localization in fission yeast is dependent on the Rax2 C-terminal region and also on Rax1.

In fission yeast, similar to budding yeast, Rax2 and Rax1 are predicted to be transmembrane proteins. I used TOPCONS membrane prediction topology software to predict membrane topology of Rax2 and Rax1 in fission yeast (Tsirigos et al. 2015). TOPCONS predicted Rax2 similar to budding yeast Rax2 to have a C-terminal transmembrane domain (1105-1125 aa), which is cytoplasmic and an N-terminal signal peptide sequence (1-22aa) (Fig. 6.5B). Most of the Rax2 protein was predicted to be in the extracytoplasmic space or outside and the transmembrane domain was predicted to be “out-in” (Fig. 6.5B). Similarly, Rax1 was predicted to have three transmembrane domains (Fig. 6.5C). Based on the localization studies and predicted domain architecture of Rax2 and Rax1, it is possible that C-terminal cytoplasmic tail of Rax2 interacts with N-terminal cytoplasmic region of Rax1 and this interaction might be important for Rax2 and Rax1’s role in regulating polarized growth (Fig. 6.5D). However, direct interaction between Rax2 and Rax1 in fission yeast has not been tested and further needs to be investigated.

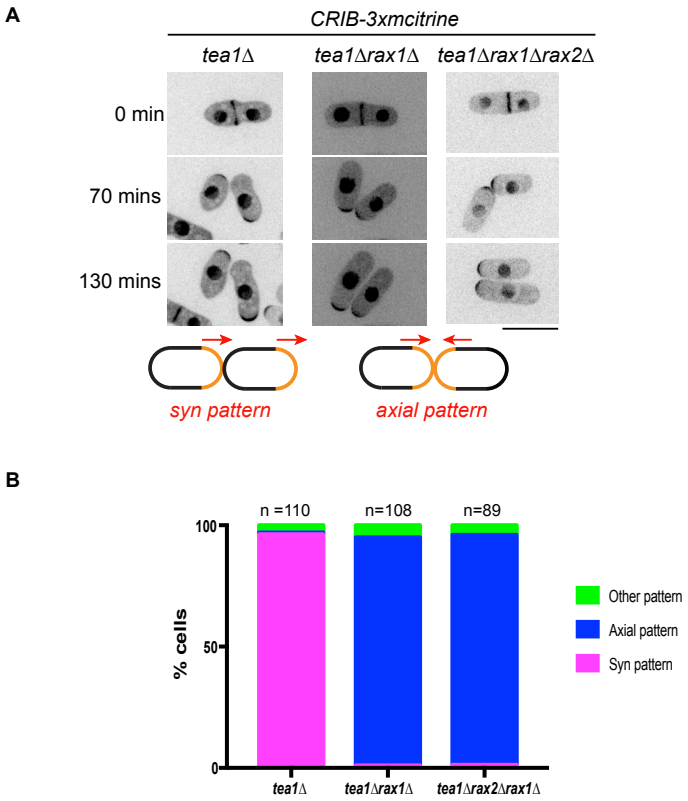

Figure 6.4. Patterns of daughter-cell growth in *rax1*Δ cells are consistent with Rax1 functioning as part of a "growth-memory cue". A) Stills from time-lapse movies of *tea1*Δ*CRIB-3xmcitrine* cells show syn growth pattern, whereas *tea1*Δ*rax1*Δ cells can no longer grow at the old ends and instead grow exclusively at the ends generated by septation in an axial pattern. Similarly *tea1*Δ*rax2*Δ*rax1*Δ *CRIB-3xmcitrine* cells also show axial growth pattern suggesting that both Rax2 and Rax1 might be working in a linear pathway to establish polarized growth. **B)** Graph showing percentage of cells growing in syn and axial growth patterns. 96% of *tea1*Δ cells show syn pattern, whereas 94% of *tea1*Δ*rax1*Δ and 95% of *tea1*Δ*rax2*Δ*rax1*Δ cells grow in an axial pattern. All movies are imaged in rich medium. Scale, 10µm.

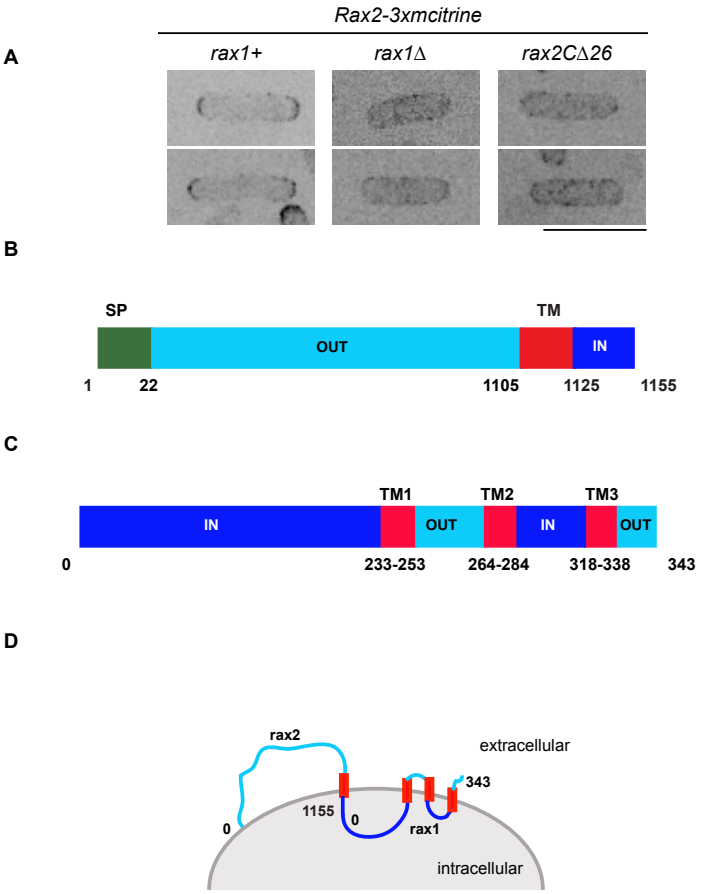

Figure 6.5. Rax1 and C-terminal region of Rax2 are required for the cortical localization of Rax2. A) Tip localization of Rax2 is perturbed in *rax1Δ cells* and 26 amino acid (Δ26C) C-terminal truncation of Rax2 compared to *rax2+* cells. **B)** Rax2 is predicted to be an "out-in" transmembrane protein. A simple domain architecture of Rax2 based on TOPCON prediction (not in scale). Rax2 is predicted to have an N-terminal signal peptide (SP), a large central region predicted to be outside (OUT), a C-terminal transmembrane domain (TM) and a cytoplamic tail (IN). **C)** Domain architecture of Rax1 based on TOPCON prediction (not in scale). Rax1 is predicted to have three transmembrane domains (TM1-3). **D)** Proposed interaction between Rax2 and Rax1 at the cell tips based on predicted domain architecture and localization studies. Scale, 10μm. (Imaged in minimal media).

6.2.4 Localization of Rax2 correlates with growth, but Rax2 is absent from septum

Next, I wanted to investigate how Rax2 acts as a landmark to establish polarized growth in fission yeast. My previous results have suggested that the growth memory-based polarity cue might be cumulative. This is based on my observation that the growth memory-based cue was inherited only from the old-growing end of the mother cell to the daughter cell inheriting this old end. Moreover, by using a premature bipolar mutant such as *for3*Δ or by imaging cells in rich medium where new end of the mother cell grow for a longer period of time compared to minimal medium, I showed that this growth memory-based cue could be inherited from both old and new-growing end of the mother cell to the daughter cells. This suggests that localization of Rax2 might correlate with growth, and that cell tips may need to grow for a certain amount of time in order to accumulate enough Rax2 to act as a growth memory-based cue. First, I wanted to check if localization of Rax2 correlates with growth. In order to address this, I did live-cell imaging of *Rax2-3xmcitrine*. Rax2 was localized only to the growing ends of the cell (Fig. 6.6A). That is, in pre-NETO cells, Rax2 was localized to only one end - the growing old end, but once cells established NETO, Rax2 was localized to both growing ends. In order to confirm that localization of Rax2 correlates with growth, I did live-cell imaging of Rax2 in a monopolar mutant *tea1*Δ cell. In *tea1*Δ cells, Rax2 was localized only to the monopolar-growing end (Fig. 6.6B).

Next, I wanted to investigate if there is any asymmetry in the amount of Rax2 at the old end compared to the new end, because such an asymmetry (if it exists) could explain why only the old-end of the mother cell normally passes on the growth memory-based cue to the daughter cell. In order to address this, I looked at the localization of Rax2 to compare amount of Rax2 present at the old end vs. new end. However, live-cell imaging of Rax2 did not show any consistent difference in the amount of Rax2 localized at old end vs. new end (Fig. 6.6C). This suggests that the simple hypothesis of asymmetry in Rax2 localization due to correlation of Rax2 localization with growth is probably incorrect. Another possibility is that this growth memory-based cue includes additional components that generate the “cumulative” properties. However, this further needs to be investigated carefully.

Even though localization of Rax2 correlates with growth, surprisingly, when cells enter mitosis, Rax2 remained at the cell tips and did not accumulate at the cell septum (Fig. 6.6E). This failure of Rax2 to accumulate at the cell septum during septation is different from the localization of known polarity proteins during septation.

Polarity proteins Tea1 and Tea4 are known to localize to the cell septum and to the cell tips during septation (Mata & Nurse 1997; Martin et al. 2005; Tatebe et al. 2005). Similarly, Cdc42, which is a key regulator of polarized growth, localizes to the growing ends during interphase and localizes to the septum during septation (Tatebe et al. 2008) (Fig. 6.6D). In order to confirm failure of Rax2 accumulation at the cell septum during septation, I constructed a *rax2-3xmcitrine bgs4-cherry* strain. β-glucan synthase-4 (Bgs4) is one of the catalytic subunits of 1-3-β-D glucan synthase, an enzyme complex involved in the synthesis of major cell wall component (1,3) β-D-glucan (Cortés et al. 2005). Bgs4 localizes to the growing cell tips during interphase and to the septum during septation (Cortés et al. 2005). Live-cell imaging of *rax2-3xmcitrine bgs4-cherry* showed that during interphase, Rax2 and Bgs4 colocalize at the growing cell tips, (Fig. 6.6E). However, during septation, Bgs4 relocalizes to the cell septum, whereas majority of Rax2 remains at the cell tips even though weak signal of Rax2 could be seen at the septum (Fig. 6.6E). This accumulation of Rax2 at the cell tips during septation might be important for its role as a landmark, as part of the mechanism that allows cell to re-identify their cell tips in the next cell cycle.

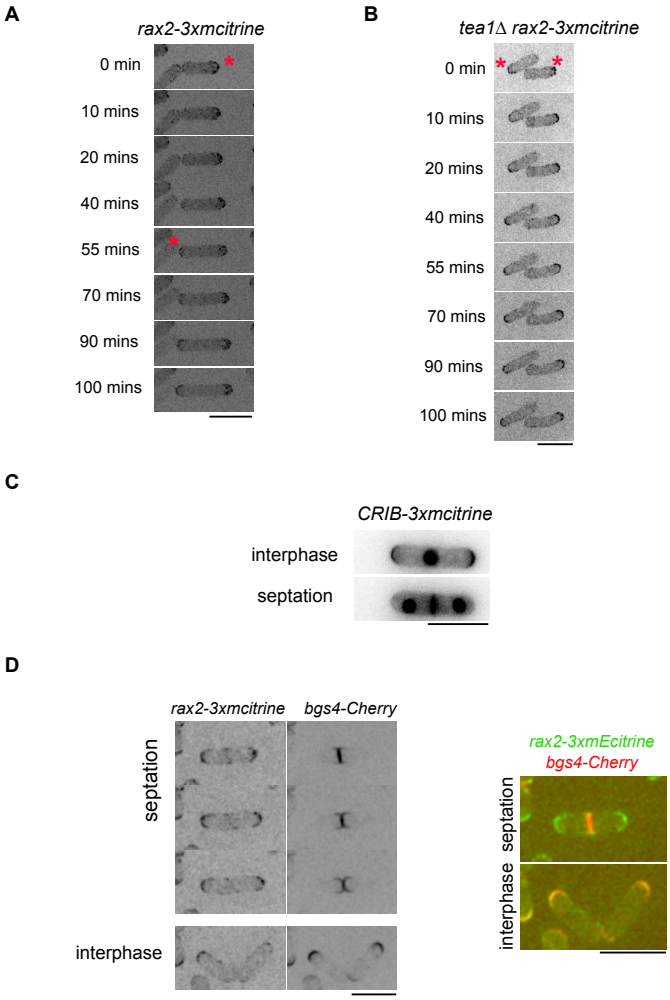

Figure 6.6 Rax2 remains at the cell tips during septation, even though growth machinery is relocalized to the cell septum A) Localization of Rax2 correlates with growth. Rax2 is initially localized to one end pre-NETO and localizes to both the ends after NETO. **B)** Rax2 is localized only to the growing end in a monopolar growing *tea1*Δ cells (* - growing ends). **C)** *CRIB-3xmcitrine* is localized to cell tips during interphase and relocalizes to septum during septation. **E)** Rax2 and Bgs4 colocalize during interphase at the cell tips, but Rax2 remains at the cell tips during septation, whereas Bgs4 relocalizes to the cell septum. (imaging in minimal medium). Scale, 10μm.

C

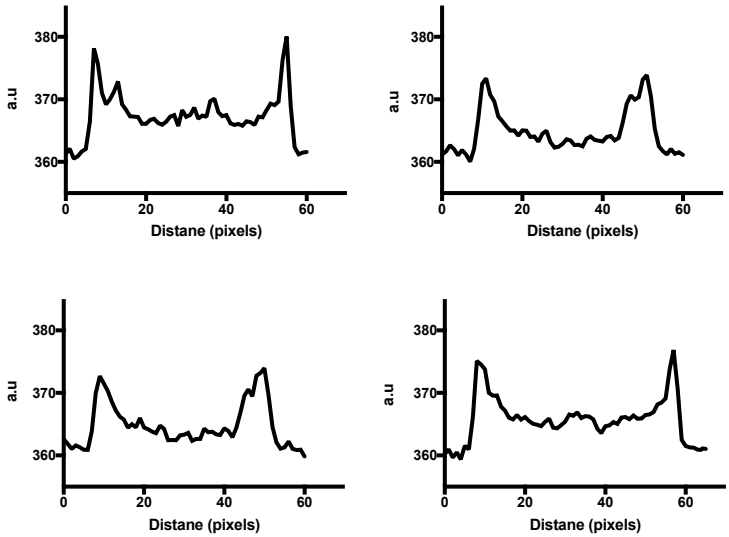

Figure 6.6C. Rax2 shows symmetric accumulation at the two cell tips. Graphs obtained by plotting line intensity of cells. Two peaks in each graph represent Rax2 intensity at the cell tips. In all the cells, both the cell tips showed similar amount of Rax2 suggesting that hypothesis of asymmetry in Rax2 localization due to correlation of Rax2 localization with growth is probably incorrect.

6.2.5 Slower dynamics of Rax2 might be important for its role as a landmark

Previously in budding yeast it was reported that Rax2 is a stable cortical landmark inherited over multiple generations (Chen et al. 2000). Time-course experiments using Rax2-myc repressed for 18 hours under *GAL1* promoter showed that the insoluble pools of Rax2 were very stable, with a half-life of about 6 hours (Chen et al. 2000). Therefore, I wanted to investigate the stability and dynamics of Rax2 at the cell tips in fission yeast. In order to address this, I did fluorescent recovery after photobleaching (FRAP) on *Rax2-3xmcitrine* strain. Since Rax2-3xmcitrine signal was very weak, it was not possible to image frequently or acquire the full Z volume because of photobleaching. Therefore, instead of standard 11 Z stacks of 0.6µm-step size, I only collected 4 Z stacks and imaged every 10 minutes post-bleach. Initially, FRAP on *Rax2-3xmcitrine* cells gave a mixture of outcomes. In some cases I observed recovery of Rax2 within 50 mins post bleach, while in other cases there was no obvious recovery. A possible explanation for cells in which Rax2 didn't recover after photobleaching is that these cells might be in mitosis during which cell growth ceases at the cell tips and therefore, new Rax2 is not being transported to the cell tips. In order to confirm this, I selected septating cells under the microscope and performed FRAP on Rax2 at the cell tip. Rax2 failed to recover to the cell tips in these septating cells (Fig. 6.7A). This suggests that indeed Rax2 localization to the cell tips correlates with growth and Rax2 is no longer transported to the cell tips when cells enter mitosis.

All these results suggest that in order to study the dynamics of Rax2, it is important to do FRAP on interphase cells. Therefore, I used *Rax2-3xmcitrine bgs4-Cherry* cells to perform FRAP. Because Rax2 doesn't accumulate at the septum, I used Bgs4 as a marker to identify (and avoid) septating cells, thereby doing FRAP only on interphase cells. I followed the following FRAP protocol. Initially I collected 2 time points 5 seconds apart as pre-bleach. 350 ms of 473nm laser was used to bleach the tip signal of Rax2. After bleaching, cells were imaged every 10 minutes for 1 hour to assay recovery of Rax2. Rax2 was almost completely recovered to the cell tips after 50 minutes (Fig. 6.7B-C).

In budding yeast, ScRax2 is transported via secretory pathway (Chen et al. 2000). Similarly, I have shown that Rax2 did not recover to cell tips upon FRAP in septating cells suggesting Rax2 might be transported via secretory pathway. Similar to Rax2, Bgs4 and Cdc42 are also transported via secretory pathway. Previously, it was shown that Bgs4 recovered to cell tips after FRAP within 20 seconds (Estravis et al. 2012). Similarly, it was previously reported that Cdc42, which is also transported

via secretory pathway has a recovery halftime of approximately 4.6 seconds (Bendezú et al. 2015). This clearly shows that unlike Bgs4 and Cdc42, Rax2 is much more stable at the cell tips. Based on these results, I propose that because Rax2 has a slower off-rate from cell tips in general, when cells enter septation, Rax2 takes much longer time to relocalize to the cell septum and hence remain at the cell tips, whereas Bgs4 and Cdc42 because of its faster dynamics relocalize to the cell septum.

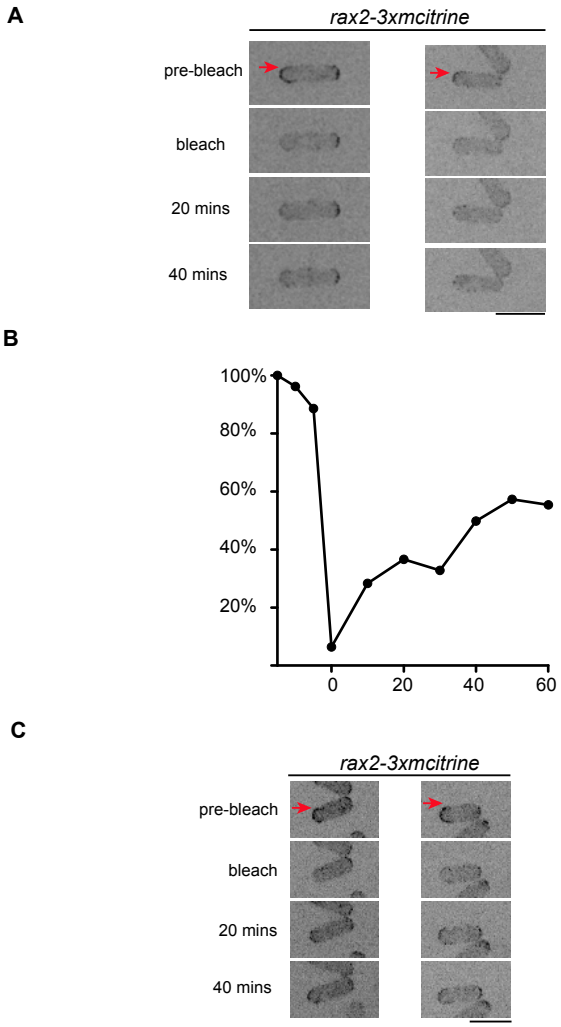

Figure 6.7. Rax2 exhibits slower dyanamics compared to Cdc42 and Bgs4. **A)** FRAP on rax2-3xmcitrine cells undergoing septation shows no recovery of Rax2 even after 40 minutes. **B)** Graph showing recovery of Rax2 after FRAP. Recovery suggests that 60% of the Rax2 is mobile pool whereas, 40% of Rax2 is stable pool and all of which recovers by 40 mins.Half-time (t1/2) for recovery of the mobile pool is 10 mins **C)** Still images from live-cell imaging shows Rax2 recovering to the cell tips after FRAP within 40 mins. Scale, 10µm.

6.2.6 Rax2-Rax1 landmarks are important for normal monopolar to bipolar growth pattern of fission yeast cells

Previously I have shown that both Rax2 and Rax1 are part of the growth memory-based polarity cue involved in establishment of polarized growth. Moreover, I have shown that this cue establishes polarized growth at the old of the daughter cell inherited from the old-growing end of the mother in *tea1*Δ cells. Next, I wanted to investigate how the Rax1-Rax2 landmark contributes to polarity establishment in wild-type fission yeast cells. In order to address this, I did live-cell imaging of *rax2*Δ*CRIB-3xmcitrine* and *rax1*Δ*CRIB-3xmcitrine* cells. Live-cell imaging of *rax2*Δ*CRIB-3xmcitrine* and *rax1*Δ*CRIB-3xmcitrine* cells showed that after cytokinesis of the mother cell, these mutants immediately undergo bipolar growth, unlike wild-type cells, which initially grow monopolar and then grow bipolar (Fig.6.8A-B) (N= 12 daughter pairs or 24 cells). A possible explanation for the immediate bipolar growth of *rax2*Δ and *rax1*Δ cells might be due to ability of Tea1 to establish polarized growth at the new ends in the absence of competition from Rax1/Rax2 landmarks at the old ends. In wild-type cells, during septation, both Tea1 and Rax2 are localized to the cell tips, whereas only Tea1 is localized to the cell septum. Therefore, upon cytokinesis, old ends that have both Tea1 and Rax2 landmarks successfully compete with the new end that only has Tea1 landmark and initiate growth at the old ends. In *rax2*Δ*/rax1*Δ cells, there is no competition from the old end; hence Tea1 landmark can establish polarized growth at both old and new ends immediately after cytokinesis. It is also possible that in the absence of competition from the old end (*rax2*Δ*/rax1*Δ), cue generated by septation might initiate polarized growth at the new end resulting in premature bipolar growth or premature bipolar growth might be due to cooperation between both septation cue and Tea1 cue present at the new end. In this way cooperation between Tea1 and Rax2 might be responsible for maintaining the normal growth pattern of fission yeast cells and lack of Rax2/Rax1 landmark leads to immediate bipolar growth (Fig. 6.9).

An alternative possibility, which I do not favour, is based on the claim by Choi *et al*. that Rax2 is required for the localization of For3 (Choi et al. 2006). However, their imaging of Rax2 was very dim, making it difficult to make any conclusions. Previously I have shown that *for3*Δ cells grow in a premature bipolar fashion. Therefore, if Rax2 were required for localization of For3, the claim of Choi *et al*. could potentially explain why *rax2*Δ cells grow in an immediate bipolar fashion. However, in my own experiments, *rax2*Δ cells did not show any of the aberrant morphology that is associated with *for3*Δ cells (data not shown). In order to investigate more

conclusively whether Rax2 is required for localization of For3, I constructed a *rax2*Δ *for3-YFP* strain. Live-cell imaging showed that For3 was localized to the cell tips in *rax2*Δ cells similar to wild-type (*rax2+*) cells suggesting that Rax2 is not required for proper localization of For3 (Fig. 6.8C). Moreover, live-cell imaging of *rax2*Δ *LifeAct-mCherry* also showed normal actin cable organization similar to wild-type (*rax2+*) cells, suggesting that localization of For3 is not dependent on Rax2 (Fig. 6.8D).

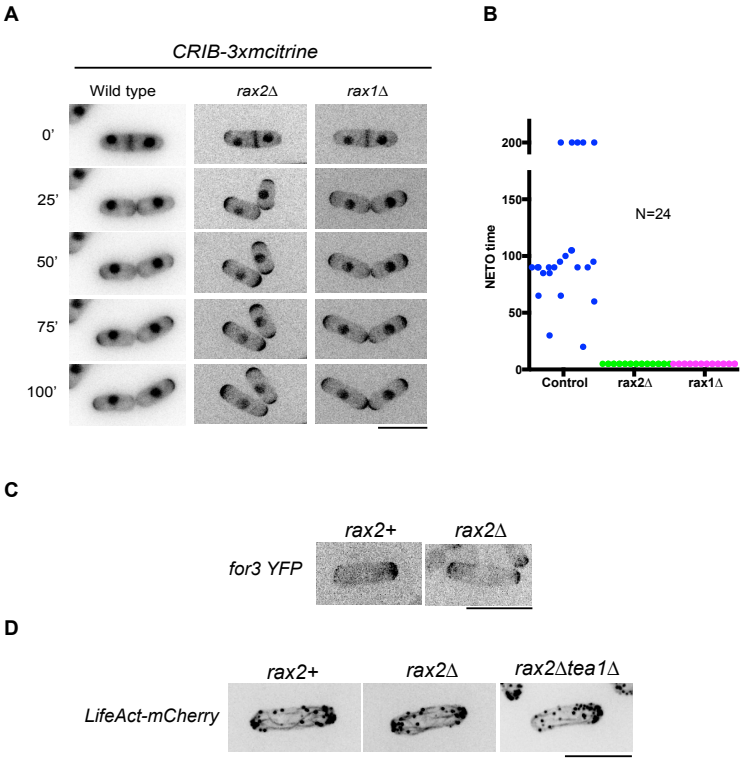

Figure 6.8. Rax2/Rax1 landmark is important for achieving normal monopolar to bipolar growth pattern of fission yeast cells A) Still images from live-cell imaging of wild-type, *rax2*Δ and *rax1*Δ cells showing immediate NETO in *rax2*Δ and *rax1*Δ cells compared to wild type cells. B) Time of NETO in wildtype (blue), *rax2*Δ (green) and *rax1*Δ (purple) cells. Time zero is the time at which septum disassembly begins. Only cells where both the daughter cells are visible in the new cell cycle are considered. **C)** Localization of *for3-YFP* in *rax2+* and *rax2*Δ cells suggesting Rax2 is not required for proper localization of For3. **D)** Actin cable organization labelled by LifeAct-mCherry in *rax2+*, *rax2*Δ and *rax2*Δ*tea1*Δ cells suggesting Rax2 is not important for actin cable organization. Scale, 10µm.

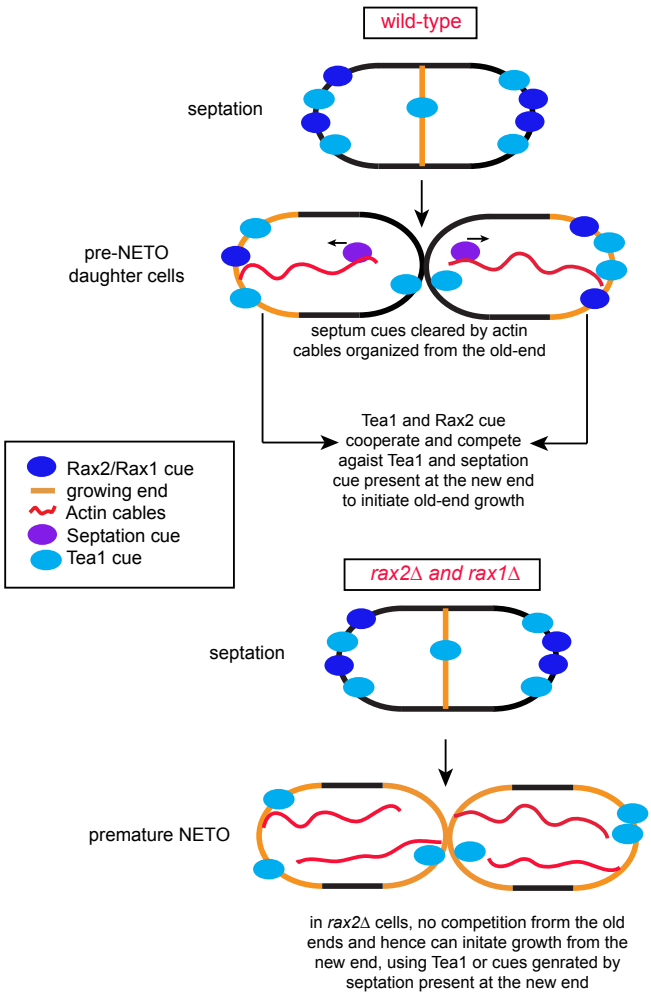

Figure 6.9. Model for role of Rax2/Rax1 landmark in maintaining normal monopolar to bipolar growth pattern of fission yeast cells. Both *rax2*Δ and *rax1*Δ cells grow in a premature bipolar fashion suggesting that Rax2/Rax1 landmark cooperate with the Tea1 landmark to establish monopolar growth at the old end in preNETO cells. Therefore, in the absence of Rax2/Rax1 landmark, cues present at the new end - generated either by septation or Tea1 cue, can initiate immediate new end growth.

6.2.7 Unlike Tea1 and Tea4, Tea3 and Pom1 do not act as "true" landmarks in fission yeast

Previously, I have shown that establishment of polarized growth at the old end of the daughter cell inherited from the old-growing end of the mother cell in a *tea1*Δ daughter pair is dependent on Rax2-Rax1 growth memory cue. In the absence of Tea1 and Rax2 cues, cells depend on a cue generated by septation and grow exclusively from the new ends. Similar to *tea1*Δ cells, mutants of *tea4*Δ, *tea3*Δ and *pom1*Δ are also known to grow in a syn pattern (Bähler & Pringle 1998; Mata & Nurse 1997; Arellano et al. 2002; Niccoli et al. 2003; Martin et al. 2005; Tatebe et al. 2005). Moreover, Tea1 binds directly to Tea4 and Tea3 *in vitro* and Tea4, Tea3 and Pom1 lose their tip localization in *tea1*Δ cells (Martin et al. 2005; Tatebe et al. 2005; Snaith et al. 2005; Padte et al. 2006; Bähler & Pringle 1998; Arellano et al. 2002) Therefore, I wanted to investigate similar to Tea1, if Tea4, Tea3 and Pom1 can also act as landmarks and identify old ends to establish polarized growth. I constructed *tea4*Δ*rax2*Δ*CRIB-3xmcitrine*, *tea3*Δ*rax2*Δ*CRIB-3xmcitrine* and *pom1*Δ*rax2*Δ*CRIB-3xmcitrine* cells. Live-cell imaging of *tea4*Δ*rax2*Δ*CRIB-3xmEcitrine* cells showed that similar to *tea1*Δ*rax2*Δ cells, *tea4*Δ*rax2*Δ cells also grow in an axial pattern (n= 112). This suggests that Tea4, similar to Tea1 also act as a landmark to identify the old ends to establish polarized growth (Fig. 6.10A-B). However, *tea3*Δ*rax2*Δ*CRIB-3xmcitrine* and *pom1*Δ*rax2*Δ*CRIB-3xmcitrine* cells did not show axial growth. Instead, one daughter cell grew bipolar, whereas the other daughter cell grew monopolar from the new end (Fig. 6.10A-B). This shows that Tea3 and Pom1 do not act as landmarks in the same way as Tea1 or Tea4. To determine whether *tea3*Δ*rax2*Δ*CRIB-3xmcitrine* and *pom1*Δ*rax2*Δ*CRIB-3xmcitrine* cells were able to establish polarized growth at the old ends by using Tea1/Tea4 landmarks, I constructed *tea1*Δ*tea3*Δ*rax2*Δ *CRIB-3xmcitrine* cells. Live-cell imaging showed that *tea4*Δ*tea3*Δ*rax2*Δ *CRIB-3xmcitrine* cells grow in an axial pattern, suggesting establishment of polarized growth at the old ends in *tea3*Δ*rax2*Δ cells were indeed by Tea1/Tea4 landmark (Fig. 6.10A).

A

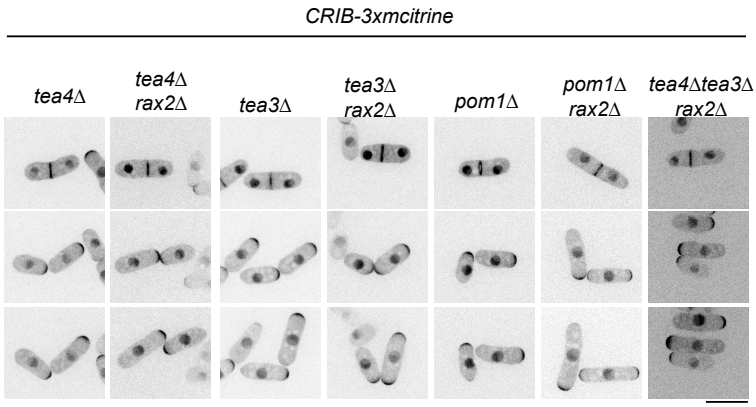

B

Genotype	→ →	← →	→ ←	→ ↔	↔ ↔
*tea1*Δ	96.25%	1.5%	.75%	1.5%	0
*tea4*Δ	96.72%	1.6%	0	1.6%	0
*tea3*Δ	78.75%	8.75%	0	12.5%	0
*pom1*Δ	93.4%	2.1%	0	4.5%	0
*tea1*Δ*rax2*Δ	0	0	96.8%	3.2%	0
*tea4*Δ*rax2*Δ	4.5%	0	92.13%	3.370%	0
*tea3*Δrax2Δ	0	2%	24.4%	69.3%	4%
*pom1*Δrax2Δ	3.2%	3.2%	0	80.64%	12.9%

Figure 6.10. Tea4 behaves as a true landmark similar to Tea1, whereas Tea3 and Pom1 do not behave as true landmarks. A) Still images from time-lapse movies of *tea4*Δ, *tea4*Δ*rax2*Δ, *tea3*Δ, *tea3*Δ*rax2*Δ, *pom1*Δ, *pom1*Δ*rax2*Δ and *tea4*Δ*tea3*Δ*rax2*Δ cells showing respective growth patterns. *tea4*Δ,*tea3*Δ and *pom1*Δ grow in syn pattern as previously reported. *tea4*Δ*rax2*Δ grow in an axial pattern suggesting Tea4 act as a landmark to establish polarized growth at the old ends. However, daughter pairs of *tea3*Δ*rax2*Δ and *pom1*Δ*rax2*Δ show one monopolar and one bipolar growth pattern suggesting Tea3 and Pom1 do not act as true landmarks to identify old ends. *tea4*Δ*tea3*Δ*rax2*Δ shows axial growth pattern suggesting that establishment of polarized growth at the old end in *tea3*Δ*rax2*Δ is indeed by Tea1/Tea4 cue. **B)** Table showing different genotypes and corresponding growth patterns. Arrows indicate direction of growth (n>100). Scale, 10μm. Imaging carried out in rich medium.

6.2.8 Polarity landmarks are important to maintain polarized growth under stresses

Previously I have shown that upon depolymerization of MTs, almost all the cells imaged in minimal medium failed to establish NETO, whereas approximately 50% of the cells imaged in rich medium established NETO (see section 5.2.2). Similarly, depolymerization of MTs gave syn and anti patterns in minimal medium, whereas gave only anti pattern in rich medium (see section 5.2.9). These results indicate that growth medium in which cells are imaged can dictate polarity growth patterns and therefore, are useful to study regulation of polarized growth. All the polarity mutants explained in this chapter till now were imaged in rich medium. Therefore, I wanted to investigate how different polarity mutants explained in this chapter behaved when imaged in minimal medium. Live-cell imaging of *tea1*Δ, *tea4*Δ, *pom1*Δ and *tea3*Δ in conditioned minimal medium showed syn growth pattern similar to when imaged in rich medium. Surprisingly, I found that that during imaging of these mutants, Cdc42 was spontaneously lost from the cell tips and relocalized to ectopic sites, hereafter referred to as 'polarity crash' (Fig. 6.11A). Next, I wanted to investigate what percentage of these mutants undergoes polarity crash. In order to study this, I did live-cell imaging of all the mutants for 15 minutes and calculated the number of cells undergoing polarity crash at the start of the movie or at any point during imaging. Approximately 50% and 40% of *tea1*Δ and *tea4*Δ cells showed polarity crashes, whereas 18% and 42.5% of *tea3*Δ and *pom1*Δ cells showed polarity crashes. Interestingly, polarity crashes observed in *tea1*Δ*, tea4*Δ *and pom1*Δ mutants were exacerbated in a *rax2*Δ background. These results indicate that apart from playing a role in establishment of polarized growth, polarity proteins Tea1, Tea4, Tea3 and Pom1 are also important for maintenance of polarized growth. Moreover, along with the MT-based landmarks Tea1 and Tea4, growth memory cue Rax2 also contribute synergistically to maintenance of polarized growth. It is important to note that even though Pom1 does not act as a true landmark, approximately 90% of the *pom1*Δ*rax2*Δ cells showed polarity crashes compared to 60% and 55% of *tea1*Δ*rax2*Δ and *tea*Δ*rax2*Δ cells respectively (Fig.6.11A). This suggests that that role of polarity proteins as landmarks and for maintenance of polarized growth is not mutually exclusive.

Next, I wanted to investigate why mutants such as *tea1*Δ*, tea4*Δ*, pom1* and *tea3*Δ exhibit polarity crashes when imaged in minimal media. I hypothesized that polarity crashes might be induced by subtle stresses to the cells in minimal medium, possibly due to nutrient limitations. Previously, it was shown that Tea4 interacts with

Win1, a MAP kinase kinase kinase (MAPKKK) of the stress-activated kinase pathway, and polarity defects were accentuated in *tea4*Δ cells exposed to osmotic stresses compared to wild type cells exposed to the same stress (Tatebe et al. 2005). Moreover, recent work from our lab shows that cells undergo polarity crash or ectopic localization of Cdc42 upon activation of Sty1 MAPK, an ortholog of mammalian p38-kinase (Mutavchiev *et al.*, Submitted). Sty1 is activated under various environmental stresses such as osmotic shock and heat stress (Tatebe et al. 2005) In order to investigate this hypothesis, I constructed a *tea4*Δ*rax2*Δ*sty1*Δ *CRIB-3xmcitrine* strain. Live-cell imaging of *tea4*Δ*rax2*Δ*sty1*Δ *CRIB-3xmcitrine* cells showed that polarity crashes were completely abolished by deleting Sty1 (Fig. 6.11B). These results indicate that apart from establishment of polarized growth, different polarity landmarks such as Tea1, Tea4, Rax2 and Rax1 are also important for maintaining polarized growth, especially under conditions of stress.

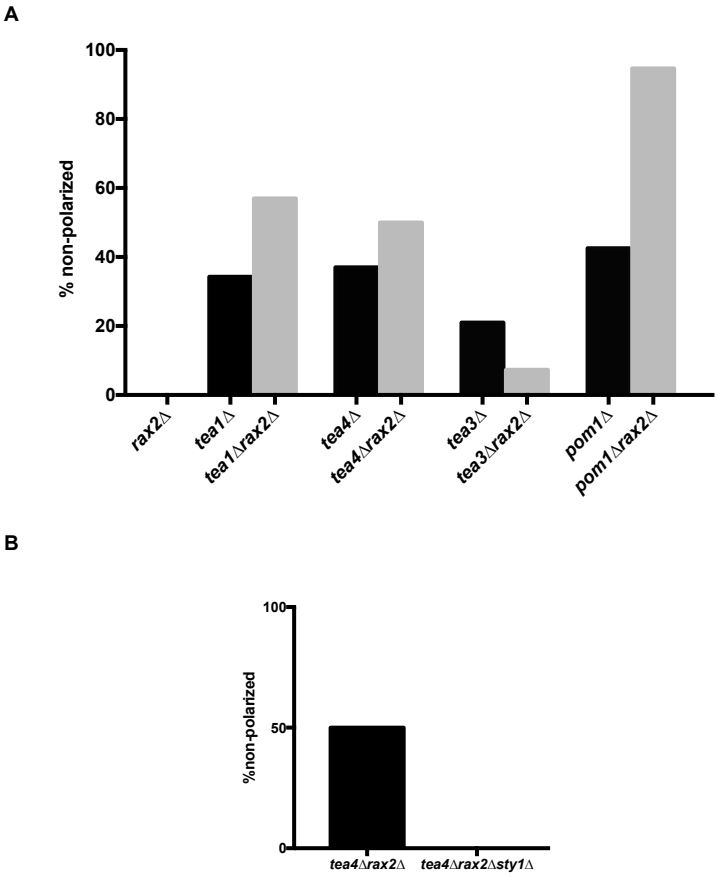

Figure 6.11. Polarity proteins Tea1, Tea4 and Pom1 are important to maintain polarized growth under stress. A) Percent of cells showing non-polarized growth (polarity crash) in different genetic background. Polarity crash is meassured by imaging different mutants for 15 mins and scoring cells where Cdc42 loses from the cell tips at he start or at any point during imaging. Landmarks *tea1* Δ and *tea4*Δ cells show similar extend of polarity crash and these polarity crashes are increased in *rax2*Δ background. pom1Δrax2Δ cells also show high polarity crash even though Pom1 is not a true landmark. This suggests that role of polarity proteins in acting as landmarks and in maintenance of polarized growth under stress are not mututally exclusive. **B)** Polarity crash is induced by subtle stresses in minimal medium. 50% of the cells undergo polarity crash in *tea4*Δ*rax2*Δ cells and this polarity crash can be rescued by deleting sty1, a kinase involved in MAPKKK cascade. This suggests that polarity proteins are important to maintain polarized growth under stresses.

6.2.9 Tea1 and Rax2 landmarks are important for re-establishment of polarized growth at the cell tips after stresses that perturb polarized growth

Previously it was shown that compared to wild-type cells, around 30% of *tea1*Δ cells show bent phenotype at 25˚C and upon temperature shift to 36˚C, the phenotype becomes stronger with 35% of cell showing bent phenotype and 20% forming T-shaped cells or branches (Mata & Nurse 1997). This suggests that Tea1 landmark is important to re-identify the cell tips during recovery from stress (temperature shift). I have shown that landmark proteins Tea1 and Rax2 contribute synergistically in maintaining polarized growth under stress. Therefore, I wanted to investigate along with Tea1, if Rax2 is also involved in re-establishment of polarity to the cell tips. In order to test this hypothesis, I first added 50μM LatA to wild-type, *rax2*Δ, *tea1*Δ and *tea1*Δ*rax2*Δ cells to depolymerize actin cytoskeleton. Apart from depolymerizing actin cytoskeleton, addition of LatA also results in activation of sty1-mediated stress signalling pathway, leading to relocalization of Cdc42-GTP from cell tips to ectopic sites (Mutavchiev *et al*., submitted). Next, I washed-out LatA using fresh media to restore actin cytoskeleton and check the number of cells able to re-establish polarized growth in wild-type, *rax2*Δ, *tea1*Δ and *tea1*Δ*rax2*Δ cells.

I followed the following strategy. I used a *CRIB-3xmcitrine LifeAct-mCherry* strain, which labels active Cdc42 and actin cytoskeleton, respectively. First, I did live-cell imaging of *CRIB-3xmcitrine LifeAct-mCherry* cells without perturbing the actin cytoskeleton for 10 mins, to visualize the intact Cdc42 polarity module and the intact actin cytoskeleton. Next, I added 50 μM LatA to depolymerize the actin cytoskeleton under the microscope. Actin cables and patches were depolymerized immediately. CRIB-3xmcitrine was relocalized from the cell tips to ectopic sites within 40 minutes. After 40 minutes, I washed out LatA thoroughly (18 washes) from the cells using fresh media under the microscope and continued imaging. Immediately after washing out LatA, actin patches reappeared and initially relocalized to the cell tips, but become depolarized, probably because Cdc42 is not yet localized to the cell tips. However, actin cables never recovered after washout (Fig.6.12A). Even though I performed very thorough washout to remove LatA, it is possible that a small amount of LatA still remain inside the cells. Previously it was reported a lower dose of LatA could depolymerize actin cables without affecting actin patches and therefore, this small amount of LatA might prevent actin cable polymerization (Martin & Chang 2006; Lo Presti & Martin 2011). In wild-type cells, CRIB-3xmcitrine relocalized from the ectopic sites to the cell tips after 70 minutes of washing out of LatA and cells reinitiated growth at the tips. Similar to wild-type cells, in *rax2*Δ cells, CRIB-

3xmcitrine relocalized to cell tips in 70 minutes and reinitiated growth possibly due to Tea1 landmark (Fig.6.12B). In *tea1*∆ cells, approximately 34% of the cells relocalized CRIB-3xcitrine and re-established polarized growth to the cells. However, in these cells, relocalization of CRIB-3xcitrine took much longer (~100 mins) compared to wild-type or *rax2*∆ cells (~70 mins). This shows that Tea1 landmark, as reported before is important for re-establishment of polarized growth after stresses that perturb actin cytoskeleton. In *tea1*∆*rax2*∆ cells, almost all the cells failed to re-establish polarized growth after LatA washout (96% cells) suggesting that both Tea1 and Rax2 landmarks are important to re-establish polarized growth after stress.

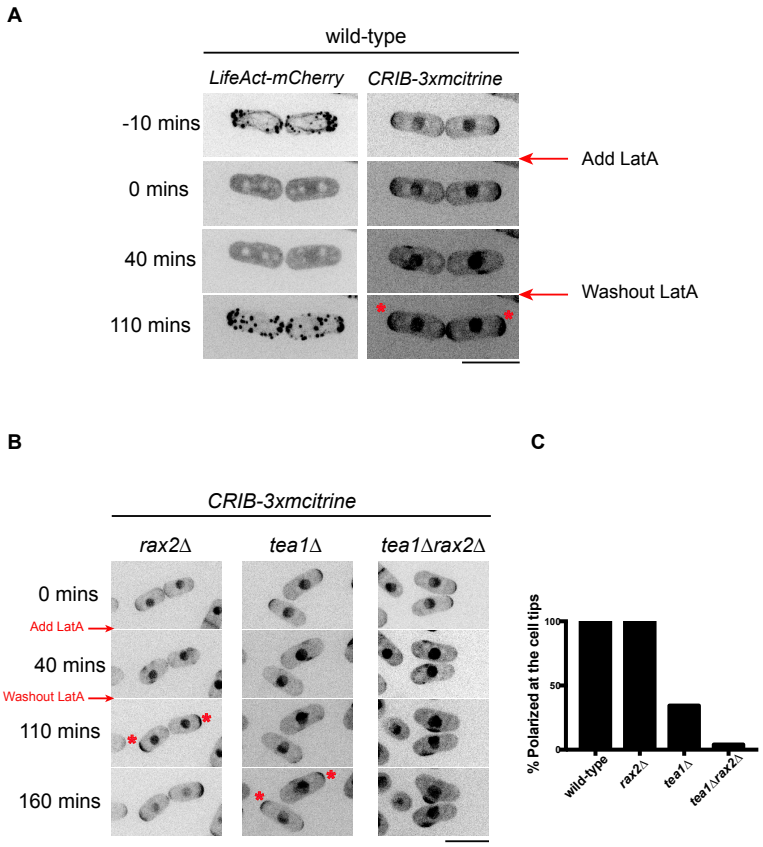

Figure 6.12. Tea1 and Rax2 landmarks are important for re-establishment of polarized growth after stress that perturb polarized growth. A) Wildtype cells re-establish polarized growth at the cell tips after washing out LatA. Two-channel imaging of actin (LifeAct-mCherry) and active Cdc42 (CRIB-3xmcitrine) in wildtype cells showing untreated (-10 mins), LatA treated (0-40 mins) and LatA washout (40-110 mins). CRIB relocalizes to cell tips after washout of LatA within 70 mins (40-100 time points) of washout of LatA. **B)** LatA washout experiments in *rax2*Δ, *tea1*Δ and *tea1*Δ*rax2*Δ cells. *rax2*Δ cells re-establish polarity similar to wildtype cells whereas *tea1*Δ*rax2*Δ cells failed to re-establish polarized growth to the cell tips. In *tea1*Δ cells some cells (34%) re-establish polarized growth albeit after much longer time (<100 mins) compared to wildtype and *rax2*Δ cells (70 mins). **C)** Percent of cells able to re-establish polarized growth to cell tips upon LatA wash-out in wildtype, *rax2*Δ, *tea1*Δ and *tea1*Δ*rax2*Δ cells. Scale, 10µm. (* - re-establishment of polarized growth).

6.3 Discussion

In this chapter I have shown that the growth memory-based cue, which I previously proposed in chapter 5 involves two predicted transmembrane proteins Rax2 and Rax1. Further, using FRAP, I have shown that Rax2 exhibits slower dynamics compared to other growth-dependent proteins such as Cdc42 and Bgs4 and this slower dynamics of Rax2 might be important for its role as a growth memory-based cue. Previously in chapter 5, I have proposed (see section 5.3.4) that co-operation and competition among three internal cues are involved in regulation of normal growth pattern of fission yeast cells. The model proposes that initially Tea1 and MT-based cue along with growth memory-based cue co-operate to establish polarized growth at the old of the daughter cells. In addition, these cues together compete with the cue generated by septation at the new end and prevent new end growth. At a later stage in cell cycle, Tea1 and MT-based cue establish bipolar growth. Further, I tested this model using yeast mutants, drug perturbations and live-cell imaging. Here, I identity Rax2 and Rax1 as the growth memory-based cue and further test the previously proposed model using live-cell imaging and *rax2*Δ mutants.

6.3.1 Rax2-Rax1 landmarks are important for maintaining normal fission yeast growth pattern

Previously, I proposed that both Tea1 and growth memory-based cue co-operate and compete against the cue generated by septation to establish monopolar old end growth in pre-NETO cells. Therefore, I predict that in the absence of growth memory cue, old end will no longer be able to successfully compete against the new end and hence initiate new end growth. Indeed in *rax2*Δ and *rax1*Δ cells, I found that cells establish premature bipolar growth instead of normal growth pattern of fission yeast. This support our model that Tea1 and Rax2 landmark cooperate and compete against the cue generated by septation at the new end in pre-NETO cells. Further, I proposed that in *tea1*Δ cells, the daughter cell that did not inherit the growth memory cue from the mother cell (old growing end) depend on a cue generated by septation to establish polarized growth. Therefore, I predict that in the absence of both Tea1 and growth memory cue, cells will use a cue generated by septation to establish polarized growth. Indeed in *tea1*Δ*rax2*Δ and *tea1*Δ*rax1*Δ cells, cells grow exclusively from the ends generated by septation (new ends), possibly by using cues generated by septation.

Here I propose a revised model for regulating the normal polarized growth pattern in fission yeast cells. Immediately after cytokinesis, both Tea1 and Rax2-Rax1 landmarks present at the cell tips co-operate to establish polarized growth at the old ends in pre-NETO cells. Further, these two landmarks compete against cue generated by septation at the new ends preventing premature bipolar growth. At a later stage in cell cycle, MTs and Tea1 helps in establishing bipolar growth. Similar competition is also reported in budding yeast to maintain a single "front" or bud site. In budding yeast, during early stages of cell polarization multiple Cdc42 clusters are formed on the membrane but only one polarity cluster or "front" is maintained. Recently it was shown that competition between different polarity proteins are responsible for maintaining this single "front" and by manipulating this competition it is possible to create and maintain multiple "fronts" leading to multiple budding (Wu et al. 2015).

An interesting unanswered question is why fission yeast cells developed such a mechanism to maintain initially monopolar and then bipolar growing cells. In fission yeast, pre-NETO, only old end is growing. Old-end is the end which was growing in the previous cell cycle and therefore, old end might have accumulated all the cell wall material to undergo sufficient remodelling to initiate growth immediately at the start of the new cell cycle. On the other hand, new end is generated by septation and therefore, new end might not have undergone sufficient remodelling to initiate growth. By undergoing initially monopolar and then bipolar, cells might be giving time for the new end to fully mature in order to initiate growth. Previously, Koyano *et. al* showed that casein case 1γ (Cki3) is critical for undergoing NETO and *cki3*Δ cells failed to undergo normal NETO and instead showed premature NETO (Koyano et al. 2015). Additionally, they showed that these premature bipolar growing *cki3*Δ cells are hypersensitive to a cell wall inhibitor calcoflour white. Based on this observation, they suggest that undergoing of NETO at proper stage of cell cycle might be important for maintaining the integrity of cell wall. In future, it will be interesting to investigate what happens to premature bipolar growing *rax2*Δ and *rax1*Δ cells upon treatment with calcoflour white. If *rax2*Δ and *rax2*Δ cells are also hypersensitive to calcoflour white, this might suggest that initially monopolar and later bipolar growing pattern of fission yeast might be important to maintain the cell wall integrity of these cells.

6.3.2 Dynamics of Rax2 might be important for growth memory-based cue

In this chapter I have shown that similar to Cdc42 and Bgs4, Rax2 is also transported via exocytic pathway and localization of Rax2 correlates with growth. Surprisingly, when growth machinery is relocalized to septum during septation, unlike Cdc42 and Bgs4, Rax2 did not accumulate at the cell septum. Moreover, FRAP on Rax2 showed that Rax2 exhibits much slower dynamics compared to Cdc42 and Bgs4. Here I propose that because of the slower dynamics of Rax2, Rax2 takes much longer time to relocalize to the cell septum during septation and hence failed to accumulate at the septum during septation. Therefore, in the new cell cycle, Rax2 landmark that is already present at the cell tips from the previous cell cycle can re-establish polarized growth.

An important unanswered question is why does Rax2 show different dynamics compared to Bgs4 even though both proteins are predicted to have transmembrane domain and are targeted via exocytic pathway. Integral membrane proteins, secretory vesicles and cell wall re-modellers are transported to and from the plasma membrane and the precise targeting and maintenance of these proteins are important for polarized growth in fission yeast (Martin & Arkowitz 2014). This regulation of polarized growth involves exocytosis and endocytosis and a balance between exo- and endocytosis is thought to maintain the polarized state (Slaughter et al. 2009; Marco et al. 2007). During polarized growth, exocytic machinery targets membrane proteins to the cell tips. Later, these proteins need to be endocytosed to recycle back to the cell interior to facilitate incorporation of new membrane proteins at the cell tips. Therefore, the dynamics of membrane proteins might be dependent on the net rate of exocytosis and endocytosis. In the case of proteins such as Bgs4, it is possible that these proteins are targeted to the cell tips by exocytosis and are recycled back quickly via endocytosis and therefore, exhibits faster dynamics. However, in the case of Rax2 it is possible that Rax2 doesn't recycle back via endocytosis, but instead uses a different mechanism and therefore, exhibits slower dynamics.

6.3.3 How does Rax2 and Rax1 'talk' to the Cdc42 polarity module?

In this chapter I have shown that Rax2-Rax1 landmark is involved in establishment of polarized growth in fission yeast. However, how this landmark 'talk' to Cdc42 polarity module is still not known and needs to be investigated. Both Rax2

and Rax1 are predicted to have transmembrane domains. In budding yeast, it was shown that localization of Sc.Rax1 and Sc.Rax2 are interdependent (Kang et al. 2004). Similarly, in fission yeast I have shown that Rax1, and C-terminal region of Rax2 is important for cortical localization of Rax2. In budding yeast where Rax2 and Rax1 were first discovered, ScRax2 and ScRax1 interact with cortical landmarks ScBud8 and ScBud9. Localization of ScRax1 and ScRax2 to the bud tip and distal pole is dependent on ScBud8, and normal localization of ScBud8 was partially dependent on ScRax1 and ScRax2 (Kang et al. 2004) ScBud8 and ScBud9 in turn interact with ScBud5 (GEF for the small GTPase ScRsr1/Bud1), resulting in activation of ScRsr1, which promotes the local activation of ScCdc42 (Park & Bi 2007). However, homologs for ScBud8 and ScBud9 have not been identified in fission yeast. Recently, it was shown that in haploid budding yeast cells, ScRax2/Rax1 act as an anchor to recruit ScNba1 and ScNis1 to cytokinetic remnants. ScNba1 directly binds to ScBem1 and ScCdc24 and inhibits ScCdc24 binding to ScRsr1, preventing local activation of ScCdc42. Thus ScRax1/Rax2 act as an anchor to recruit proteins that inhibit activation of ScCdc42 at the previous site of budding (cytokinetic remnants) (Meitinger et al. 2014). However, a homolog for Nba1 and Nis1 does not exist in fission yeast. Moreover, in fission yeast Rax1/Rax2 seems to promote rather than inhibit polarized growth. However, it is possible that similar to haploid budding yeast cells, Rax2-Rax1 could act as a scaffold to recruit other proteins important for regulating polarized growth.

References

Adames, N.R. & Cooper, J. a., 2000. Microtubule interactions with the cell cortex causing nuclear movements in Saccharomyces cerevisiae. *Journal of Cell Biology*, 149(4), pp.863–874.

Adams, A.E.M. et al., 1990. CDC42 and CDC43, Two Additional Genes Involved in Budding and the Establishment of Cell Polarity in the Yeast Saccharomyces cerevisiae. , 130(2), pp.299–312.

Aghamohammadzadeh, S. & Ayscough, K.R., 2009. Differential requirements for actin during yeast and mammalian endocytosis. *Nature cell biology*, 11(8), pp.1039–42. Available at: http://dx.doi.org/10.1038/ncb1918.

Akhmanova, A. & Hoogenraad, C.C., 2015. Microtubule minus-end-targeting proteins. *Current Biology*, 25(4), pp.R162–R171. Available at: http://dx.doi.org/10.1016/j.cub.2014.12.027.

Akhmanova, A. & Steinmetz, M.O., 2015. Control of microtubule organization and dynamics: two ends in the limelight. *Nature reviews. Molecular cell biology*, 16(12), pp.711–26. Available at: http://www.nature.com/doifinder/10.1038/nrm4084%5Cnhttp://www.ncbi.nlm.nih.gov/pubmed/26562752.

Akhmanova, A. & Steinmetz, M.O., 2010. Microtubule +TIPs at a glance. *Journal of Cell Science*, 123(20), pp.3415–3419. Available at: http://jcs.biologists.org/cgi/doi/10.1242/jcs.062414.

Akhmanova, A. & Steinmetz, M.O., 2008. Tracking the ends: a dynamic protein network controls the fate of microtubule tips. *Nature reviews. Molecular cell biology*, 9(4), pp.309–322.

Akira yamashita et al., 2005. The Roles of Fission Yeast Ase1 in Mitotic Cell Division, Meiotic Nuclear Oscillation, and Cytokinesis Checkpoint Signaling. *Molecular biology of the cell*, 16(8), pp.1–13.

Almonacid, M. et al., 2015. Active diffusion positions the nucleus in mouse oocytes. *Nature Cell Biology*, 17(4), pp.470–479. Available at: http://dx.doi.org/10.1038/ncb3131.

Almonacid, M. et al., 2009. Spatial Control of Cytokinesis by Cdr2 Kinase and Mid1/Anillin Nuclear Export. *Current Biology*, 19(11), pp.961–966. Available at: http://dx.doi.org/10.1016/j.cub.2009.04.024.

Arellano, M. et al., 2002. Tea3p Is a Cell End Marker Activating Polarized Growth in Schizosaccharomyces pombe. , 12(2), pp.751–756.

Asnacios, A. & Hamant, O., 2012. The mechanics behind cell polarity. *Trends in cell*

biology, 22(11), pp.584–91. Available at: http://www.ncbi.nlm.nih.gov/pubmed/22980034 [Accessed October 14, 2014].

Bähler, J., Wu, J.Q., et al., 1998. Heterologous modules for efficient and versatile PCR-based gene targeting in Schizosaccharomyces pombe. *Yeast*, 14(10), pp.943–951.

Bähler, J., Steever, A.B., et al., 1998. Role of Polo Kinase and Mid1p in Determining the Site of Cell Division in Fission Yeast. , 143(6), pp.1603–1616.

Bähler, J. & Pringle, J.R., 1998. Pom1p, a fission yeast protein kinase that provides positional information for both polarized growth and cytokinesis. *Genes and Development*, 12(9), pp.1356–1370.

Barral, Y. et al., 2000. Compartmentalization of the cell cortex by septins is required for maintenance of cell polarity in yeast. *Molecular Cell*, 5(5), pp.841–851.

Behrens, R. & Nurse, P., 2002. Roles of fission yeast tea1p in the localization of polarity factors and in organizing the microtubular cytoskeleton. *The Journal of cell biology*, 157(5), pp.783–93. Available at: http://www.pubmedcentral.nih.gov/articlerender.fcgi?artid=2173414&tool=pmcentrez&rendertype=abstract [Accessed October 17, 2014].

Bendezú, F.O. et al., 2015. Spontaneous Cdc42 Polarization Independent of GDI-Mediated Extraction and Actin-Based Trafficking. *PLOS Biology*, 13(4), p.e1002097. Available at: http://dx.plos.org/10.1371/journal.pbio.1002097.

Bendezú, F.O. & Martin, S.G., 2011. Actin cables and the exocyst form two independent morphogenesis pathways in the fission yeast. *Molecular biology of the cell*, 22(1), pp.44–53. Available at: http://www.pubmedcentral.nih.gov/articlerender.fcgi?artid=3016976&tool=pmcentrez&rendertype=abstract [Accessed November 10, 2014].

Bendezú, F.O. & Martin, S.G., 2013. Cdc42 explores the cell periphery for mate selection in fission yeast. *Current biology : CB*, 23(1), pp.42–7. Available at: http://www.ncbi.nlm.nih.gov/pubmed/23200991 [Accessed November 10, 2014].

Bicho, C.C. et al., 2010. A catalytic role for Mod5 in the formation of the Tea1 cell polarity landmark. *Current biology : CB*, 20(19), pp.1752–7. Available at: http://www.pubmedcentral.nih.gov/articlerender.fcgi?artid=3094757&tool=pmcentrez&rendertype=abstract [Accessed October 27, 2014].

Bieling, P. et al., 2008. CLIP-170 tracks growing microtubule ends by dynamically recognizing composite EB1/tubulinbinding sites. *Journal of Cell Biology*, 183(7), pp.1223–1233.

Bieling, P. et al., 2007. Reconstitution of a microtubule plus-end tracking system in vitro. *Nature*, 450(7172), pp.1100–1105. Available at:

http://www.ncbi.nlm.nih.gov/pubmed/18059460%5Cnhttp://www.nature.com/doifinder/10.1038/nature06386.

Borrego-Pinto, J. et al., 2012. Samp1 is a component of TAN lines and is required for nuclear movement. *Journal of Cell Science*, 125(5), pp.1099–1105. Available at: http://jcs.biologists.org/cgi/doi/10.1242/jcs.087049.

Brouhard, G.J. et al., 2008. XMAP215 Is a Processive Microtubule Polymerase. *Cell*, 132(1), pp.79–88.

Browning, H., Hackney, D.D. & Nurse, P., 2003. Targeted movement of cell end factors in fission yeast. *Nature cell biology*, 5(9), pp.812–8. Available at: http://www.ncbi.nlm.nih.gov/pubmed/12894167.

Brunner, D. & Nurse, P., 2000. CLIP170-like tip1p spatially organizes microtubular dynamics in fission yeast. *Cell*, 102(5), pp.695–704.

Bryant, D.M. & Mostov, K.E., 2008. From cells to organs: building polarized tissue. *Nature reviews. Molecular cell biology*, 9(11), pp.887–901. Available at: http://www.pubmedcentral.nih.gov/articlerender.fcgi?artid=2921794&tool=pmcentrez&rendertype=abstract [Accessed July 10, 2014].

Burke, T. a et al., 2014. Homeostatic actin cytoskeleton networks are regulated by assembly factor competition for monomers. *Current biology : CB*, 24(5), pp.579–85. Available at: http://www.ncbi.nlm.nih.gov/pubmed/24560576 [Accessed August 20, 2014].

Busch, K.E. et al., 2004. Tea2p kinesin is involved in spatial microtubule organization by transporting Tip1p on microtubules. *Developmental Cell*, 6(6), pp.831–843.

Busch, K.E. & Brunner, D., 2004. The Microtubule Plus End-Tracking Proteins mal3p and tip1p Cooperate for Cell-End Targeting of Interphase Microtubules. *Current Biology*, 128(2), pp.189–190.

Carazo-Salas, R.E., Antony, C. & Nurse, P., 2005. The kinesin Klp2 mediates polarization of interphase microtubules in fission yeast. *Science (New York, N.Y.)*, 309(July), pp.297–300.

Chang, E.C. et al., 1994. Cooperative interaction of S. pombe proteins required for mating and morphogenesis. *Cell*, 79(1), pp.131–141.

Chang, F. & Martin, S.G., 2009. Shaping fission yeast with microtubules. *Cold Spring Harbor perspectives in biology*, 1(1), p.a001347. Available at: http://www.pubmedcentral.nih.gov/articlerender.fcgi?artid=2742080&tool=pmcentrez&rendertype=abstract [Accessed November 6, 2014].

Chang, F. & Nurse, P., 1996. How Fission Yeast Fission in the Middle. *Cell*, 84(2), pp.191–194. Available at: http://linkinghub.elsevier.com/retrieve/pii/S0092867400809733.

Chant, J., 1999. C p i y.

Chant, J. & Herskowitz, I., 1991. Genetic control of bud site selection in yeast by a set of gene products that constitute a morphogenetic pathway. *Cell*, 65, pp.1203–1212.

Chen, T., 2000. Multigenerational Cortical Inheritance of the Rax2 Protein in Orienting Polarity and Division in Yeast. *Science*, 290(5498), pp.1975–1978. Available at: http://www.sciencemag.org/cgi/doi/10.1126/science.290.5498.1975 [Accessed November 10, 2014].

Chen, T. et al., 2000. Multigenerational cortical inheritance of the Rax2 protein in orienting polarity and division in yeast. *Science (New York, N.Y.)*, 290(5498), pp.1975–1978.

Choi, E., Lee, K. & Song, K., 2006. Molecules and Function of rax2p in the Polarized Growth of Fission Yeast. , 22(2), pp.146–153.

Chowdhury, S. & Gustin, M.C., 1992. The Yeast Cytoskeleton and Osmotic-Stress - Phenotype-Specific Suppressors of an Actin. *Molecular Biology of the Cell*, 3(3), pp.A153–A153.

Coffman, V.C. et al., 2013. The formins Cdc12 and For3 cooperate during contractile ring assembly in cytokinesis. *The Journal of cell biology*, 203(1), pp.101–14. Available at: http://www.pubmedcentral.nih.gov/articlerender.fcgi?artid=3798249&tool=pmcentrez&rendertype=abstract [Accessed November 10, 2014].

Coll, P.M. et al., 2003. Gef1p, a New Guanine Nucleotide Exchange Factor for Cdc42p, Regulates Polarity in Schizosaccharomyces pombe. *Molecular biology of the cell*, 14(May), pp.2559–2569.

Cortés, J.C.G. et al., 2005. The novel fission yeast (1,3)beta-D-glucan synthase catalytic subunit Bgs4p is essential during both cytokinesis and polarized growth. *Journal of cell science*, 118(Pt 1), pp.157–174.

D'Alessandro, M. et al., 2015. Amphiphysin 2 Orchestrates Nucleus Positioning and Shape by Linking the Nuclear Envelope to the Actin and Microtubule Cytoskeleton. *Developmental Cell*, 35(2), pp.186–198. Available at: http://linkinghub.elsevier.com/retrieve/pii/S153458071500619X.

Daga, R.R. & Chang, F., 2005. Dynamic positioning of the fission yeast cell division plane. *Proceedings of the National Academy of Sciences of the United States of America*, 102(23), p.8228.

Daga, R.R., Yonetani, A. & Chang, F., 2006. Asymmetric microtubule pushing forces in nuclear centering. *Current biology : CB*, 16(15), pp.1544–50. Available at: http://www.ncbi.nlm.nih.gov/pubmed/16890530 [Accessed November 10, 2014].

Das, M. et al., 2012. Oscillatory dynamics of Cdc42 GTPase in the control of polarized growth. *Science (New York, N.Y.)*, 337(6091), pp.239–43. Available at: http://www.pubmedcentral.nih.gov/articlerender.fcgi?artid=3681419&tool=pmcentrez&rendertype=abstract [Accessed October 16, 2014].

Das, M. et al., 2015. Phosphorylation-dependent inhibition of Cdc42 GEF Gef1 by 14-3-3 protein Rad24 spatially regulates Cdc42 GTPase activity and oscillatory dynamics during cell morphogenesis. *Molecular Biology of the Cell*, 26(19), pp.3520–3534. Available at: http://www.molbiolcell.org/cgi/doi/10.1091/mbc.E15-02-0095.

Das, M. et al., 2007. Regulation of Cell Diameter, For3p Localization, and Cell Symmetry by Fission Yeast Rho-GAP Rga4p. *Molecular biology of the cell*, 18(December), pp.986–994.

Das, M. et al., 2009. The conserved NDR kinase Orb6 controls polarized cell growth by spatial regulation of the small GTPase Cdc42. *Current biology : CB*, 19(15), pp.1314–9. Available at: http://www.ncbi.nlm.nih.gov/pubmed/19646873 [Accessed November 10, 2014].

Desai, A. & Mitchison, T.J., 1997. MICROTUBULE POLYMERIZATION. , pp.83–117.

Dixit, R. et al., 2009. Microtubule plus-end tracking by CLIP-170 requires EB1. *Proceedings of the National Academy of Sciences of the United States of America*, 106(2), pp.492–497.

Drummond, D.R. & Cross, R.A., 2000. Dynamics of interphase microtubules in Schizosaccharomyces pombe. *Current Biology*, 10(13), pp.766–775.

Dupin, I. & Etienne-Manneville, S., 2011. Nuclear positioning: mechanisms and functions. *The international journal of biochemistry & cell biology*, 43(12), pp.1698–707. Available at: http://www.ncbi.nlm.nih.gov/pubmed/21959251 [Accessed October 27, 2014].

East, D. a & Mulvihill, D.P., 2011. Regulation and function of the fission yeast myosins. *Journal of cell science*, 124(Pt 9), pp.1383–90. Available at: http://www.ncbi.nlm.nih.gov/pubmed/21502135 [Accessed November 6, 2014].

Estravis, M., Rincón, S.A. & Pérez, P., 2012. Cdc42 regulation of polarized traffic in fission yeast. *Communicative and Integrative Biology*, 5(4), pp.370–373.

Etienne-Manneville, S., 2004. Cdc42--the centre of polarity. *Journal of cell science*, 117(Pt 8), pp.1291–1300.

Etienne-Manneville, S., 2013. Microtubules in cell migration. *Annual review of cell and developmental biology*, 29, pp.471–99. Available at: http://www.ncbi.nlm.nih.gov/pubmed/23875648.

Etienne-Manneville, S. & Hall, A., 2002. Rho GTPases in cell biology. *Nature*, 420(6916), pp.629–635.

Eustratios Bananis et al., 2004. Microtubule-Dependent Movement of Late Endocytic Vesicles In Vitro: Requirements for Dynein and Kinesin. *Molecular biology of the cell*, 15(8), pp.1–13.

Farhan, H. & Hsu, V.W., 2015. Cdc42 and Cellular Polarity: Emerging Roles at the Golgi. *Trends in Cell Biology*, 26(4), pp.241–248. Available at: http://dx.doi.org/10.1016/j.tcb.2015.11.003.

Feierbach, B. & Chang, F., 2001. Roles of the fission yeast formin for3p in cell polarity, actin cable formation and symmetric cell division. *Current Biology*, 11(21), pp.1656–1665. Available at: http://linkinghub.elsevier.com/retrieve/pii/S0960982201005255.

Feierbach, B., Verde, F. & Chang, F., 2004. Regulation of a formin complex by the microtubule plus end protein tea1p. *The Journal of cell biology*, 165(5), pp.697–707. Available at: http://www.pubmedcentral.nih.gov/articlerender.fcgi?artid=2172381&tool=pmcentrez&rendertype=abstract [Accessed October 17, 2014].

Frigault, M.M. et al., 2009. Live-cell microscopy - tips and tools. *Journal of cell science*, 122(Pt 6), pp.753–767.

Fujita, A. et al., 2004. Rax1 , a protein required for the establishment of the bipolar budding pattern in yeast. , 327, pp.161–169.

Gachet, Y. & Hyams, J.S., 2005. Endocytosis in fission yeast is spatially associated with the actin cytoskeleton during polarised cell growth and cytokinesis. *Journal of cell science*, 118(Pt 18), pp.4231–42. Available at: http://www.ncbi.nlm.nih.gov/pubmed/16141239 [Accessed October 19, 2014].

Garcia, M.A. et al., 2001. Fission yeast ch-TOG/XMAP215 homologue Alp14 connects mitotic spindles with the kinetochore and is a component of the Mad2-dependent spindle checkpoint. *EMBO Journal*, 20(13), pp.3389–3401.

Garcia, M.A., Koonrugsa, N. & Toda, T., 2002. Spindle ± kinetochore attachment requires the combined action of Kin I-like Klp5 / 6 and Alp14 / Dis1-MAPs in ® ssion yeast. *EMBO Journal*, 21(22), pp.6015–6024.

Gardner, M.K., Zanic, M. & Howard, J., 2013. Microtubule catastrophe and rescue. *Current Opinion in Cell Biology*, 25(1), pp.1–9. Available at: http://dx.doi.org/10.1016/j.ceb.2012.09.006.

Gladfelter, A.S., Pringle, J.R. & Lew, D.J., 2001. The septin cortex at the yeast mother-bud neck. *Current Opinion in Microbiology*, 4(6), pp.681–689.

Gomes, E.R., Jani, S. & Gundersen, G.G., 2005. Nuclear movement regulated by

Cdc42, MRCK, myosin, and actin flow establishes MTOC polarization in migrating cells. *Cell*, 121(3), pp.451–63. Available at: http://www.ncbi.nlm.nih.gov/pubmed/15882626 [Accessed November 3, 2014].

Goode, B.L. & Eck, M.J., 2007. Mechanism and function of formins in the control of actin assembly. *Annual review of biochemistry*, 76, pp.593–627. Available at: http://www.ncbi.nlm.nih.gov/pubmed/17373907 [Accessed October 17, 2014].

Goodwin, S.S. & Vale, R.D., 2010. Patronin Regulates the Microtubule Network by Protecting Microtubule Minus Ends. *Cell*, 143(2), pp.263–274. Available at: http://dx.doi.org/10.1016/j.cell.2010.09.022.

Goryachev, A.B. & Pokhilko, A. V., 2008. Dynamics of Cdc42 network embodies a Turing-type mechanism of yeast cell polarity. *FEBS Letters*, 582(10), pp.1437–1443.

Grallert, A. et al., 2007. In vivo movement of the type V myosin Myo52 requires dimerisation but is independent of the neck domain. *Journal of cell science*, 120(Pt 23), pp.4093–8. Available at: http://www.ncbi.nlm.nih.gov/pubmed/18003699 [Accessed November 10, 2014].

Graziano, B.R. & Weiner, O.D., 2014. Self-organization of protrusions and polarity during eukaryotic chemotaxis. *Current Opinion in Cell Biology*, 30(1), pp.60–67. Available at: http://dx.doi.org/10.1016/j.ceb.2014.06.007.

Gundersen, G.G. & Worman, H.J., 2013. Nuclear positioning. *Cell*, 152(6), pp.1376–89. Available at: http://www.pubmedcentral.nih.gov/articlerender.fcgi?artid=3626264&tool=pmcentrez&rendertype=abstract [Accessed July 11, 2014].

Gupta, K.K. et al., 2009. Minimal plus-end tracking unit of the cytoplasmic linker protein CLIP-170. *Journal of Biological Chemistry*, 284(11), pp.6735–6742.

Hachet, O. et al., 2011. A phosphorylation cycle shapes gradients of the DYRK family kinase Pom1 at the plasma membrane. *Cell*, 145(7), pp.1116–28. Available at: http://www.ncbi.nlm.nih.gov/pubmed/21703453 [Accessed November 10, 2014].

Hagan, I. & Yanagida, M., 1997. Evidence for cell cycle-specific, spindle pole body-mediated, nuclear positioning in the fission yeast Schizosaccharomyces pombe. *Journal of cell science*, 110 (Pt 1, pp.1851–66. Available at: http://www.ncbi.nlm.nih.gov/pubmed/9296386.

Hayles, J. & Nurse, P., 2001. A journey into space. , 2(September).

Heerssen, H.M., Pazyra, M.F. & Segal, R. a, 2004. Dynein motors transport activated Trks to promote survival of target-dependent neurons. *Nature neuroscience*, 7(6), pp.596–604.

Hendershott, M.C. & Vale, R.D., 2014. Regulation of microtubule minus-end dynamics by CAMSAPs and Patronin. *Proceedings of the National Academy of Sciences of the United States of America*, 111(16), pp.5860–5. Available at: http://www.pubmedcentral.nih.gov/articlerender.fcgi?artid=4000804&tool=pmcentrez&rendertype=abstract.

Hirokawa, N., Noda, Y., et al., 2009. Kinesin superfamily motor proteins and intracellular transport. *Nature reviews. Molecular cell biology*, 10(10), pp.682–96. Available at: http://dx.doi.org/10.1038/nrm2774%5Cnhttp://www.ncbi.nlm.nih.gov/pubmed/19773780.

Hirokawa, N., Nitta, R. & Okada, Y., 2009. The mechanisms of kinesin motor motility: lessons from the monomeric motor KIF1A. *Nature reviews. Molecular cell biology*, 10(12), pp.877–884. Available at: http://dx.doi.org/10.1038/nrm2807.

Hoebe, R. a et al., 2007. Controlled light-exposure microscopy reduces photobleaching and phototoxicity in fluorescence live-cell imaging. *Nature biotechnology*, 25(2), pp.249–53. Available at: http://www.ncbi.nlm.nih.gov/pubmed/17237770 [Accessed August 21, 2014].

Holleran, E.A., Karki, S. & Holzbaur, E.L.F., 1998. The Role of the Dynactin Complex in Intracellular Motility. *International Review of Cytology*, 182, pp.69–109.

Howell, A.S. et al., 2009. Singularity in Polarization: Rewiring Yeast Cells to Make Two Buds. *Cell*, 139(4), pp.731–743. Available at: http://dx.doi.org/10.1016/j.cell.2009.10.024.

Huang, J. et al., 2012. Nonmedially assembled F-actin cables incorporate into the actomyosin ring in fission yeast. *The Journal of cell biology*, 199(5), pp.831–47. Available at: http://www.pubmedcentral.nih.gov/articlerender.fcgi?artid=3514790&tool=pmcentrez&rendertype=abstract [Accessed November 10, 2014].

Huang, K.M. & Snider, M.D., 1995. Isolation of protein glycosylation mutants in the fission yeast Schizosaccharomyces pombe. *Molecular biology of the cell*, 6(5), pp.485–96. Available at: http://www.pubmedcentral.nih.gov/articlerender.fcgi?artid=301210&tool=pmcentrez&rendertype=abstract [Accessed August 10, 2013].

Huang, Y. et al., 2007. Polarity Determinants Tea1p, Tea4p, and Pom1p Inhibit Division-Septum Assembly at Cell Ends in Fission Yeast. *Developmental Cell*, 12(6), pp.987–996.

Huang, Y., Yan, H. & Balasubramanian, M.K., 2008. Assembly of normal actomyosin rings in the absence of Mid1p and cortical nodes in fi ssion yeast. *Journal of Cell*

Biology, 183(6), pp.979–988.

Irazoqui, J.E., Gladfelter, A.S. & Lew, D.J., 2003. Scaffold-mediated symmetry breaking by Cdc42p. *Nature cell biology*, 5(12), pp.1062–1070.

Isermann, P. & Lammerding, J., 2013. Nuclear mechanics and mechanotransduction in health and disease. *Current Biology*, 23(24), pp.R1113–R1121. Available at: http://dx.doi.org/10.1016/j.cub.2013.11.009.

Jacobs, C.W. et al., 1988. Functions of Microtubules in the Saccharomyces cerevisiae Cell Cycle. , 130(2), pp.299–312.

Janson, M.E. et al., 2007. Crosslinkers and Motors Organize Dynamic Microtubules to Form Stable Bipolar Arrays in Fission Yeast. *Cell*, 128(2), pp.357–368.

Johnson, D.I. (University of M. & Pringle, J.R. (University of M., 1990. Gene Involved in the Development of Cell Polarity. , 111(July), pp.143–152.

Kaksonen, M., Sun, Y. & Drubin, D.G., 2003. A Pathway for Association of Receptors, Adaptors, and Actin during Endocytic Internalization. *Cell*, 115(4), pp.475–487.

Kang, P.J. et al., 2004. Marking Cortical Sites for Bipolar Bud-site Selection in Yeast □. , 15(November), pp.5145–5157.

Kardon, J.R. & Vale, R.D., 2009. Regulators of the cytoplasmic dynein motor. *Nature reviews. Molecular cell biology*, 10(12), pp.854–865. Available at: http://dx.doi.org/10.1038/nrm2804.

Karki, S. & Holzbaur, E.L., 1999. Cytoplasmic dynein and dynactin in cell division and intracellular transport. *Current Opinion in Cell Biology*, 11(1), pp.45–53.

Kelly, F.D. & Nurse, P., 2011. Spatial control of Cdc42 activation determines cell width in fission yeast. *Molecular biology of the cell*, 22(20), pp.3801–11. Available at: http://www.pubmedcentral.nih.gov/articlerender.fcgi?artid=3192860&tool=pmcentrez&rendertype=abstract.

Kim, H. et al., 2003. The kelch repeat protein, Tea1, is a potential substrate target of the p21-activated kinase, Shk1, in the fission yeast, Schizosaccharomyces pombe. *The Journal of biological chemistry*, 278(32), pp.30074–82. Available at: http://www.ncbi.nlm.nih.gov/pubmed/12764130 [Accessed November 1, 2014].

King, J.S. & Insall, R.H., 2009. Chemotaxis: finding the way forward with Dictyostelium. *Trends in Cell Biology*, 19(10), pp.523–530.

King, M.C., Drivas, T.G. & Blobel, G., 2008. A network of nuclear envelope membrane proteins linking centromeres to microtubules. *Cell*, 134(3), pp.427–38. Available at: http://www.pubmedcentral.nih.gov/articlerender.fcgi?artid=2617791&tool=pmce

ntrez&rendertype=abstract [Accessed November 10, 2014].

Knight, A.W. & Billinton, N., 2001. Distinguishing GFP from Cellular Autofluorescence. , (October).

Kobielak, A., Pasolli, H.A. & Fuchs, E., 2004. Mammalian formin-1 participates in adherens junctions and polymerization of linear actin cables. *Nature cell biology*, 6(1), pp.21–30. Available at: http://www.pubmedcentral.nih.gov/articlerender.fcgi?artid=2605950&tool=pmcentrez&rendertype=abstract.

Kokkoris, K., Gallo Castro, D. & Martin, S.G., 2014. The Tea4-PP1 landmark promotes local growth by dual Cdc42 GEF recruitment and GAP exclusion. *Journal of cell science*, 127(Pt 9), pp.2005–16. Available at: http://www.ncbi.nlm.nih.gov/pubmed/24554432 [Accessed November 6, 2014].

Kovar, D.R., 2006. Molecular details of formin-mediated actin assembly. *Current Opinion in Cell Biology*, 18(1), pp.11–17.

Kovar, D.R., Sirotkin, V. & Lord, M., 2011. Three's company: the fission yeast actin cytoskeleton. *Trends in cell biology*, 21(3), pp.177–87. Available at: http://www.pubmedcentral.nih.gov/articlerender.fcgi?artid=3073536&tool=pmcentrez&rendertype=abstract [Accessed November 10, 2014].

Koyano, T. et al., 2015. Casein kinase 1?? acts as a molecular switch for cell polarization through phosphorylation of the polarity factor Tea1 in fission yeast. *Genes to Cells*, 20(12), pp.1046–1058.

Kozubowski, L. et al., 2008. Symmetry-Breaking Polarization Driven by a Cdc42p GEF-PAK Complex. *Current Biology*, 18(22), pp.1719–1726. Available at: http://dx.doi.org/10.1016/j.cub.2008.09.060.

Lansbergen, G. et al., 2006. CLASPs Attach Microtubule Plus Ends to the Cell Cortex through a Complex with LL5?? *Developmental Cell*, 11(1), pp.21–32.

Lansbergen, G. & Akhmanova, A., 2006. Microtubule plus end: A hub of cellular activities. *Traffic*, 7(5), pp.499–507.

Lee, I.-J., Coffman, V.C. & Wu, J.-Q., 2012. Contractile-ring assembly in fission yeast cytokinesis: Recent advances and new perspectives. *Cytoskeleton (Hoboken, N.J.)*, 69(10), pp.751–63. Available at: http://www.ncbi.nlm.nih.gov/pubmed/22887981 [Accessed November 10, 2014].

Lee, W.L., Bezanilla, M. & Pollard, T.D., 2000. Fission yeast myosin-I, Myo1p, stimulates actin assembly by Arp2/3 complex and shares functions with WASp. *Journal of Cell Biology*, 151(4), pp.789–799.

Lewkowicz, E. et al., 2008. The microtubule-binding protein CLIP-170 coordinates mDia1 and actin reorganization during CR3-mediated phagocytosis. *Journal of*

Cell Biology, 183(7), pp.1287–1298.

Li, R. & Bowerman, B., 2010. Symmetry Breaking in Biology. , pp.1–5.

Liakopoulos, D. et al., 2003. Asymmetric loading of Kar9 onto spindle poles and microtubules ensures proper spindle alignment. *Cell*, 112(4), pp.561–574.

Lippincott-schwartz, J., Snapp, E. & Kenworthy, A., 2001. STUDYING PROTEIN DYNAMICS IN LIVING CELLS. , 2(June).

Loïodice, I. et al., 2005. Ase1p Organizes Antiparallel Microtubule Arrays during Interphase and Mitosis in Fission Yeast. *Molecular biology of the cell*, 16(8), pp.1–13.

Luxton, G.W.G. et al., 2010. Linear arrays of nuclear envelope proteins harness retrograde actin flow for nuclear movement. *Science (New York, N.Y.)*, 329(5994), pp.956–9. Available at: http://www.pubmedcentral.nih.gov/articlerender.fcgi?artid=3938394&tool=pmcentrez&rendertype=abstract [Accessed October 7, 2014].

Luxton, G.W.G. et al., 2011. TAN lines: a novel nuclear envelope structure involved in nuclear positioning. *Nucleus (Austin, Tex.)*, 2(3), pp.173–81. Available at: http://www.pubmedcentral.nih.gov/articlerender.fcgi?artid=3149877&tool=pmcentrez&rendertype=abstract [Accessed October 29, 2014].

Macara, I.G. & McCaffrey, L., 2013. Cell polarity in morphogenesis and metastasis. *Philosophical transactions of the Royal Society of London. Series B, Biological sciences*, 368(1629), p.20130012. Available at: http://www.pubmedcentral.nih.gov/articlerender.fcgi?artid=3785962&tool=pmcentrez&rendertype=abstract.

Machesky, L.M. & Insall, R.H., 1999. Signaling to actin dynamics. *Journal of Cell Biology*, 146(2), pp.267–272.

Mallik, R. & Gross, S.P., 2004. Molecular motors: Strategies to get along. *Current Biology*, 14(22), pp.971–982.

Marco, E. et al., 2007. Endocytosis Optimizes the Dynamic Localization of Membrane Proteins that Regulate Cortical Polarity. *Cell*, 129(2), pp.411–422.

Marcus, S. et al., 1995. Shk1, a homolog of the Saccharomyces cerevisiae Ste20 and mammalian p65PAK protein kinases, is a component of a Ras/Cdc42 signaling module in the fission yeast Schizosaccharomyces pombe. *Proceedings of the National Academy of Sciences*, 92(13), pp.6180–6184. Available at: http://www.pnas.org/content/92/13/6180%5Cnhttp://www.ncbi.nlm.nih.gov/pubmed/7597098%5Cnhttp://www.pnas.org/content/92/13/6180.full.pdf%5Cnhttp://www.pnas.org/content/92/13/6180.short.

Marks, J., Hagan, I.M. & Hyams, J.S., 1986. Growth polarity and cytokinesis in fission yeast: the role of the cytoskeleton. *J Cell Sci Suppl*, 5(229), pp.229–241.

Martín-García, R. & Mulvihill, D.P., 2009. Myosin V spatially regulates microtubule dynamics and promotes the ubiquitin-dependent degradation of the fission yeast CLIP-170 homologue, Tip1. *Journal of cell science*, 122(Pt 21), pp.3862–72. Available at: http://www.ncbi.nlm.nih.gov/pubmed/19808886 [Accessed November 10, 2014].

Martin, S.G., 2009. Microtubule-dependent cell morphogenesis in the fission yeast. *Trends in cell biology*, 19(9), pp.447–54. Available at: http://www.ncbi.nlm.nih.gov/pubmed/19713114 [Accessed October 1, 2014].

Martin, S.G. et al., 2007. Regulation of the Formin for3p by cdc42p and bud6p □. , 18(October), pp.4155–4167.

Martin, S.G., 2015. Spontaneous cell polarization: Feedback control of Cdc42 GTPase breaks cellular symmetry. *BioEssays*, 37(11), pp.1193–1201.

Martin, S.G. et al., 2005. Tea4p links microtubule plus ends with the formin for3p in the establishment of cell polarity. *Developmental cell*, 8(4), pp.479–91. Available at: http://www.ncbi.nlm.nih.gov/pubmed/15809031 [Accessed November 10, 2014].

Martin, S.G. & Arkowitz, R. a, 2014. Cell polarization in budding and fission yeasts. *FEMS microbiology reviews*, 38(2), pp.228–53. Available at: http://www.ncbi.nlm.nih.gov/pubmed/24354645 [Accessed November 10, 2014].

Martin, S.G. & Berthelot-Grosjean, M., 2009. Polar gradients of the DYRK-family kinase Pom1 couple cell length with the cell cycle. *Nature*, 459(7248), pp.852–856. Available at: http://dx.doi.org/10.1038/nature08054.

Martin, S.G. & Chang, F., 2006. Dynamics of the formin for3p in actin cable assembly. *Current biology : CB*, 16(12), pp.1161–70. Available at: http://www.ncbi.nlm.nih.gov/pubmed/16782006 [Accessed November 10, 2014].

Martin, S.G. & Chang, F., 2005. ND ES SC. , 4(8), pp.1046–1049.

Mata, J. & Nurse, P., 1998. Discovering the poles in yeast. *Trends in Cell Biology*, 8(4), pp.163–167. Available at: http://linkinghub.elsevier.com/retrieve/pii/S0962892498012240.

Mata, J. & Nurse, P., 1997. tea1 and the Microtubular Cytoskeleton Are Important for Generating Global Spatial Order within the Fission Yeast Cell. *Cell*, 89(6), pp.939–949. Available at: http://linkinghub.elsevier.com/retrieve/pii/S0092867400802792.

McCaffrey, L.M. & Macara, I.G., 2009. Widely conserved signaling pathways in the establishment of cell polarity. *Cold Spring Harbor perspectives in biology*, 1(2),

pp.1–18.

Meitinger, F. et al., 2014. A Memory System of Negative Polarity Cues Prevents Replicative Aging. *Cell*, 159(5), pp.1056–1069. Available at: http://linkinghub.elsevier.com/retrieve/pii/S0092867414013026.

Miki, F. et al., 2004. Two-hybrid search for proteins that interact with Sad1 and Kms1, two membrane-bound components of the spindle pole body in fission yeast. *Molecular genetics and genomics : MGG*, 270(6), pp.449–61. Available at: http://www.ncbi.nlm.nih.gov/pubmed/14655046 [Accessed November 10, 2014].

Minc, N. et al., 2009. Establishing new sites of polarization by microtubules. *Current biology : CB*, 19(2), pp.83–94. Available at: http://www.pubmedcentral.nih.gov/articlerender.fcgi?artid=2820583&tool=pmcentrez&rendertype=abstract [Accessed October 17, 2014].

Mishra, M. et al., 2013. In vitro contraction of cytokinetic ring depends on myosin II but not on actin dynamics. *Nature cell biology*, 15(7), pp.853–9. Available at: http://www.ncbi.nlm.nih.gov/pubmed/23770677 [Accessed November 3, 2014].

Mitchison, J.M. & Nurse, P., 1985. Growth in cell length in the fission yeast Schizosaccharomyces pombe. *Journal of cell science*, 75, pp.357–376.

Mitchison, T. & Kirschner, M., 1984. Dynamic instability of microtubule growth. *Nature*, 312(5991), pp.237–42. Available at: http://www.ncbi.nlm.nih.gov/pubmed/6504138.

Monici, M., 2005. Cell and tissue autofluorescence research and diagnostic applications. *Biotechnology annual review*, 11, pp.227–56. Available at: http://www.ncbi.nlm.nih.gov/pubmed/16216779 [Accessed August 7, 2013].

Moores, C.A. & Milligan, R.A., 2006. Lucky 13 - microtubule depolymerisation by kinesin-13 motors. *Journal of Cell Science*, 119(19), pp.3905–3913. Available at: http://jcs.biologists.org/content/119/19/3905.abstract.

Moseley, J.B. et al., 2009. A spatial gradient coordinates cell size and mitotic entry in fission yeast. *Nature*, 459(7248), pp.857–860. Available at: http://dx.doi.org/10.1038/nature08074.

Motegi, F., Arai, R. & Mabuchi, I., 2001. Identification of two type V myosins in fission yeast, one of which functions in polarized cell growth and moves rapidly in the cell. *Molecular biology of the cell*, 12(5), pp.1367–1380.

Mulvihill, D.P., Edwards, S.R. & Hyams, J.S., 2006. A critical role for the type V myosin, Myo52, in septum deposition and cell fission during cytokinesis in Schizosaccharomyces pombe. *Cell motility and the cytoskeleton*, 63(3), pp.149–61. Available at: http://www.ncbi.nlm.nih.gov/pubmed/16421926 [Accessed

November 10, 2014].

Nakano, K. et al., 2002. The small GTPase Rho3 and the diaphanous/formin For3 function in polarized cell growth in fission yeast. *J Cell Sci*, 115(Pt 23), pp.4629–4639. Available at: http://www.ncbi.nlm.nih.gov/entrez/query.fcgi?cmd=Retrieve&db=PubMed&dopt=Citation&list_uids=12415007.

Nakano, K., Arai, R. & Mabuchi, I., 1997. The small GTP-binding protein Rho1 is a multifunctional protein that regulates actin localization, cell polarity, and septum formation in the fission yeast Schizosaccharomyces pombe. *Genes to cells : devoted to molecular & cellular mechanisms*, 2(11), pp.679–94. Available at: http://www.ncbi.nlm.nih.gov/pubmed/9491802.

Nakaseko, Y. et al., 2001. M phase-specific kinetochore proteins in fission yeast: Microtubule-associating Dis1 and Mtc1 display rapid separation and segregation during anaphase. *Current Biology*, 11(8), pp.537–549.

Nakata, T. & Hirokawa, N., 2003. Microtubules provide directional cues for polarized axonal transport through interaction with kinesin motor head. *Journal of Cell Biology*, 162(6), pp.1045–1055.

Nelson, W.J., 2003. Adaptation of core mechanisms to generate cell polarity. , 422(April).

Nelson, W.J., 2009. Remodelling Epithelial Cell Organization: Transitions Between Front-Rear and Apical Basal Polarity. *Cold Spring Harbor Perspectives in Biology*, 1(7), pp.1–19.

Niccoli, T., Arellano, M. & Nurse, P., 2003. Role of Tea1p, Tea3p and Pom1p in the determination of cell ends in Schizosaccharomyces pombe. *Yeast (Chichester, England)*, 20(16), pp.1349–58. Available at: http://www.ncbi.nlm.nih.gov/pubmed/14663827 [Accessed November 1, 2014].

Niccoli, T. & Nurse, P., 2002. Different mechanisms of cell polarisation in vegetative and shmooing growth in fission yeast. *Journal of cell science*, 115(Pt 8), pp.1651–62. Available at: http://www.ncbi.nlm.nih.gov/pubmed/11950884.

Nogales, E., 2001. S Tructural I Nsights Into. *Annual Reviews Biochem*, 69, pp.277–302.

Ottilie, S. et al., 1995. Fission yeast pak1+ encodes a protein kinase that interacts with Cdc42p and is involved in the control of cell polarity and mating. *The EMBO journal*, 14(23), pp.5908–19. Available at: http://www.pubmedcentral.nih.gov/articlerender.fcgi?artid=394709&tool=pmcentrez&rendertype=abstract.

Padte, N.N. et al., 2006. The Cell-End Factor Pom1p Inhibits Mid1p in Specification

of the Cell Division Plane in Fission Yeast. *Current Biology*, 16(24), pp.2480–2487.

Pan, K.Z. et al., 2014. Cortical regulation of cell size by a sizer cdr2p. *eLife*, 3, p.e02040. Available at: http://www.pubmedcentral.nih.gov/articlerender.fcgi?artid=3956294&tool=pmcentrez&rendertype=abstract [Accessed October 21, 2014].

Paoletti, A. & Chang, F., 2000. Analysis of mid1p , a Protein Required for Placement of the Cell Division Site , Reveals a Link between the Nucleus and the Cell Surface in Fission Yeast. , 11(August), pp.2757–2773.

Park, H.-O. & Bi, E., 2007. Central Roles of Small GTPases in the Development of Cell Polarity in Yeast and Beyond. *Microbiology and Molecular Biology Reviews*, 71(1), pp.48–96. Available at: http://www.pubmedcentral.nih.gov/articlerender.fcgi?artid=1847380&tool=pmcentrez&rendertype=abstract.

Pelham, R.J. & Chang, F., 2001. Role of actin polymerization and actin cables in actin-patch movement in Schizosaccharomyces pombe. *Nature cell biology*, 3(3), pp.235–44. Available at: http://www.ncbi.nlm.nih.gov/pubmed/11231572.

Perrin, B.J. & Ervasti, J.M., 2010. The actin gene family: Function follows isoform. *Cytoskeleton*, 67(10), pp.630–634.

Petersen, J. & Nurse, P., 2007. TOR signalling regulates mitotic commitment through the stress MAP kinase pathway and the Polo and Cdc2 kinases. *Nature cell biology*, 9(11), pp.1263–1272.

Petersen, J. & Russell, P., 2016. Growth and the environment of Schizosaccharomyces pombe. *Cold Spring Harbor Protocols*, 2016(3), pp.210–226.

Petrie, R.J., Doyle, A.D. & Yamada, K.M., 2009. Random versus directionally persistent cell migration. *Nature reviews. Molecular cell biology*, 10(8), pp.538–49. Available at: http://dx.doi.org/10.1038/nrm2729.

Pfaendtner, J. et al., 2010. Structure and dynamics of the actin filament. *Journal of Molecular Biology*, 396(2), pp.252–263. Available at: http://dx.doi.org/10.1016/j.jmb.2009.11.034.

Phillips, M.J. & Voeltz, G.K., 2015. Structure and function of ER membrane contact sites with other organelles. *Nature reviews. Molecular cell biology*, 17(2), pp.1–14. Available at: http://www.ncbi.nlm.nih.gov/pubmed/26627931.

Piel, M. & Tran, P.T., 2009. Cell shape and cell division in fission yeast. *Current biology : CB*, 19(17), pp.R823-7. Available at: http://www.pubmedcentral.nih.gov/articlerender.fcgi?artid=2997724&tool=pmce

ntrez&rendertype=abstract [Accessed November 10, 2014].

Pollard, T.D., 2007a. Regulation of actin filament assembly by Arp2/3 complex and formins. *Annual review of biophysics and biomolecular structure*, 36, pp.451–477.

Pollard, T.D., 2007b. Regulation of actin filament assembly by Arp2/3 complex and formins. *Annual review of biophysics and biomolecular structure*, 36, pp.451–77. Available at: http://www.ncbi.nlm.nih.gov/pubmed/17477841 [Accessed July 10, 2014].

Pollard, T.D., Blanchoin, L. & Mullins, R.D., 2000. MOLECULARMECHANISMS CONTROLLING ACTIN FILAMENTDYNAMICS INNONMUSCLE CELLS.

Pollard, T.D. & Cooper, J.A., 2009. Actin, a central player in cell shape and movement. *Science (New York, N.Y.)*, 326(5957), pp.1208–12. Available at: http://www.pubmedcentral.nih.gov/articlerender.fcgi?artid=3677050&tool=pmcentrez&rendertype=abstract.

Lo Presti, L., Chang, F. & Martin, S.G., 2012. Myosin Vs organize actin cables in fission yeast. *Molecular biology of the cell*, 23(23), pp.4579–91. Available at: http://www.pubmedcentral.nih.gov/articlerender.fcgi?artid=3510019&tool=pmcentrez&rendertype=abstract [Accessed November 10, 2014].

Lo Presti, L. & Martin, S.G., 2011. Shaping fission yeast cells by rerouting actin-based transport on microtubules. *Current biology : CB*, 21(24), pp.2064–9. Available at: http://www.ncbi.nlm.nih.gov/pubmed/22137473 [Accessed November 5, 2014].

Pruyne, D. & Bretscher, a, 2000. Polarization of cell growth in yeast. I. Establishment and maintenance of polarity states. *Journal of cell science*, 113 (Pt 3, pp.365–375.

Pruyne, D.W., Schott, D.H. & Bretscher, A., 1998. Tropomyosin-containing Actin Cables Direct the Myo2p-dependent Polarized Delivery of Secretory Vesicles in Budding Yeast. *Journal of Cell Biology*, 143(7), pp.1931–1945.

Quinlan, M.E., 2016. Cytoplasmic Streaming in the *Drosophila* Oocyte. *Annual Review of Cell and Developmental Biology*, 32(1), p.annurev-cellbio-111315-125416. Available at: http://www.annualreviews.org/doi/10.1146/annurev-cellbio-111315-125416.

Qyang, Y. et al., 2002. The p21-activated kinase, Shk1, is required for proper regulation of microtubule dynamics in the fission yeast, Schizosaccharomyces pombe. *Molecular Microbiology*, 44(2), pp.325–334.

Radcliffe, P. et al., 1998. Identification of novel temperature-sensitive lethal alleles in essential beta-tubulin and nonessential alpha 2-tubulin genes as fission yeast

polarity mutants. *Molecular biology of the cell*, 9(7), pp.1757–1771.

Reinsch, S. & Gönczy, P., 1998. Mechanisms of nuclear positioning. , 2295, pp.2283–2295.

Reinsch, S. & Karsenti, E., 1997. Movement of nuclei along microtubules in Xenopus egg extracts. *Current Biology*, 7(3), pp.211–214. Available at: http://www.sciencedirect.com/science/article/pii/S0960982297700927.

Revilla-Guarinos, M.T. et al., 2016. Rga6 is a Fission Yeast Rho GAP Involved in Cdc42 Regulation of Polarized Growth. *Molecular biology of the cell*. Available at: http://www.ncbi.nlm.nih.gov/pubmed/26960792.

Riedl, J. et al., 2008. Lifeact: a versatile marker to visualize F-actin. *Nature methods*, 5(7), pp.605–7. Available at: http://www.pubmedcentral.nih.gov/articlerender.fcgi?artid=2814344&tool=pmcentrez&rendertype=abstract [Accessed July 10, 2014].

Rincón, S. a, Estravís, M. & Pérez, P., 2014. Cdc42 regulates polarized growth and cell integrity in fission yeast. *Biochemical Society transactions*, 42(1), pp.201–5. Available at: http://www.ncbi.nlm.nih.gov/pubmed/24450652.

Rincon, S. a & Paoletti, A., 2012. Mid1/anillin and the spatial regulation of cytokinesis in fission yeast. *Cytoskeleton (Hoboken, N.J.)*, 69(10), pp.764–77. Available at: http://www.ncbi.nlm.nih.gov/pubmed/22888038 [Accessed November 10, 2014].

Roberts, A.J. et al., 2013. Functions and mechanics of dynein motor proteins. *Nature reviews. Molecular cell biology*, 14(11), pp.713–26. Available at: http://www.pubmedcentral.nih.gov/articlerender.fcgi?artid=3972880&tool=pmcentrez&rendertype=abstract.

Roque, H. et al., 2010. The fission yeast XMAP215 homolog dis1p is involved in microtubule bundle organization. *PLoS ONE*, 5(12).

Rupes, I., Jia, Z. & Young, P.G., 1999. Ssp1 promotes actin depolymerization and is involved in stress response and new end take-off control in fission yeast. *Molecular biology of the cell*, 10(5), pp.1495–1510.

Samejima, I. et al., 2010. Fission yeast Mto1 regulates diversity of cytoplasmic microtubule organizing centers. *Current biology : CB*, 20(21), pp.1959–65. Available at: http://www.pubmedcentral.nih.gov/articlerender.fcgi?artid=2989437&tool=pmcentrez&rendertype=abstract [Accessed November 3, 2014].

Sandblad, L. et al., 2006. The Schizosaccharomyces pombe EB1 Homolog Mal3p Binds and Stabilizes the Microtubule Lattice Seam. *Cell*, 127(7), pp.1415–1424.

Sanders, S.L. & Herskowitz, I., 1996. The Bud4 protein of yeast, required for axial budding, is localized to the mother/bud neck in a cell cycle-dependent manner.

Journal of Cell Biology, 134(2), pp.413–427.

Saunders, T.E. et al., 2012. Noise Reduction in the Intracellular Pom1p Gradient by a Dynamic Clustering Mechanism. *Developmental Cell*, 22(3), pp.558–572. Available at: http://dx.doi.org/10.1016/j.devcel.2012.01.001.

Sawin, K.E., 1998. Chapter 8: GFP Fusion Proteins as Probes for Cytology in Fission Yeast. *Methods in Cell Biology*, 58, pp.123–138.

Sawin, K.E., Lourenco, P.C.C. & Snaith, H. a, 2004. Microtubule Nucleation at Non-Spindle Pole Body Microtubule-Organizing Centers Requires Fission Yeast Centrosomin-Related Protein mod20p. *Current Biology*, 128(2), pp.189–190.

Sawin, K.E. & Nurse, P., 1998. Regulation of Cell Polarity by Microtubules in Fission Yeast. , 142(2), pp.457–471.

Sawin, K.E. & Snaith, H. a, 2004. Role of microtubules and tea1p in establishment and maintenance of fission yeast cell polarity. *Journal of cell science*, 117(Pt 5), pp.689–700. Available at: http://www.ncbi.nlm.nih.gov/pubmed/14734657 [Accessed November 10, 2014].

Sawin, K.E. & Tran, P.T., 2006. Cytoplasmic microtubule organization in fission yeast. *Yeast (Chichester, England)*, 23(13), pp.1001–14. Available at: http://www.ncbi.nlm.nih.gov/pubmed/17072892.

Schirenbeck, A. et al., 2005. The Diaphanous-related formin dDia2 is required for the formation and maintenance of filopodia. *Nature cell biology*, 7(6), pp.619–625. Available at: http://www.ncbi.nlm.nih.gov/pubmed/15908944.

Shelley, M.J., 2016. The Dynamics of Microtubule/Motor-Protein Assemblies in Biology and Physics. *Annual Review of Fluid Mechanics*, 48(1), pp.487–506. Available at: http://dx.doi.org/10.1146/annurev-fluid-010814-013639.

Shiozaki, K. & Russell, P., 1995. Cell-cycle control linked to extracellular environment by MAP kinase pathway in fission yeast. *Nature*, 378(6558), pp.739–743.

Sirotkin, V. et al., 2005. Interactions of WASp, myosin-I, and verprolin with Arp2/3 complex during actin patch assembly in fission yeast. *Journal of Cell Biology*, 170(4), pp.637–648.

Sirotkin, V. et al., 2010. Quantitative Analysis of the Mechanism of Endocytic Actin Patch Assembly and Disassembly in Fission Yeast. *Molecular biology of the cell*, 21(24), pp.4325–4337.

Slaughter, B.D., Smith, S.E. & Li, R., 2009. Symmetry Breaking in the Life Cycle of the Budding Yeast. , 1(3), p.18.

Slep, K.C. & Vale, R.D., 2007. Structural Basis of Microtubule Plus End Tracking by XMAP215, CLIP-170, and EB1. *Molecular Cell*, 27(6), pp.976–991.

Snaith, H.A. & Sawin, K.E., 2003. Fission yeast mod5p regulates polarized growth

through anchoring of tea1p at cell tips. , 573(1954), pp.647–651.

Snaith, H. a et al., 2011. Characterization of Mug33 reveals complementary roles for actin cable-dependent transport and exocyst regulators in fission yeast exocytosis. *Journal of cell science*, 124(Pt 13), pp.2187–2199.

Snaith, H. a, Samejima, I. & Sawin, K.E., 2005. Multistep and multimode cortical anchoring of tea1p at cell tips in fission yeast. *The EMBO journal*, 24(21), pp.3690–9. Available at: http://www.pubmedcentral.nih.gov/articlerender.fcgi?artid=1276721&tool=pmcentrez&rendertype=abstract [Accessed October 17, 2014].

Snell, V. & Nurse, P., 1994. Genetic analysis of cell morphogenesis in fission yeast--a role for casein kinase II in the establishment of polarized growth. *The EMBO journal*, 13(9), pp.2066–2074.

Sohrmann, M. et al., 1996. The dmf1/mid1 gene is essential for correct positioning of the division septum in fission yeast. *Genes and Development*, 10(21), pp.2707–2719.

St Johnston, D. & Ahringer, J., 2010. Cell polarity in eggs and epithelia: Parallels and diversity. *Cell*, 141(5), pp.757–774.

Starr, D. a & Han, M., 2002. Role of ANC-1 in tethering nuclei to the actin cytoskeleton. *Science (New York, N.Y.)*, 298(5592), pp.406–9. Available at: http://www.ncbi.nlm.nih.gov/pubmed/12169658 [Accessed November 10, 2014].

Stauber, T. et al., 2006. A Role for Kinesin-2 in COPI-Dependent Recycling between the ER and the Golgi Complex. *Current Biology*, 16(22), pp.2245–2251.

Suzuki, A. & Ohno, S., 2006. The PAR-aPKC system: lessons in polarity. *Journal of cell science*, 119(Pt 6), pp.979–987.

Sveiczer, A., Novak, B. & Mitchison, J.M., 1996. The size control of fission yeast revisited. *Journal of cell science*, 109, pp.2947–2957.

Sweeney, H.L. & Houdusse, A., 2010. Structural and functional insights into the Myosin motor mechanism. *Annual review of biophysics*, 39, pp.539–557.

Tahirovic, S. & Bradke, F., 2009. Neuronal Polarity. *Cold Spring Harbor perspectives in biology*, 17, pp.267–310.

Tamura, K. et al., 2013. Myosin XI-i links the nuclear membrane to the cytoskeleton to control nuclear movement and shape in Arabidopsis. *Current biology : CB*, 23(18), pp.1776–81. Available at: http://www.ncbi.nlm.nih.gov/pubmed/23973298 [Accessed November 10, 2014].

Tatebe, H. et al., 2008. Pom1 DYRK regulates localization of the Rga4 GAP to ensure bipolar activation of Cdc42 in fission yeast. *Current biology : CB*, 18(5), pp.322–30. Available at:

http://www.pubmedcentral.nih.gov/articlerender.fcgi?artid=2277499&tool=pmcentrez&rendertype=abstract [Accessed October 7, 2014].

Tatebe, H. et al., 2005. Wsh3/Tea4 is a novel cell-end factor essential for bipolar distribution of Tea1 and protects cell polarity under environmental stress in S. pombe. *Current biology : CB*, 15(11), pp.1006–15. Available at: http://www.ncbi.nlm.nih.gov/pubmed/15936270 [Accessed October 17, 2014].

Terenna, C.R. et al., 2008. Physical Mechanisms Redirecting Cell Polarity and Cell Shape in Fission Yeast. *Current Biology*, 18(22), pp.1748–1753. Available at: http://dx.doi.org/10.1016/j.cub.2008.09.047.

Thompson, B.J., 2013. Cell polarity: models and mechanisms from yeast, worms and flies. *Development (Cambridge, England)*, 140(1), pp.13–21. Available at: http://www.ncbi.nlm.nih.gov/pubmed/23222437 [Accessed November 10, 2014].

Tolic-Nørrelykke, I.M. et al., 2005. Nuclear and division-plane positioning revealed by optical micromanipulation. *Current biology : CB*, 15(13), pp.1212–6. Available at: http://www.ncbi.nlm.nih.gov/pubmed/16005294 [Accessed November 10, 2014].

Toya, M. et al., 2001. Identification and functional analysis of the gene for type I myosin in fission yeast. *Genes to cells : devoted to molecular & cellular mechanisms*, 6(3), pp.187–199.

Tran, P.T. et al., 2001. A Mechanism for Nuclear Positioning in Fission Yeast Based on Microtubule Pushing 7. , 153(2), pp.397–411.

Tran, P.T., Paoletti, A. & Chang, F., 2004. Imaging green fluorescent protein fusions in living fission yeast cells. *Methods*, 33(3), pp.220–225.

Tropini, C. et al., 2012. Islands containing slowly hydrolyzable GTP analogs promote microtubule rescues. *PLoS ONE*, 7(1).

Tsirigos, K.D. et al., 2015. The TOPCONS web server for consensus prediction of membrane protein topology and signal peptides. *Nucleic acids research*, 43(W1), pp.W401-7. Available at: http://www.pubmedcentral.nih.gov/articlerender.fcgi?artid=4489233&tool=pmcentrez&rendertype=abstract.

Uemura, T. & Tanagida, M., 1986. Mitotic spindle pulls but fails to separate chromosomes in type II DNA topoisomerase mutants: uncoordinated mitosis. *The EMBO journal*, 5(5), pp.1003–1010.

Ullal, P. et al., 2015. The DYRK-family kinase Pom1 phosphorylates the F-BAR protein Cdc15 to prevent division at cell poles. *The Journal of Cell Biology*, 211(3), pp.653–668. Available at: http://www.jcb.org/cgi/doi/10.1083/jcb.201504073.

Vavylonis, D. et al., 2008. Assembly mechanism of the contractile ring for cytokinesis

by fission yeast. *Science (New York, N.Y.)*, 319(5859), pp.97–100. Available at: http://www.ncbi.nlm.nih.gov/pubmed/18079366.

Verde, F., Mata, J. & Nurse, P., 1995. Fission Yeast Cell Morphogenesis : Identification of. , 131(6), pp.1529–1538.

Vicente-Manzanares, M. et al., 2009. Non-muscle myosin {II} takes centre stage in cell adhesion and migration. *Nature Reviews Molecular Cell Biology*, 10(11), pp.778–790. Available at: http://www.nature.com/nrm/journal/v10/n11/full/nrm2786.html.

Walczak, C.E., Gayek, S. & Ohi, R., 2013. Microtubule-Depolymerizing Kinesins. *Annual Review of Cell and Developmental Biology*, 29(1), pp.417–441. Available at: http://www.annualreviews.org/doi/abs/10.1146/annurev-cellbio-101512-122345.

Wedlich-Soldner, R. & Li, R., 2003. Spontaneous cell polarization: undermining determinism. *Nature cell biology*, 5(April), pp.267–270.

Wei, B. et al., 2016. Unique Spatiotemporal Activation Pattern of Cdc42 by Gef1 and Scd1 Promotes Different Events during Cytokinesis. *Molecular biology of the cell*, 27(8), pp.1235–1245. Available at: http://www.molbiolcell.org/content/27/8/1235?etoc.

Welte, M.A., 2004. Bidirectional transport along microtubules. *Current Biology*, 14(13), pp.525–537.

Win, T.Z. et al., 2001. Two type V myosins with non-overlapping functions in the fission yeast Schizosaccharomyces pombe: Myo52 is concerned with growth polarity and cytokinesis, Myo51 is a component of the cytokinetic actin ring. *Journal of cell science*, 114(Pt 1), pp.69–79.

Wood, E. & Nurse, P., 2013. Pom1 and cell size homeostasis in fission yeast. *Cell Cycle*, 12(19), pp.3228–3236.

Wood, E. & Nurse, P., 2015. Sizing up to Divide: Mitotic Cell-Size Control in Fission Yeast. *Annual review of cell and developmental biology*, 31, pp.11–29. Available at: http://www.ncbi.nlm.nih.gov/pubmed/26566110.

Woolner, S. & Bement, W.M., 2009. Unconventional myosins acting unconventionally. *Trends in Cell Biology*, 19(6), pp.245–252.

Woźniak, M.J. & Allan, V.J., 2006. Cargo selection by specific kinesin light chain 1 isoforms. *The EMBO journal*, 25(23), pp.5457–68. Available at: http://emboj.embopress.org/content/25/23/5457.abstract.

Wu, C.F. et al., 2015. Role of competition between polarity sites in establishing a unique front. *eLife*, 4(NOVEMBER2015), pp.1–33.

Wu, J. et al., 2003. Spatial and Temporal Pathway for Assembly and Constriction of

the Contractile Ring in Fission Yeast Cytokinesis. , 5, pp.723–734.

Wu, X. et al., 2010. Ultraviolet irradiation induces autofluorescence enhancement via production of reactive oxygen species and photodecomposition in erythrocytes. *Biochemical and biophysical research communications*, 396(4), pp.999–1005. Available at: http://www.ncbi.nlm.nih.gov/pubmed/20471364 [Accessed November 10, 2014].

Zahner, J.E., Harkins, H. a & Pringle, J.R., 1996. Genetic analysis of the bipolar pattern of bud site selection in the yeast Saccharomyces cerevisiae. *Molecular and cellular biology*, 16(4), pp.1857–1870.

Zhang, D., Vjestica, A. & Oliferenko, S., 2012. Plasma membrane tethering of the cortical ER necessitates its finely reticulated architecture. *Current biology : CB*, 22(21), pp.2048–52. Available at: http://www.ncbi.nlm.nih.gov/pubmed/23041194 [Accessed January 23, 2015].

Zhang, D., Vjestica, A. & Oliferenko, S., 2010. The cortical ER network limits the permissive zone for actomyosin ring assembly. *Current Biology*, 20(11), pp.1029–1034. Available at: http://dx.doi.org/10.1016/j.cub.2010.04.017.